Effects of Sex, Strain Rate, and Age on the Tensile and Compressive Material Properties of Human Rib Cortical Bone

Michael John Katzenberger Jr.

Thesis submitted to the faculty of the Virginia Polytechnic Institute and State University in partial fulfillment of the requirements for the degree of

Master of Science
in
Biomedical Engineering

Andrew R. Kemper, Chair
Warren N. Hardy
Amanda M. Agnew

August 22, 2019
Blacksburg, VA

Keywords: rib, thorax, thoracic injury, bone, biomechanics, stress, strain, tension, compression

Effects of Sex, Strain Rate, and Age on the Tensile and Compressive Material Properties of Human Rib Cortical Bone

Michael J. Katzenberger Jr.

ACADEMIC ABSTRACT

The objective of this study was to evaluate the effects of sex, loading rate, and age on the tensile and compressive material properties of human rib cortical bone over a wide range of subject demographics. Tension coupons were tested from sixty-one (n = 61) subjects (M = 32, F = 29) ranging in age from 17 to 99 years of age (Avg. = 56.4 ± 26.2 yrs.). Compression samples were tested from thirty (n = 30) subjects (M = 19, F = 11) ranging in age from 18 to 95 years of age (Avg. = 49.0 ± 23.9 yrs.). For each subject, one coupon/sample was tested to failure on a material testing system at a targeted strain rate of 0.005 strain/s, while a second coupon/sample was tested at 0.5 strain/s. A load cell was used to measure axial load for both the tension coupons and compression samples. An extensometer was used to measure displacement within the gage length of the tension coupons and a deflectometer was used to measure displacement of the compression samples. Tension data were obtained from fifty-eight (n = 58) coupons at 0.005 strain/s and fifty-eight (n = 58) coupons at 0.5 strain/s, with fifty-five (n = 55) matched pairs. Compression data were obtained from thirty (n = 30) compression samples at 0.005 strain/s and thirty (n = 30) samples at 0.5 strain/s. The elastic modulus, yield stress, yield strain, ultimate stress, elastic strain energy density (SED), plastic SED, and total SED were then calculated for each tensile and compression test. In addition, failure stress and failure strain were calculated for each tension test. There were no significant differences in the tensile material properties between sexes and no significant interactions between age and sex for either method of loading. In regard to the differences in tensile material properties with respect to loading rate, yield stress, yield strain, failure stress, ultimate stress, elastic SED, plastic SED, and total SED were significantly lower at 0.005 strain/s compared to 0.5 strain/s. All material properties were significantly lower at 0.005 strain/s compared to 0.5 strain/s in compression. Spearman correlation analyses showed that all tensile material properties had significant negative correlations with age at 0.005 strain/s except modulus. At 0.5 strain/s, all tensile material properties except yield strain had significant negative correlations with age. No significant correlations were observed in material properties with respect to advanced age in compression at either loading rate. Although the results revealed that the tensile material properties of human rib cortical bone varied significantly with respect to chronological age, the R^2 values only ranged from 0.15 - 0.62, indicating that there may be other underlying variables that better account for the variance within a given population. Overall, this is the first study to analyze the effects of sex, loading rate, and age on tensile material properties of human rib cortical bone using a reasonably large sample size and the first study to test the compressive material properties of human rib cortical bone. The results of this study provide data that allows FEMs to better assess thoracic injury risk for all vehicle occupants. Additionally, this study provides the necessary data to more accurately model and assess differences in the material response of the rib cage for nearly all vehicle occupants of driving age.

Effects of Sex, Strain Rate, and Age on the Tensile and Compressive Material Properties of Human Rib Cortical Bone

Michael J. Katzenberger Jr.

GENERAL AUDIENCE ABSTRACT

The thorax is one of the most frequently injured body regions in motor vehicle collisions (MVCs), and severe thoracic injuries have been shown to increase mortality risk. Finite element models (FEMs) of the human body are frequently used to evaluate thoracic injury risk. However, the accuracy of these models is dependent on the biomechanical data used to validate them. Although the material properties of bone have been shown to vary with respect to age and loading rate, previous studies that have evaluated the material properties of human rib cortical bone were limited to a small number of subjects, a narrow age range, one loading rate, and one loading mode (tension). Therefore, the purpose of this study was to evaluate the effects of sex, age, and loading rate on the tensile and compressive material properties of rib cortical bone over a wide range of subject demographics. Tension coupons were tested from sixty-one (n = 61) subjects (M = 32, F = 29) ranging in age from 17 to 99 years (Avg. = 56.4 ± 26.2 years). Compression samples were tested from thirty (n = 30) subjects (M = 19, F = 11) ranging in age from 18 to 95 years (Avg. = 49.0 ± 23.9 years). For each subject, one coupon/sample was tested to failure on a material testing system at a targeted strain rate of 0.005 strain/s, while the other coupon was tested at 0.5 strain/s. A load cell was used to measure axial load for both the tension coupons and compression samples. An extensometer was used to measure displacement within the gage length of the tension coupons and a deflectometer was used to measure displacement of the compression samples. There were no significant differences in material properties between sexes and no significant interactions between age and sex for either method of loading. In regard to the differences in tensile material properties with respect to loading rate, yield stress, yield strain, failure stress, ultimate stress, elastic SED, plastic SED, and total SED were significantly lower at 0.005 strain/s compared to 0.5 strain/s. All material properties were significantly lower at 0.005 strain/s compared to 0.5 strain/s in compression. In regard to the effect of age, all tensile material properties had significant negative correlations with age at except the modulus at 0.005 strain/s and yield strain at 0.5 strain/s. No significant correlations were observed in material properties with respect to advanced age in compression at either loading rate. Overall, this is the first study to provide the tension and compression data needed to more accurately model and assess differences in the material response of the rib cage for nearly all vehicle occupants of driving age.

`

ACKNOWLEDGEMENTS

First, I would like to thank my thesis advisor, Dr. Andrew Kemper. Dr. Kemper taught me the fundamentals of injury biomechanics and provided his expertise in material testing during this research project.

I would like to thank my committee members, Dr. Amanda Agnew and Dr. Warren Hardy, for their time and contributions.

I would also like to personally thank Dr. Devon Albert. She is currently a post-doc in the Center for Injury Biomechanics at Virginia Tech, and she helped me in many different facets of grad school. Additionally, I would like to acknowledge all the undergraduate assistants who helped with sample preparation and data processing.

I must express gratitude to my family for providing me with unfailing support and continuous encouragement throughout my years of study. This accomplishment would not have been possible without them. Thank you.

Finally, this work would not be possible without the generous contributions of the anatomical donors.

TABLE OF CONTENTS

`

LIST OF FIGURES

`

`

`

`

LIST OF TABLES

`

CHAPTER 1: INTRODUCTION

The thorax is one of the most frequently injured body regions in motor vehicle collisions (MVCs), and severe thoracic injuries have been shown to increase mortality risk [1, 2]. A study that analyzed injuries sustained in frontal impacts documented in the National Automotive Sampling System (NASS) from 1988 to 1994 showed that chest injuries constituted 37.6% of all AIS 3+ injuries, 46.3% of all AIS 4+ injuries, and 43.3 % of all AIS 5+ injuries [3]. A more recent study analyzing data from the NASS Crashworthiness Data System for frontal, single-impact crashes from 2000 to 2011 found that the thorax had a higher risk for AIS 3+, 4+, and 5+ injuries in both belted and unbelted occupants compared to the head, which is also frequently injured in MVCs [4]. In regard to thoracic injuries, it has been reported that elderly vehicle occupants are more likely to sustain severe chest injuries during MVCs [1]. Furthermore, it has been shown that elderly vehicle occupants have a higher mortality risk from these injuries in comparison to younger vehicle occupants [5, 6]. These epidemiological findings are supported by experimental post-mortem human subjects (PMHS) studies that have shown that rib fractures are the most commonly observed skeletal injury during frontal loading [7]. In addition, PMHS studies have reported that thoracic injury tolerance decreases significantly with advanced age [8, 9]. However, the decrease in structural injury tolerance of the thorax with advanced age is likely attributed to changes in the geometric properties, material properties, or a combination of both, since chronological age does not directly represent the biological mechanisms at play.

In order to characterize the structural response of the ribs, different types of bending tests have been performed on whole rib segments and intact whole ribs. A number of studies have performed three-point bending tests on whole rib segments to evaluate the effects of geometry and loading rate [10-13]. These studies have shown that the structural response of the ribs varies with respect to rib region and rib level and that these structural changes are accompanied by changes in the cross-sectional geometry [11, 14]. In addition, the maximum bending moment and energy absorption of human ribs in three-point bending has been shown to increase significantly with increased loading rate [15]. Although three-point bending tests provide valuable structural data, the boundary conditions are not representative of those seen *in vivo*. Furthermore, linear-elastic beam equations and correction factors used to calculate stress and strain for these types of tests do not produce accurate material response data [14]. In order to evaluate the structural response of

the ribs in a more realistic loading condition, a number of studies have performed anterior-posterior (A-P) bending tests on intact whole ribs [16-20]. Murach *et al.* (2017) reported that structural properties of whole ribs in A-P bending could be predicted by rib cross-sectional geometry, and the prediction was improved when using a combination of cross-sectional and gross geometric variables [18] . However, obtaining accurate cross-sectional geometry measurements of the ribs is difficult due to the fact that the cortical shell is extremely thin. Consequently, histologic analysis, high resolution CT, or cortical bone mapping techniques are required, all of which are difficult to obtain for large sections of the ribs. Agnew *et al.* (2015) performed A-P bending tests on 140 ribs from 47 subjects (Age = 6 - 99 yrs.) and reported statistically significant negative relationships for percent displacement and linear structural stiffness with respect to advancing age, but noted that age did not explain the majority of the variance in each of the structural variables [21]. Additionally, Schafman *et al.* (2016) reported that a number of rib structural properties showed negative relationships with respect to age and some relationships with respect to sex, but only a small amount of the variance could be explained by chronological-age (7 - 39%) or sex (3 - 17%) [16]. Although these studies provide valuable structural data and geometric data, current finite element models (FEMs) are not able to accurately predict the fracture location and timing with these data alone [19]. The results of these rib bending studies indicate that other variables across the anatomical hierarchy need to be evaluated to more fully understand the underlying reason for the observed changes in structural response within a given population, e.g., material properties, bone mineral density, microstructure, etc.

Several comprehensive studies have analyzed the effect of age on the material properties of human cortical bone. Data obtained from these studies show that the ultimate stress, ultimate strain, and energy absorption consistently decrease with advanced age, regardless of the type of bone tested [22-24]. However, these results are primarily based on data from human femoral and tibial samples, and different bones may produce different material responses due to variance in microarchitecture [23]. Therefore, the magnitude of material properties from other skeletal elements cannot necessarily be used to estimate the material properties of rib cortical bone. Kemper *et al.* (2005) conducted the first study on the tensile material properties of human rib cortical bone. This study performed tension tests on rib cortical bone coupons from six PMHS and reported that some material properties decreased with advanced age, such as failure strain and strain energy density, but not failure stress [25]. Subsequently, Kemper *et al.* (2007) tested rib

`

cortical bone from six more male subjects and did not find a significant correlation between any material properties and age [14]. Subit *et al.* (2011) used different testing procedures than Kemper *et al.* to obtain rib cortical bone material properties from three subjects and also did not find significant correlations with respect to age [26]. However, all three of these studies had very small subject sample sizes, ranging from three to six subjects per study. A recently published study by Albert *et al.* (2017) performed tensile tests on rib cortical bone from twenty seven (n = 27) subjects and found that the modulus, yield stress, failure stress, failure strain, and strain energy density (SED) of human rib cortical bone in tensile loading decreased significantly with advanced age [27]. Although this study had a substantially larger dataset than the previous studies, the sample size was biased towards older subjects (Avg. = 70.5 ± 18.1 yrs.). Experimental studies have yet to analyze the material properties of rib cortical bone for the entire population of vehicle occupants. Due to large inter-subject variance within a given population, more subjects are needed to reasonably capture human variability and comprehensively evaluate the trends in material properties with respect to sex and age. In addition, the vast majority of the literature pertaining to the material response of rib cortical bone has been conducted at a single loading rate (0.5 strain/s). Although the viscoelastic properties of cortical bone in general have been well established in the literature, there are currently no studies that have specifically evaluated the effect of strain rate on the tensile material properties of human rib cortical bone [28-31]. Given that the thorax experiences multiple different dynamic loading rates during an MVC, the collection of material data at multiple rates is necessary to model the rate-dependent effects of rib cortical bone.

Furthermore, the literature focused on quantifying the material properties of rib cortical bone has been limited to tensile testing. However, during the dynamic loading conditions observed in an MVC, the ribs withstand loading in both tension and compression due to the natural curvature of the rib. For example, in a frontal, blunt loading condition, the cutaneous side of the rib is placed in tension, while the pleural side of the rib is placed in compression. Studies have shown that the material response of cortical bone, e.g., the shape of the stress versus strain curve and the material property values, differs between tensile and compressive loading, i.e., the stress-strain response is asymmetric [32, 33]. Therefore, it is necessary to quantify both the tensile and compressive material response of rib cortical bone to accurately model the material response of rib cortical bone. Although there have been a number of studies that have investigated the compressive material properties of the cortical bone, these studies have been primarily limited to the testing of

`

femoral or tibial bone [28, 34]. There are currently no studies that have attempted to fabricate and test compression samples of rib cortical bone. This is likely due to the fact that the cortical shell is very thin in human ribs, even in the thicker posterior cortical shell (Avg. cortical thickness = 0.7 to 1.2 mm), which makes it extremely challenging to obtain a precisely machined compression coupon for material testing [35].

While age and/or sex related differences in the structural response of the thorax are likely due to changes in both the geometric and material properties, it is currently unknown which geometric or material variables account for the majority of the variance in the structural properties of the ribs. Consequently, several whole body FEM studies have evaluated the effects of age and/or sex on the response of the thorax by attempting to account for changes in both geometric and material properties [36-38]. Although these parametric studies have shown that age dependent material and geometric properties affect the response and injury risk of the model, they primarily focus on how geometric and material changes affect the global response of the model with limited or no validation data for particular demographics [36-38]. In addition, whole body FEMs and FEMs of isolated ribs are typically unable to accurately predict the number, location, and/or timing of rib fractures [36, 39-41]. Logically, the accuracy of these models depends on the biomechanical data available for validation. Currently, there is a lack of experimental data available for FEMs to validate the anisotropic, age-dependent, rate-dependent, asymmetric material behavior of human rib cortical bone. Consequently, many FEMs use non-rate dependent, isotropic, symmetric, elastic-plastic material models when modeling rib cortical bone, which do not necessarily represent the response of the thorax at the range of strain rates observed during MVCs [36, 41-43]. In addition, some FEMs have used material data from long bones when attempting to model the effects of strain rate and/or age on the response and injury tolerance of the thorax [37, 40]. However, it has been shown that the material response of cortical bone can vary between skeletal elements due to differences in micro-architecture [23]. FEM studies that have implemented material properties from human rib cortical bone have been limited the use of the tensile data from Kemper et al. (2005, 2007) [36, 39, 43]. Although combining the data from these two studies results in a wide range of subject ages (18 to 81), the material data was only obtained for a single loading rate, and the small number of subjects (n=12) does not accurately represent the variance observed in the population. In addition, these data do not account for the differences between the tensile and compressive material properties of cortical bone. Overall, obtaining a more comprehensive

`

material property data set for human rib cortical bone would allow FEMs to better model and assess how differences in the material response of the rib cage affect thoracic response, as well as more accurately evaluate the relative effects of geometric and material variables.

Research Objectives

In order to address the present needs in the fields of injury biomechanics and automotive safety, two research studies were carried out in this thesis to quantify the material properties of human rib cortical bone to provide data for finite element models to more accurately predict the material response of the thorax during dynamic loading. Specific emphasis was placed on evaluating changes in material properties of rib cortical bone with respect to sex, loading rate, and age. The main research objectives of this thesis are as follows:

1) Quantify the effects of sex, loading rate, and age on the tensile material properties of human rib cortical bone using a large subject population over a wide age range

2) Develop novel methods to fabricate and test human rib cortical bone samples in compression

3) Quantify the effects of sex, loading rate, and age on the compressive material properties of human rib cortical bone over a wide age range

`

CHAPTER 2: EFFECTS OF SEX, LOADING RATE, AND AGE ON THE TENSILE MATERIAL PROPERTIES OF HUMAN RIB CORTICAL BONE

Introduction

A combination of cross-sectional geometry, gross geometry, and material properties is hypothesized to contribute to the structural response of human ribs. A recent study reported that cross-sectional geometry and whole rib geometry explain 35% to 75% of variance in rib structural response [18]. Given that the structural response of bone can be affected by both the geometry and material properties, it is likely that the remaining variance is at least partially explained by material properties. Previous studies have quantified the material properties of human rib cortical bone through tensile testing [14, 25, 26]. However, these studies had very small subject sample sizes, ranging from three to six subjects per study, and included primarily older subjects. While it has been shown that elderly occupants are more likely to sustain severe thoracic injuries due to an MVC and have a higher mortality risk from these injuries compared to younger vehicle occupants, the fatal crash rate per mile driven for 16 to 19 year-olds is nearly 3 times the rate for drivers over the age of 20, as of 2017 [5, 6, 44]. Due to large inter-subject variance within a given population, a relatively large sample size is needed to reasonably capture human variability and comprehensively evaluate the trends in material properties with respect to sex and age. In addition, the vast majority of the literature pertaining to the material response of rib cortical bone has been conducted at a single loading rate (0.5 strain/s). Although extensive tensile and compression testing conducted on human tibia and femur cortical bone has shown that cortical bone is viscoelastic, the effect of strain rate on the material properties of rib cortical bone has yet to be adequately studied [28, 29]. Therefore, the goals of the current study were to quantify the tensile material properties of human rib cortical bone over a wide age range, and evaluate differences in the material response with respect to sex, loading rate, and age.

Methods

Sixty-one (n = 61) subjects (Male [M] = 32, Female [F] = 29) ranging from 17 to 99 years of age (Avg. = 56.4 ± 26.2 yrs.) were used in this study. Data were obtained from two sources. Fifty-eight (n = 58) tension coupons were tested at 0.005 strain/s, and thirty-one (n = 31) tension coupons were tested at 0.5 strain/s in the current study. In addition, data were obtained from Albert *et al.* (2017), which comprised of twenty-seven (n = 27) additional tension coupons previously tested at

0.5 strain/s using the same test procedures and subject pool as the current study [45]. Subject demographics including sex, age, height, and weight are included in Table A1.

All ribs used in this study were ethically obtained through the Body Donor Program at The Ohio State University and Lifeline of Ohio with no known bone disease reported. Whole ribs were excised from the body, wrapped in normal saline soaked gauze, stored in air-tight plastic bags, and frozen at -20 °C until testing [46-50]. Rib levels 3-7 were used in this study. The rib level and rib side (left/right) were selected at random; however, the rib level and rib side taken from each subject were occasionally limited by the tissue available. Kemper et al. (2005, 2007) tested multiple samples per subject and found no significant differences in the tensile material properties of rib cortical bone with respect to region (anterior, lateral, posterior) or rib level [14, 25]. Therefore, it was assumed that there were no significant differences in material properties with respect to region, rib level, or side (right versus left) [10].

A series of steps were taken to obtain two dog-bone shaped coupons from each subject for testing [14, 25, 45]. All specimens were kept hydrated with normal saline throughout each fabrication process. First, ribs were thawed and the soft tissue was removed. Then, a 3 cm longitudinal segment of the rib was cut using a low speed diamond saw. Two cuts were then made with the diamond saw parallel to the long axis of the rib on the cutaneous side of the segment to obtain a rectangular coupon (Figure 1). The coupon was taken from a location on the cutaneous side of the rib with the least amount of natural curvature, i.e., the anterior to lateral portion of the rib. Fine grit sand paper was used to carefully remove all trabecular bone from the rectangular coupon, leaving only cortical bone. The remaining cortical bone was sanded to a constant thickness ranging from 0.508 mm (0.020 in.) to 0.635 mm (0.025 in.) with a tolerance of ± 0.0635 mm (± 0.0025 in.). Next, the sample was milled into a "dog-bone" shaped coupon using a Computer Numerical Control (CNC) mill (MAXNC 10, MAXNC Inc., Chandler, AZ). Coupon dimensions were based on those used by Kemper *et al.* (2005) [25]. Each coupon was sanded until the sample thickness was uniform with a tolerance of ± 0.0127 mm (± 0.0005 in.). The minimum uniform thickness was 0.2286 ± 0.0127 mm (0.009 ± 0.0005 in.) and the maximum uniform thickness was 0.4318 ± 0.0127 mm (0.017 ± 0.0005 in.). The final thickness and width of the gage length, i.e., the rectangular section in the middle of the coupon, of each sample were measured with dial calipers before testing to quantify the initial cross-sectional area.

Uniaxial tensile tests were performed to failure on a servo-hydraulic high-rate Material Testing System (810 MTS, MTS Systems Corporation, Eden Prairie, MN) with a slack adapter, which allowed the piston to reach a constant velocity before loading the coupon [14, 25, 45]. Custom designed coupon grips with sandpaper covered grip faces were used to clamp the coupon and prevent the coupon from slipping during testing (Figure 1) [14, 25, 45]. The top and bottom grips were carefully aligned to ensure that the coupons experienced a strictly tensile load [25]. A uniaxial load cell (1500ASK-100, Interface, Scottsdale, AZ) was used to measure the axial load experienced by the coupon, and an extensometer (632.13F-20, MTS, Eden Prairie, MN) was used to measure the displacement in the gage length.

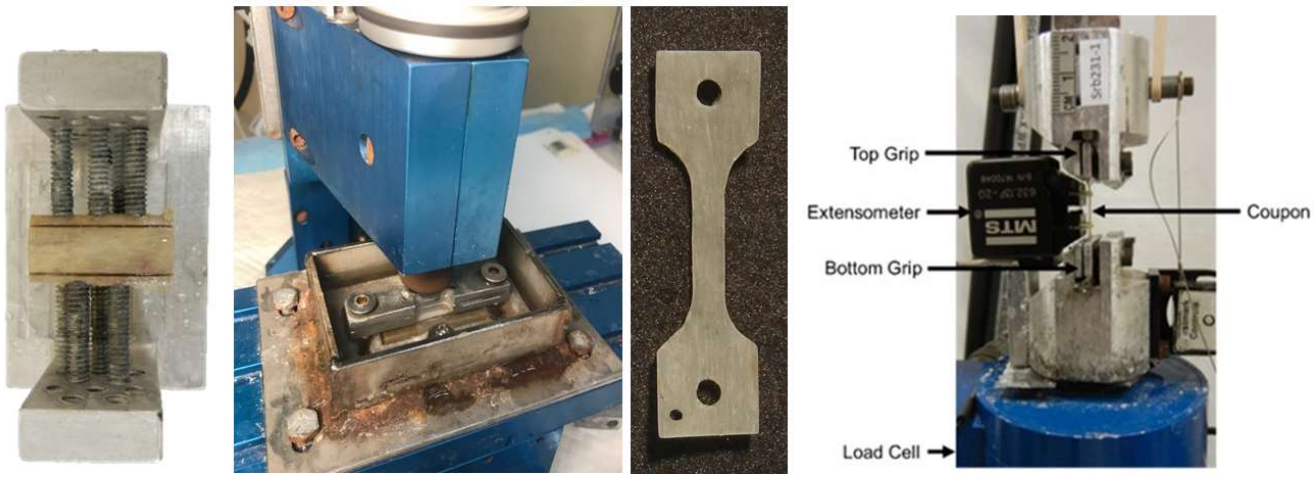

Figure 1: Parallel cuts made on the cutaneous side of a 3 cm rib segment (left), rectangular cortical coupon milled into a dog-bone coupon in CNC mill (left-center), final dog-bone coupon (right-center), front view of tension experimental setup (right).

For each subject, one coupon was tested to failure in tension at a targeted strain rate of 0.005 strain/s, while the other coupon was tested at 0.5 strain/s. The targeted strain rate of 0.5 strain/s was selected for this study because it was the average strain rate measured by strain gages on the ribs of PMHS during frontal belt loading tests that simulated a 48 kph sled test, and it was the same strain rate used in previous studies that evaluated the tensile material properties of human rib cortical bone [14, 25, 45, 51]. The slower strain rate, 0.005 strain/s, was targeted for three reasons. First, the slower loading rate was approximately the same order of magnitude as the lowest loading rate used by previous studies that have analyzed the effects of strain rate on cortical bone from other skeletal elements [18, 31]. Second, the ribs experienced a wide range of loading rates (0.034

to 0.706 strain/s) during table-top belt loading tests that simulated belt loading observed in a 48 kph frontal collision. It has been shown that most MVCs occur between 24 and 33 kph [52]. Therefore, it is likely that the thorax will experience loading rates closer to 0.005 strain/s in lower speed collisions. Third, it was two orders of magnitude lower than 0.5 strain/s, which increased the chance of detecting differences in material response with respect to strain rate since the inter-subject variance within a given strain rate can be relatively large [53]. For the 0.005 strain/s tests, data were collected at 500 Hz and filtered with a 5 - 80 Hz notch filter (Figure A1). For the 0.5 strain/s tests, data were collected at 40100.2 Hz and filtered at SAE CFC 180 (Figure A1) [54].

The filtered data were used to the calculate elastic modulus, yield stress, yield strain, failure stress, failure strain, ultimate stress, elastic strain energy density (SED), plastic SED, and total SED (Figure A2). Stress was calculated by dividing the force by the initial cross-sectional area of the gage length. Strain was calculated by dividing the change in length between the extensometer blades by the initial length between the blades. The yield point was calculated as the point of intersection between the stress-strain curve and a straight line that was offset by 0.1% strain and parallel to the elastic portion of the curve [55, 56]. The elastic modulus was quantified by the slope of the elastic portion of the stress-strain curve between approximately 10% and 50% of the yield point. Failure stress and failure strain were the stress and strain at the time of failure, while ultimate stress was the maximum stress experienced by the coupon. Failure strain for all tests was the same as the ultimate/maximum strain. Total SED was calculated as the area under the stress-strain curve, with elastic SED and plastic SED defined as the area under the stress-strain curve before and after the yield point, respectively. A test was deemed successful if the coupon fractured within the gage length. For several subjects, two successful tests were obtained at a single loading rate. For those cases, the two tests were averaged, and the material properties were reported as one data point. Characteristic average curves were quantified for each decade at both loading rates using the procedure published by Lessley *et al.* (2004) [57].

Statistical analyses were conducted to determine if there was a significant correlation between the material properties and sex, loading rate, and age. The alpha (α) value was set at 0.05 to determine significance for all analyses and p-values were reported for all correlations. If the p-value was less than α, the correlation was deemed significant. All material properties were tested for normality at each loading rate using a Shapiro-Wilk test (W) (Table A2). An analysis of variance (ANOVA)

was performed across all subjects, with age treated as a continuous variable, to evaluate the effects of sex and the interaction between age and sex on the material properties at each loading rate. The effect of sex was also analyzed with age treated as a discrete variable. For this analysis, the subjects were grouped into three age groups: young (Age = 17 - 35 years, M = 12, F = 8), middle aged (36 - 65 years, M = 8, F = 6), and elderly (66+ years, M = 12, F = 14). These age groups were based on an epidemiological study assessing the effect of age on thoracic injury tolerance [58]. A Tukey's honestly significant difference (HSD) multiple comparison test was then conducted to determine if there were significance differences with respect to sex within each age group. To evaluate whether or not there were differences in the material properties with respect to loading rate, either a paired t-test (t) or a Wilcoxon signed-rank (S) test was conducted. If the data for a given material property were normally distributed at both loading rates, a paired t-test was used. A Wilcoxon signed-rank test, which does not assume normally distributed data, was used if the material property data were not normally distributed for one or both of the loading rates. Because at least one material property was not normally distributed, the Spearman's rank correlation coefficient (ρ), which is a nonparametric bivariate correlation, was determined for each material property with respect to age. Linear regression analyses were also performed to determine the R^2 value for each material property with respect to age.

Results

Material property data were successfully obtained from a total of one hundred twenty-one (n = 121) tension coupons (Figures A3-A11, Table A1). From the current study, material property data were obtained from fifty-eight (n = 58) subjects at 0.005 strain/s (M = 32, F = 26, Avg. = 56.9 ± 26.1 yrs.). The average strain rate for these tests was 0.00515 strain/s. From both the current study and Albert *et al.* (2017), material property data were obtained from fifty-eight (n = 58) subjects at 0.5 strain/s (M = 31, F = 27, Avg. = 57.3 ± 26.3 yrs.). The average strain rate for these tests was 0.504 strain/s. A total of fifty-five (n = 55) subjects had matched 0.005 strain/s and 0.5 strain/s data pairs (M = 31, F = 24, Avg. = 57.8 ± 26.1 yrs.). Four subjects in the 0.005 strain/s group and one subject in the 0.5 strain/s group had two successful tests using two different coupons for the given loading rate.

Two statistical analyses were performed to evaluate the effect of sex on the material properties, where age was treated as either a continuous or discrete variable. No significant differences were found in the material properties with respect to sex or the interaction between age and sex when age was treated as a continuous variable (Table 1). The same results were obtained when analyzing the effect of sex on material properties within age groups (i.e., young, middle aged, and elderly) (Table 2). Therefore, males and females were grouped together for the correlation analyses with respect to age.

Table 1: ANOVA results for the effect of sex on tensile material properties at each strain rate.

Material Property Variable	0.005 strain/s		0.5 strain/s	
	Sex	Sex*Age	Sex	Sex*Age
	p-value	p-value	p-value	p-value
Modulus	0.2437	0.9037	0.8274	0.4021
Yield Stress	0.7303	0.7452	0.8090	0.4751
Yield Strain	0.1825	0.3344	0.4077	0.8957
Failure Stress	0.5388	0.8496	0.4492	0.9353
Failure Strain	0.5406	0.2445	0.2055	0.2286
Ultimate Stress	0.7027	0.6567	0.4738	0.9427
Elastic SED	0.9808	0.6881	0.7377	0.3875
Plastic SED	0.7930	0.4246	0.2610	0.3684
Total SED	0.8000	0.4247	0.2654	0.4141

Table 2: Tukey HSD results for the effect of sex on tensile material properties within each age group at each strain rate.

Material Property Variable	0.005 strain/s			0.5 strain/s		
	Young	Middle	Elderly	Young	Middle	Elderly
	p-value	p-value	p-value	p-value	p-value	p-value
Modulus	0.9695	0.9535	0.9468	0.9954	1.0000	0.9998
Yield Stress	1.0000	0.9613	0.9948	0.9521	0.8910	0.6133
Yield Strain	0.6752	1.0000	0.9997	0.9884	1.0000	0.9767
Failure Stress	0.9501	0.7377	0.9971	0.9396	0.9921	0.9738
Failure Strain	0.9947	0.9630	1.0000	0.5890	0.9997	0.9810
Ultimate Stress	0.9963	0.7362	0.9967	0.9462	0.9888	0.9747
Elastic SED	0.9994	0.9492	0.9996	1.0000	1.0000	0.9878
Plastic SED	1.0000	0.6009	1.0000	0.6815	0.9958	0.9698
Total SED	1.0000	0.5913	1.0000	0.7138	0.9963	0.9662

When comparing material properties between loading rates, yield strain ($p < 0.0001$), yield stress ($p < 0.0001$), failure stress ($p < 0.0001$), ultimate stress, ($p < 0.0001$), elastic SED ($p < 0.0001$), plastic SED ($p = 0.0184$), and total SED ($p = 0.0064$) were significantly higher at 0.5 strain/s than 0.005 strain/s (Figure 2, Table 3). Modulus ($p = 0.9664$) and failure strain ($p = 0.3246$) were not significantly different between loading rates (Figure 2, Table 3). It should be noted that several material properties were not normally distributed (Table A2). For those variables, the Wilcoxon signed-rank test was used.

Table 3: Statistical analysis for the effect of loading rate on tensile material properties.

Material Property Variable	Paired t-test		Wilcoxon Signed Rank Test	
	t	p-value	S	p-value
Modulus	0.042	0.9664	42	0.7284
Yield Stress	-5.328	**<0.0001**	-532	**<0.0001**
Yield Strain	-7.404	**<0.0001**	-644	**<0.0001**
Failure Stress*	-6.770	<0.0001	-619	**<0.0001**
Failure Strain*	-0.994	0.3246	-136	0.2582
Ultimate Stress*	-6.270	<0.0001	-592	**<0.0001**
Elastic SED	-2.436	**<0.0001**	-278	**<0.0001**
Plastic SED*	-6.717	0.0182	-625	**0.0184**
Total SED*	-2.876	0.0057	-319	**0.0064**

Notes: An asterisk (*) indicates a parameter that was not normally distributed and that the Wilcoxon Signed Rank Test should be used. Bold text indicates a significant p-value for the appropriate statistical test.

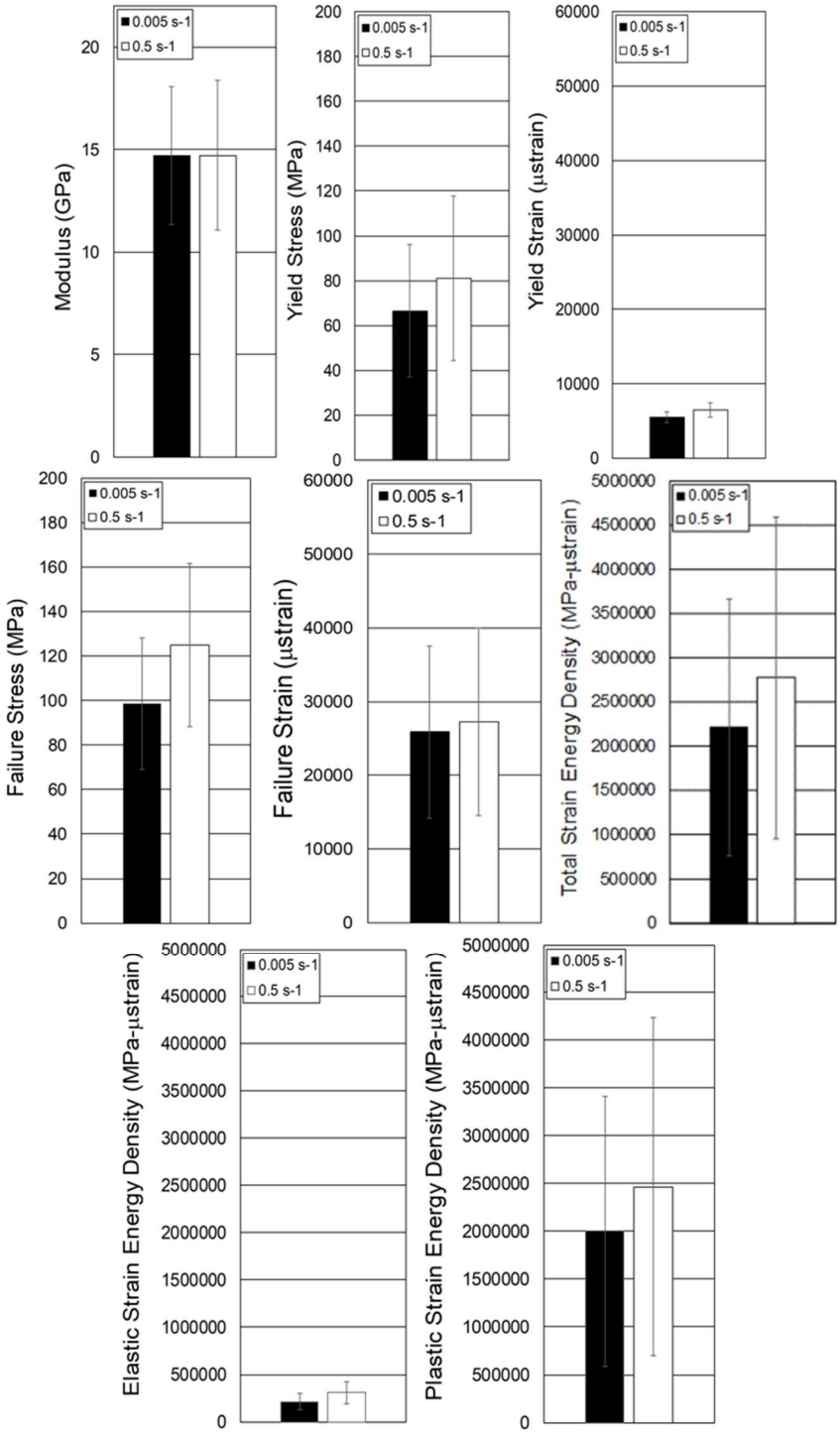

Figure 2: Average tensile material property values for each loading rate with ± 1 S.D. indicated by error bars.

For both the 0.005 strain/s and 0.5 strain/s tests, a number of material properties had significant negative correlations with respect to age (Table 4). Yield stress, failure stress, ultimate stress, failure strain, elastic SED, plastic SED, and total SED all decreased significantly with increasing age at both loading rates (Figure 4, Figures 6 – 10). Yield strain had a significant negative correlation with age at 0.005 strain/s, but not at 0.5 strain/s (Figure 5). Modulus had a significant negative correlation with age at 0.5 strain/s, but not at 0.005 strain/s (Figure 3). At both loading rates, the R^2 values were the highest for total SED and plastic SED. Conversely, the R^2 values were lowest for modulus, yield strain, elastic SED, and yield stress. The R^2 values for plastic versus elastic SED illustrate that the plastic SED accounted for 55 - 61% of the variance in material properties with respect to age, while elastic SED accounted for only 18 - 19%. The characteristic average stress-strain curves for each decade of life for each loading rate are shown in Figure 11. Individual stress-strain curves are plotted with the respective characteristic average curves in the Appendix (Figures A3 – A11).

Table 4: Spearman's rank correlation analysis for the effect of age on tensile material properties.

Material Property Variable	0.005 strain/s tests				0.5 strain/s tests		
	ρ	**R^2**	**p-value**		**ρ**	**R^2**	**p-value**
Modulus	-0.188	0.041	0.1569		-0.445	0.241	**0.0005**
Yield Stress	-0.389	0.145	**0.0025**		-0.462	0.237	**0.0003**
Yield Strain	-0.527	0.226	**<.0001**		-0.197	0.041	0.1375
Failure Stress	-0.594	0.358	**<.0001**		-0.785	**0.556**	**<.0001**
Failure Strain	-0.703	**0.527**	**<.0001**		-0.697	**0.490**	**<.0001**
Ultimate Stress	-0.624	0.397	**<.0001**		-0.787	**0.559**	**<.0001**
Elastic SED	-0.451	0.178	**0.0004**		-0.424	0.194	**0.0009**
Plastic SED	-0.744	**0.547**	**<.0001**		-0.791	**0.611**	**<.0001**
Total SED	-0.745	**0.551**	**<.0001**		-0.792	**0.623**	**<.0001**

Notes: Bold text indicates a significant p-value or an R^2 value ≥ 0.49.

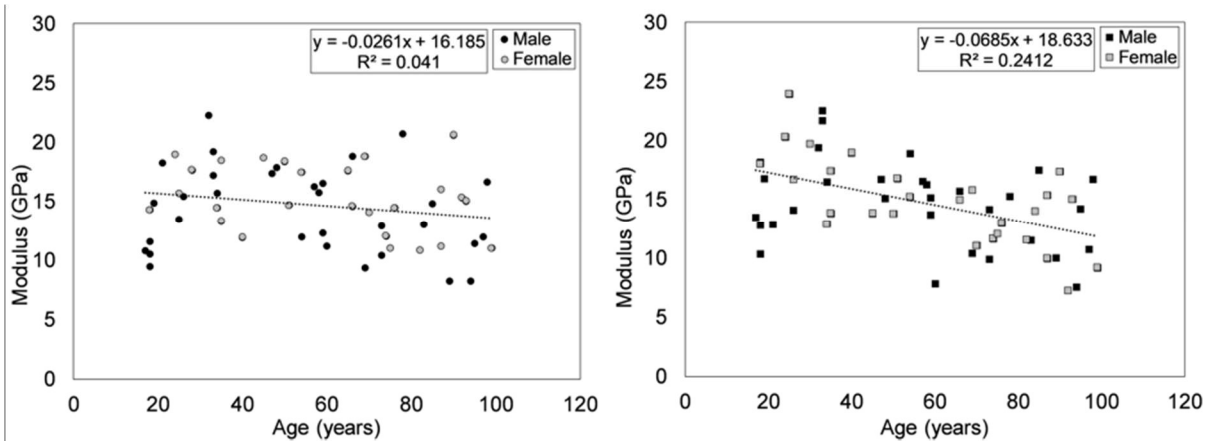

Figure 3: Modulus versus age at 0.005 strain/s (left) and 0.5 strain/s (right) in tension.

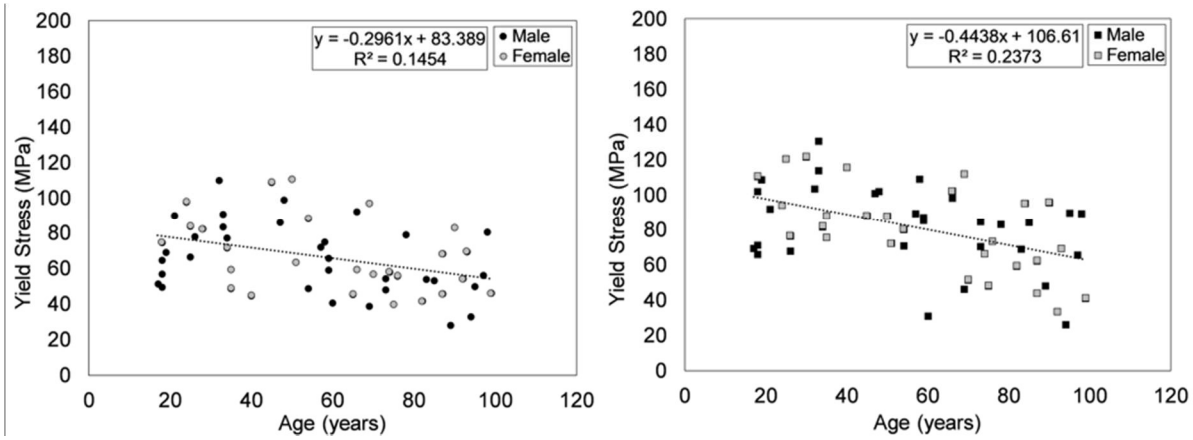

Figure 4: Yield stress versus age at 0.005 strain/s (left) and 0.5 strain/s (right) in tension.

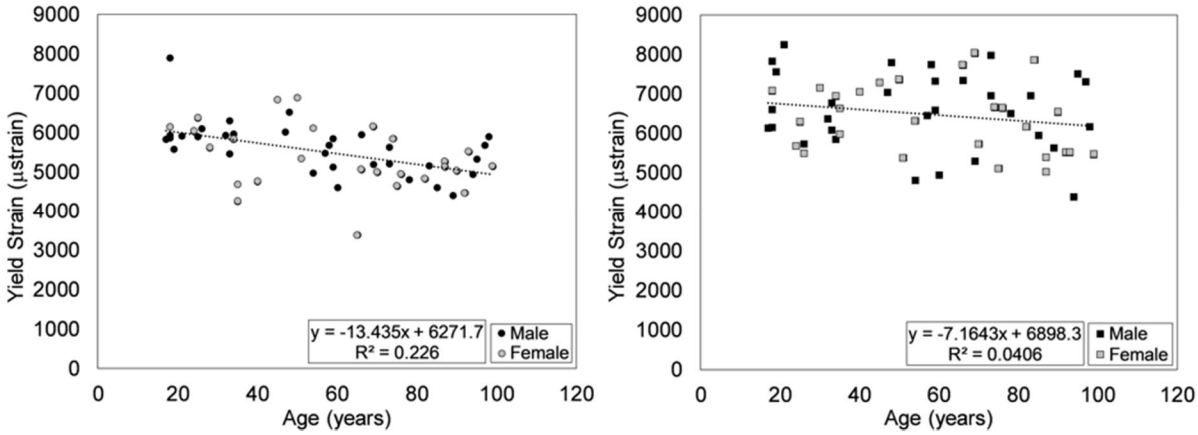

Figure 5: Yield strain versus age at 0.005 strain/s (left) and 0.5 strain/s (right) in tension.

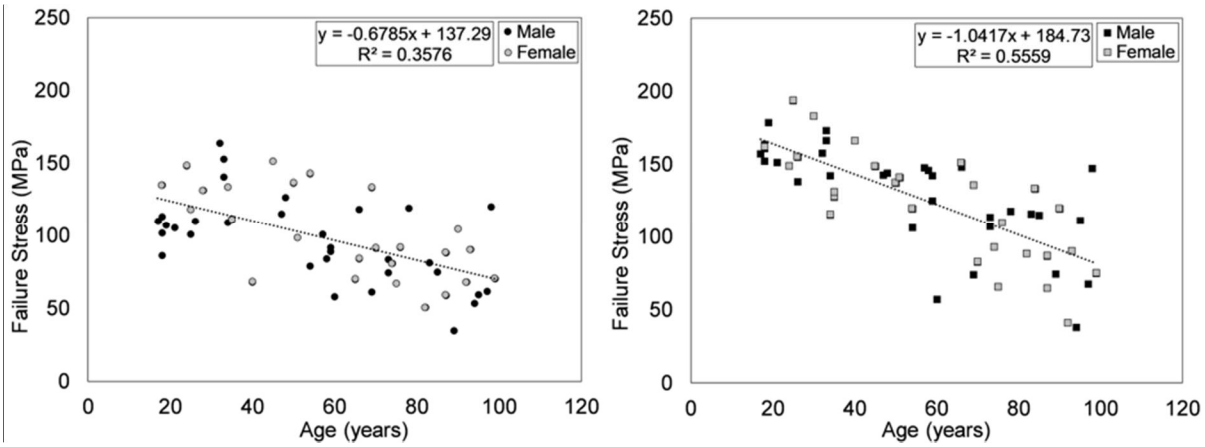

Figure 6: Failure stress versus age at 0.005 strain/s (left) and 0.5 strain/s (right) in tension.

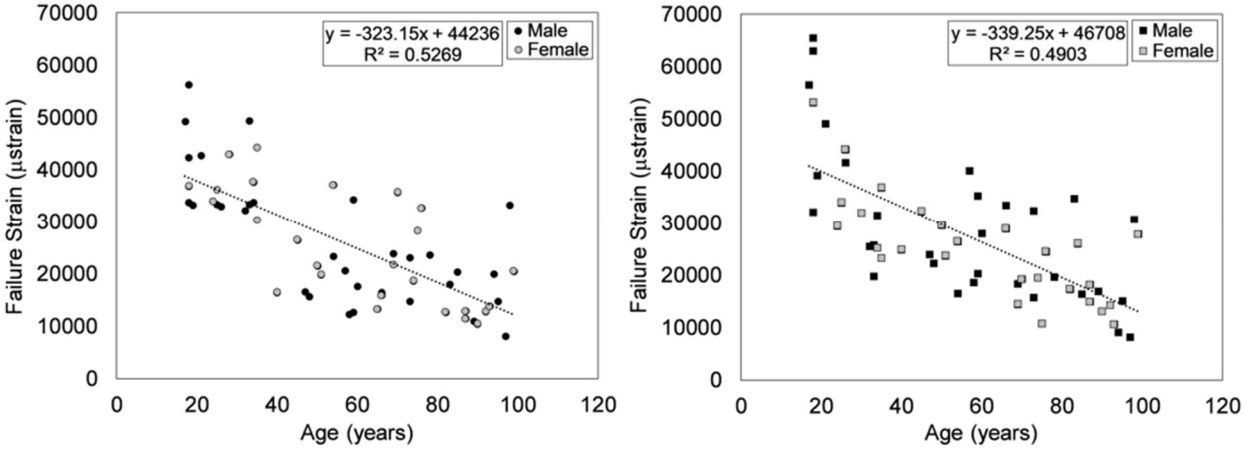

Figure 7: Failure strain versus age at 0.005 strain/s (left) and 0.5 strain/s (right) in tension.

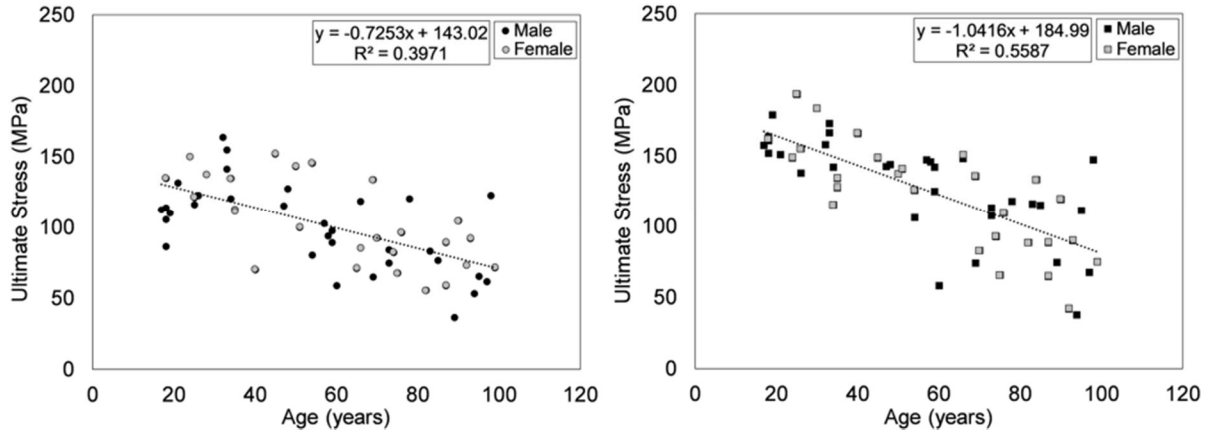

Figure 8: Ultimate stress versus age at 0.005 strain/s (left) and 0.5 strain/s (right) in tension.

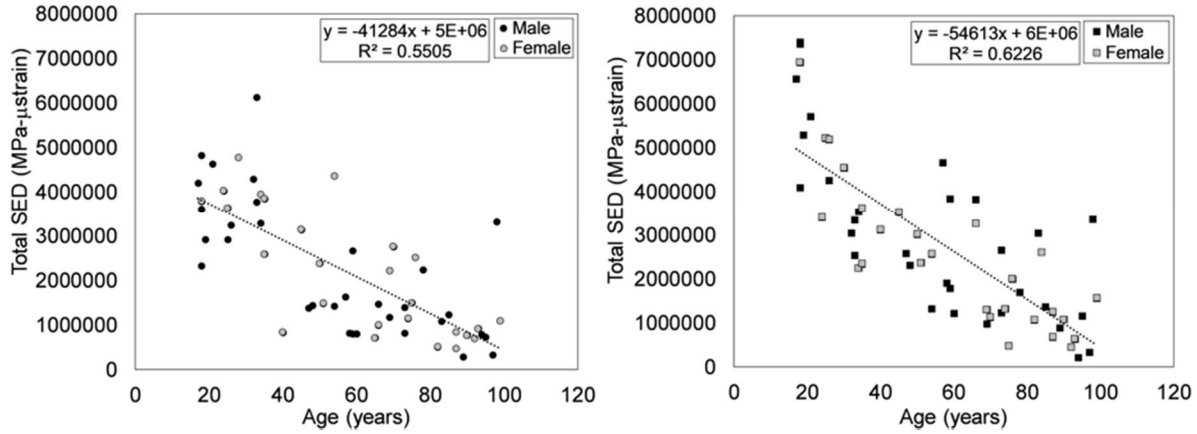

Figure 9: Total strain energy density versus age at 0.005 strain/s (left) and 0.5 strain/s (right) in tension.

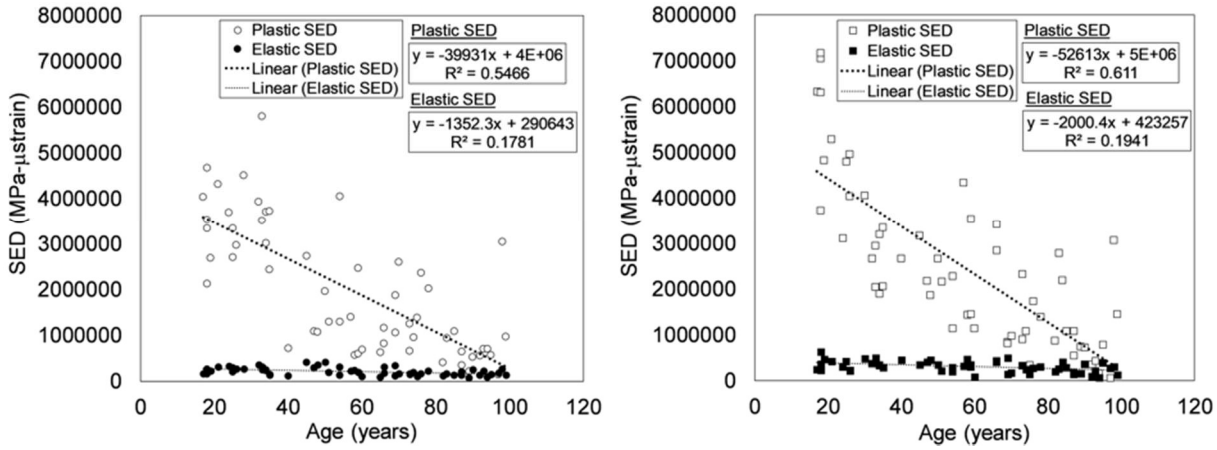

Figure 10: Tensile plastic and elastic strain energy density versus age at 0.005 strain/s (left) and 0.5 strain/s (right).

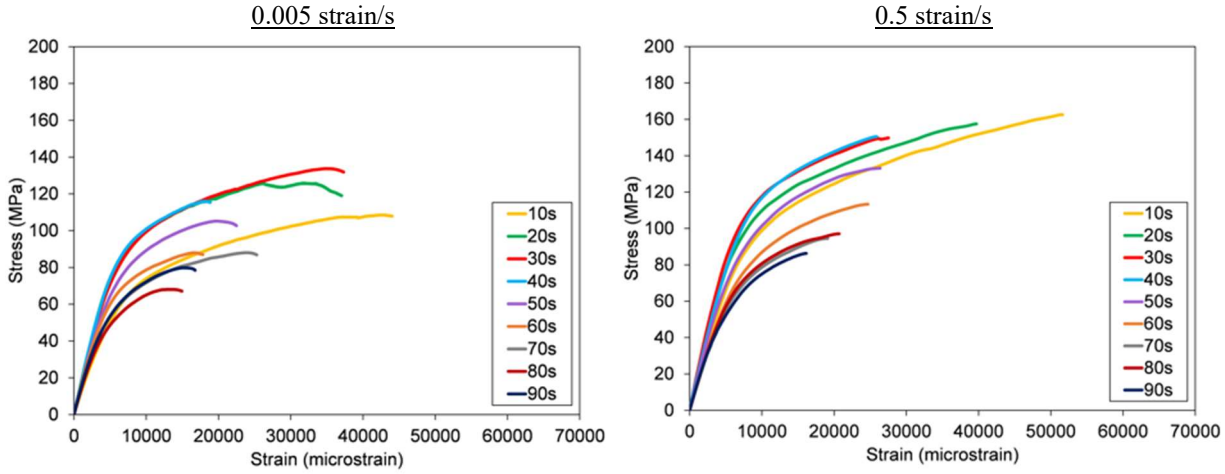

Figure 11: Characteristic average stress versus strain curves for each decade of life for 0.005 strain/s (left) and 0.5 strain/s (right) tests.

Discussion

In regard to the effects of loading rate on the material response of human rib cortical bone, the results of the current study were consistent with previous research performed at similar loading rates. The current study found that the yield stress, yield strain, failure stress, ultimate stress, elastic SED, plastic SED, and total SED were all significantly higher at 0.5 strain/s than 0.005 strain/s, while there was no significant difference in the modulus or failure strain between loading rates. This is fairly consistent with the trends reported by McElhaney (1966), who tested embalmed human femoral cortical bone in compression at strain rates ranging from 0.001 to 1500 strain/s. From the lowest to highest loading rates, McElhaney (1966) reported considerable increases in the ultimate stress and modulus and a considerable decrease in the maximum strain with increased loading rate. At the lower end of the loading rate spectrum, increases in ultimate stress and energy absorption were reported from 0.001 strain/s to 0.1 strain/s, which are the same trends seen in the current study between 0.005 strain/s and 0.5 strain/s. In regard to ultimate strain, McElhaney (1966) reported that ultimate strain decreased when the loading rate increased from 1 strain/s to 1500 strain/s, but observed a slight increase in ultimate strain from 0.001 strain/s to 0.1 strain/s. This slight increase in ultimate strain was also observed in the current study from 0.005 strain/s to 0.5 strain/s. Although the tests conducted by McElhaney (1966) were performed in compression, similar trends in material properties with respect to loading rate were quantified in bovine tibial cortical bone coupons in tension by Crowninshield and Pope (1974) [31]. Crowninshield and Pope (1974) tested samples at several loading rates ranging from 0.001 strain/s to 1000 strain/s and found that the yield stress and ultimate stress significantly increased with an increase in strain rate, while ultimate strain decreased with an increase in strain rate. Crowninshield and Pope (1974) also reported that modulus was not greatly affected by strain rate and that the ultimate strain had the greatest scatter of any quantity measured in that study. In regard to the energy absorption to failure, it is important to note that the data from McElhaney (1966) and Crowninshield and Pope (1974) both show that energy absorption increases slightly from 0.001 strain/s to ~0.1 strain/s before transitioning to a distinct steady decrease in energy absorption with increased loading rate [28, 31, 59]. The increase in SED up to ~ 0.1 strain/sec is consistent with the current study, which showed a significant increase in SED from 0.005 strain/s to 0.5 strain/s. Lastly, Currey *et al.* (1975) performed tensile tests on bovine femoral bone at several loading rates ranging from 0.0001 strain/s to 0.16 strain/s [60]. The study reported a significant increase in modulus, yield stress,

yield strain, and ultimate stress with increased loading rate, which are all consistent with the current study with the exception of modulus. Although the differences in the modulus and ultimate strain between the two low-range strain rates evaluated in the current study were not significant, the results showed significant differences in the yield stress/strain, ultimate stress, and energy absorption that were also seen in previous studies. In regard to the yield stress/strain, it is important to note that although the method for determining the yield point, i.e., the end of the elastic region, is well defined in the literature, it is an approximation. Differences in the shape of the curve in this transition region due to rate effects can affect the calculated yield point. It is also possible that the elastic energy increased at the higher loading rate due to the viscosity. Overall, the results of the current study illustrate that FEMs should implement rate dependence for yield stress/strain, ultimate stress, and strain energy density in order to validate the response of the thorax at multiple loading rates. However, additional strain rates need to be evaluated to fully characterize the viscoelastic properties of rib cortical bone.

No significant correlations were found when assessing the effect of sex on the material properties of rib cortical bone in the current study. While Kemper *et al.* (2005) found that male rib cortical bone had significantly higher ultimate strain and significantly lower modulus than female rib cortical bone, the subject size was limited to only 3 males and 3 females, and the females were older on average than the males. Previous studies that analyzed humeral, tibial, and femoral cortical bone tensile material properties with large subject sizes observed conflicting results. No significant differences between sexes were found in Lindahl and Lindgren (1967) or Burstein *et al.* (1976). [23, 24]. A more recent study reported a significantly higher tensile strength of human femoral cortical bone in males than in females [61]. Conversely, McCalden *et al.* (1993) reported that female cortical bone experienced greater ultimate stress than male cortical bone, even after accounting for differences in porosity [22]. The findings of some of these studies seem to contradict what is known about the effects of sex and aging on material properties. Several studies have shown that the bone mineral density (BMD) of cortical bone decreases more rapidly with advancing age in females than in males, and that decreases in BMD are correlated with a decrease in ultimate stress and modulus [22, 62, 63]. Therefore, one would expect to find significantly lower ultimate tensile stress and modulus values for females compared to males, especially for older subjects. While this trend may exist across the entire human population, a large degree of inter-subject variation in material properties also exists per study. Given the random sampling of the

population used in the current study and previous studies, inter-subject variation could unintentionally skew the results. It is possible that more male and female samples would be needed per decade to detect differences between sexes, if such differences exist. Additionally, a significant amount of bone loss in ribs is due to endocortical loss, i.e., expansion of the medullary cavity, including the complex process of trabecularization of the cortex [64, 65]. As a result, observation of intracortical porosity as the cortex disappears is limited, and the effects of differential bone loss due to this mechanism may not be seen from purely cortical coupon testing. In other words, sex differences may be more attributed to geometric changes rather than material changes. Agnew *et al.* (2018) found sex differences in almost all rib structural bending properties, likely reflecting these morphometric changes to rib geometry. Future work should further explore these explanations.

The results of the current study were consistent with the findings of previous studies that have quantified the tensile material response of rib cortical bone at 0.5 strain/s. Kemper *et al.* (2005) reported that the ultimate stress, ultimate strain, and total SED all significantly decrease with advanced age, while the modulus increases. However, the data was limited to only 6 subjects (Avg. age = 50.2 yrs.), which also included one 18 year old. The removal of that subject resulted in no correlation between modulus and age for a 5 subject sample size (Avg. age = 56.6 yrs.). In order to compare the current data to previous studies that used the same methodology, material properties from Kemper *et al.* (2005) and Kemper *et al.* (2007) were plotted with the current results (Figure 12). Kemper *et al.* (2005) tested 19 coupons per subject and Kemper *et al.* (2007) tested 8 coupons per subject. Therefore, the material properties were averaged per subject to obtain a single data point. The scatter plots of the combined data show that the values are consistent between studies for a given age and that the trends with respect to increased age are similar. While the R^2 values of the linear trend line from the combined data slightly decreased, the correlations remained the same. Similar trends were observed in material property data with advanced age in the 0.005 strain/s tests. Specifically, all material properties except modulus significantly decreased with increasing age at 0.005 strain/s. While there was a significant decrease in modulus with increased age at 0.5 strain/s, the R^2 value for modulus at 0.5 strain/s was only 0.241, indicating a weak correlation. Previous studies also reported weak trends or no significant correlations between modulus and age [14, 22, 24]. Overall, these results illustrated that the testing procedures for tensile

coupons of rib cortical bone used in this study produced consistent results and trends with age at multiple loading rates.

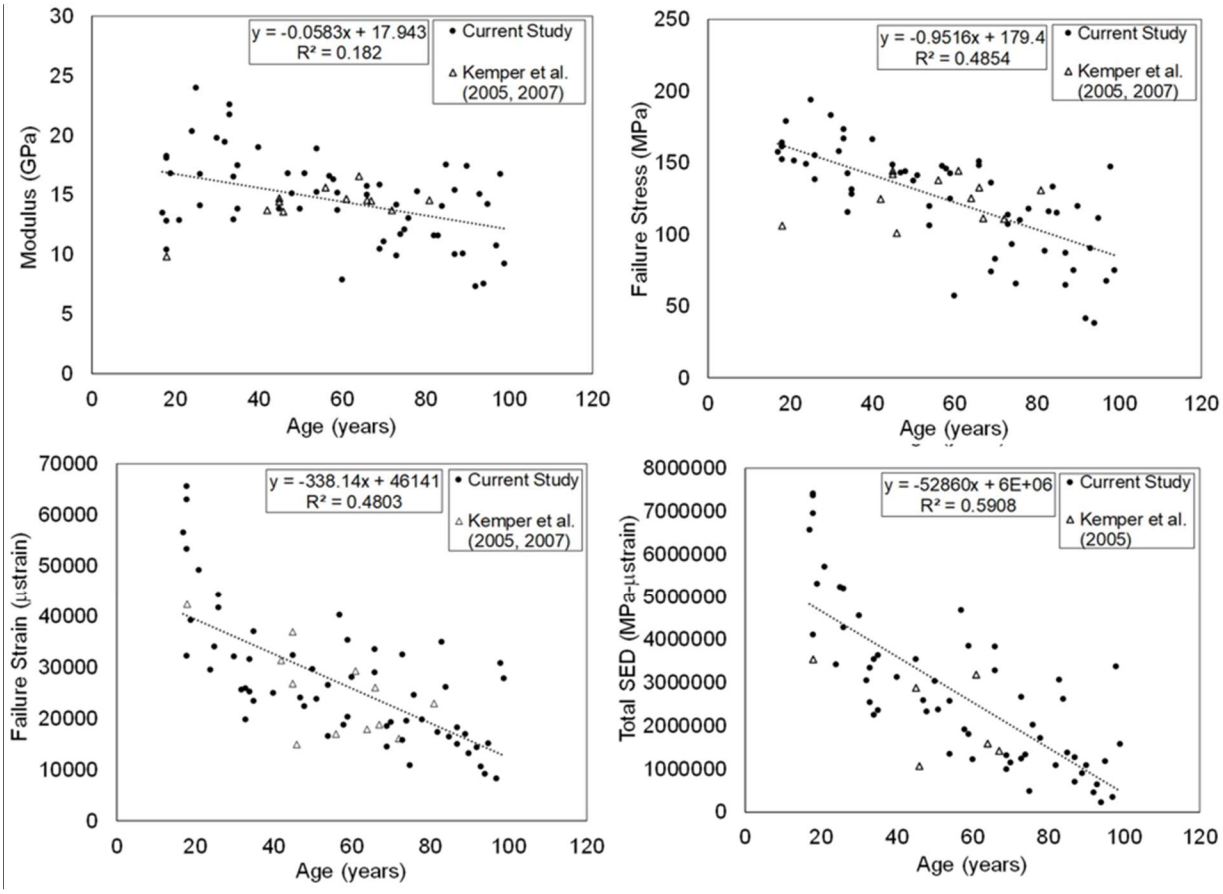

Figure 12: Comparison of modulus (top left), failure stress (top right), failure strain (bottom left), and total SED (bottom right) values to the data reported by Kemper *et al.* (2005, 2007).
Notes: Trend lines are based on the combined data. Modulus was calculated slightly differently by Kemper *et al.* (2005, 2007).

In regard to the design and statistical power of the age analysis in the current study, the target sample size for this study was determined based on previous studies [22, 23]. The correlations between age and femoral cortical bone material properties from McCalden et al. (1993) were analyzed to select desired effect sizes of 0.8 and 0.35, i.e., the highest and second lowest correlation coefficients that were significant, for the Pearson correlation coefficient (r) for the current study. Then, a power analysis was performed in R 3.6.0 [66] using package pwr [67] with an alpha level of 0.05, a desired power of 0.8, and the stated effect size. This yielded target sample sizes of

approximately 9 and 61 subjects for the effect sizes of 0.8 and 0.35, respectively. The current study had the additional goals of achieving an approximately balanced number of subjects per decade and more subjects per decade than in previous studies on human cortical bone (1 to 11 subjects per decade; Avg. = 4.0-5.1) (Table A3) [22, 23]. As stated in the results, the number of successfully tested subjects in the current study were 58 at 0.005 strain/s (4-8 subjects/decade; Avg. = 6.4 subjects/decade) and 58 at 0.5 strain/s (4-8 subjects/decade; Avg. = 6.4 subjects/decade). When combined with the data from Kemper et al. (2005, 2007) the analysis for the 0.5 strain/s tests included 70 subjects (5-9 subjects/decade; Avg. = 7.8 subjects/decade).

The design of the study and the number of subjects have important implications on the interpretation of the p-values from the age correlation analysis. In this analysis, the number of subjects and the correlation coefficient alone determine the p-value for a given material property. Therefore, any correlation coefficients above the desired effect size (~0.35), will have a p-value below 0.05, i.e., a significant p-value given an alpha level of 0.05. In fact, several of the correlation analyses between age and material properties resulted in spearman correlation coefficients between 0.38 and 0.62, which were deemed statistically significant despite low R^2 values. However, it is important to note that significance does not indicate that the observed correlation with age is meaningful. Therefore, significance should be interpreted in conjunction with other metrics such as R^2 values to indicate whether the observed relationships between the material properties and age are biologically meaningful.

The trends with respect to age observed in the current study were comparable to those reported by previous studies on other skeletal elements. Previous studies that tested tibial and femoral cortical bone coupons found that yield stress and yield strain decreased with advanced age [22, 23]. Burstein *et al.* (1976) performed tensile tests on human tibial and femoral cortical bone from subjects aged 21 to 86 and reported that ultimate strain and energy absorption also had significant negative correlations with age, which agrees with the data from the current study. Lindahl and Lindgren (1967) performed tensile tests on human tibial and femoral cortical bone samples from subjects aged 15 to 89 and found that ultimate tensile stress and ultimate tensile strain decreased with age, while modulus showed no change [24]. Lastly, McCalden *et al.* (1993) performed tensile tests on human femora from subjects aged 20 to 102 and found that ultimate strain and energy

absorption decreased with age while modulus did not, which also agrees with the data from the current study.

Several previous studies have attributed the decreases in material properties with advanced age to reduced post-yield deformation experienced by the samples [22, 23]. Among all the material properties evaluated in the current study, total SED and plastic SED had the strongest correlations with age, suggesting samples from younger subjects were more ductile and samples from older subjects were more brittle. The percent change between the average value for the youngest subjects (10 – 19 yrs.) and the oldest subjects (90 – 99 yrs.) was -70% at 0.005 strain/s and -82% at 0.5 strain/s for total SED and -73% and -85% for plastic SED. In addition, the high R^2 values indicate that the total and plastic SED explained a large portion of the variance with respect to age (Figure 9 and Figure 10). Conversely, the low R^2 values at each loading rate for elastic SED show that elastic SED explained a very small portion of the variance, and the percent change between the average values for the youngest subjects and the oldest subjects was much smaller (-15% and -38%) (Figure 10). Similar trends were seen by McCalden *et al.* (1993), who reported that the plastic energy of femoral cortical bone in tension significantly decreased with age, but the elastic energy did not [22]. The relationship between the plastic/yield strain and age reported in the current study showed the same relationship as plastic/elastic SED and age (Figure 13). Specifically, plastic strain had much higher R^2 values (0.51 and 0.49) and percent changes between the average values for the youngest subjects and the oldest subjects (-68% and -77%) than yield strain ($R^2 = 0.22$ and 0.04, % change = -15% and -12%). The relationship between the plastic stress and age ($R^2 = 0.42$ and 0.62, % change = -59% and -79%) versus yield stress and age ($R^2 = 0.15$ and 0.24, % change = -3% and -27%) was similar to that seen for plastic/yield strain and age, but less pronounced (Figure 14). Overall, these data clearly show that post-yield behavior is driving the correlation between total SED and age.

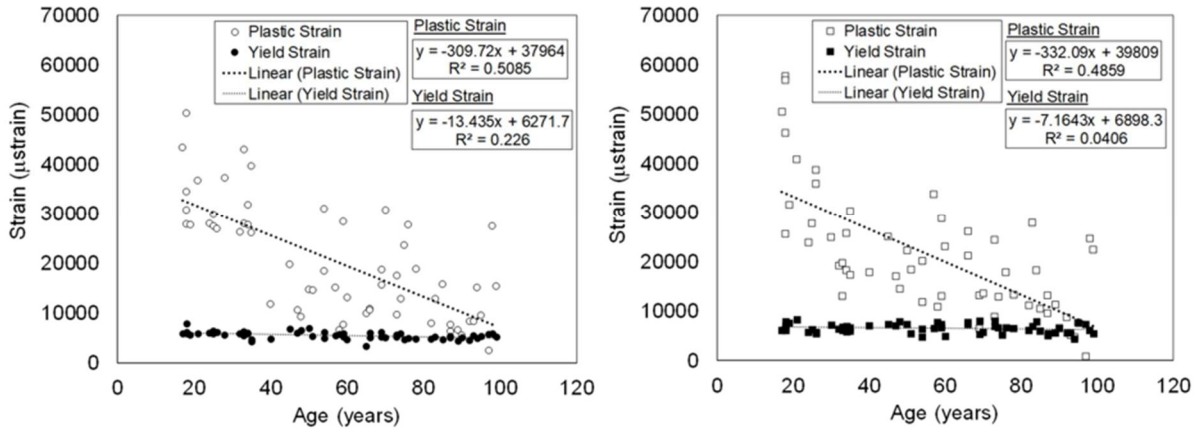

Figure 13: Plastic and yield strain versus age at 0.005 strain/s (left) and 0.5 strain/s (right).

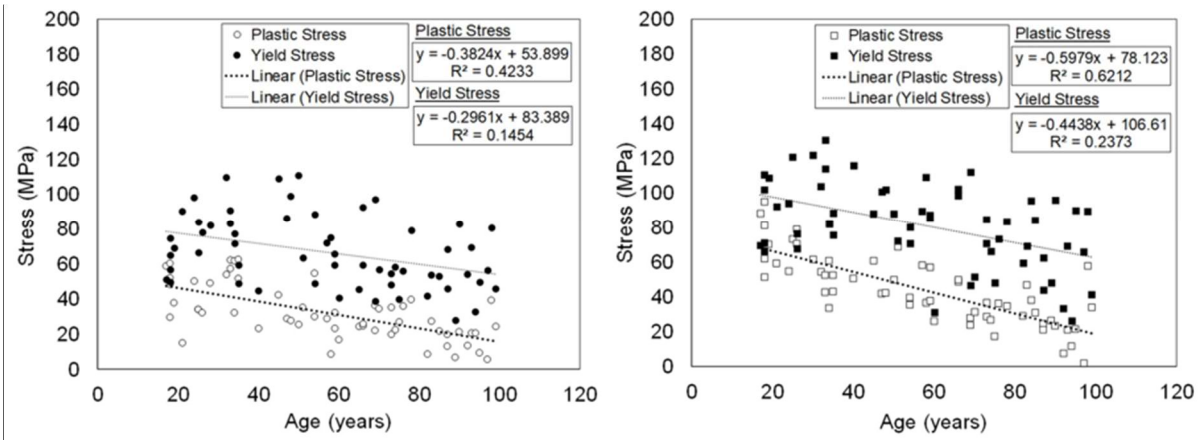

Figure 14: Plastic and yield stress versus age at 0.005 strain/s (left) and 0.5 strain/s (right).

The degree of the plasticity of bone in tension is often attributed to the ductility of collagen, the dominant protein in bone. Collagen's ability to absorb energy in tensile loading is crucial to preventing catastrophic bone fractures, unlike the inorganic materials in bone, e.g., hydroxyapatite, which provide stiffness and strength in compression. It has been shown that the collagen network in cortical bone experiences a 50% decrease in energy absorption during aging due to an increase in the percentage of denatured collagen [68]. During plastic strain, the relative motion of mineralized collagen fibrils is resisted by the interfibrillar matrix of non-collagenous proteins [69]. Therefore, the relationship between the relative percentage of non-collagenous molecules in the interfibrillar matrix of cortical bone and the resistance to plastic strain should potentially be investigated. Overall, further investigation into how the material properties of the rib cortex change in regard to bone composition at a microstructural level may result in a better understanding of

why thoracic fracture risk increases with advanced age, since advancing chronological age is not truly a biological mechanism of change.

While there were significant correlations between several material properties and age, the R^2 values and linear trend line slopes were relatively low for some variables (Table 4). As seen in Figure 7 (right), a total of 7 subjects aged ≤35 years old had a lower total SED than three different subjects between 60 and 69 years old at 0.5 strain/s. This implies that, while chronological age is the simplest and most easily obtainable variable to evaluate, there are likely underlying variables that may better account for the reported decreases in material properties. As mentioned previously, collagen degradation could have negative effects on the material properties of cortical bone and should be studied in conjunction with human rib material property research [60, 70]. A decrease in bone mineral density (BMD), i.e., the relative volume of the bone versus porous space, has also been shown to have significant negative correlations with cortical bone material properties [22, 53, 71]. Kemper *et al.* (2005) reported that a decrease in cortical bone BMD correlated with a significant decrease in the ultimate tensile strain of rib cortical bone [25]. In addition, an increase in cortical porosity has been reported to be a key anatomical change responsible for fractures in elderly subjects [72]. For example, McCalden *et al.* (1993) reported that as porosity increases, the ultimate stress of human femoral cortical bone decreases [22]. However, due to a lack of studies evaluating the microstructure and local BMD of rib cortical bone, the effects of microstructure and local BMD on the material and structural response of rib cortical bone are still not fully understood. Additionally, several of these underlying variables may also be linked with age, confounding the relationship between histological characteristics and material properties. Therefore, future research should investigate the effects of cortical bone mineralization, local BMD, and microstructure on tensile material properties of rib cortical bone in order to better understand the underlying variables associated with increased fracture risk.

It is important to note that the material response of cortical bone can vary between bones due to differences in the micro-architecture. Burstein *et al.* (1976) reported that the ultimate strain and energy of tibial cortical bone decrease significantly with age, while ultimate stress, ultimate strain, elastic modulus, and energy significantly decrease with age for femoral cortical bone. Burstein *et al.* (1976) attributed the differences between the tibial and femoral specimens to differences at the tissue and structural level, which vary based on the normal loading conditions that different bones

are subjected to during life. Due to the fact that the ribs withstand different types of loading in everyday life than the femur, tibia, or fibula, and bone is known to remodel in response to the forces/stresses that are placed upon it, the microstructure of the ribs is likely inherently different than the long bones in the lower extremity. Consequently, the magnitudes of the material properties for rib cortical bone are likely different as well. This difference is illustrated when comparing trends in ultimate stress and ultimate strain with respect to age between different studies (Figure 15). It is important to note that McCalden et al. (1993) performed tests at 0.03 strain/s, and Burstein et al. (1976) performed tests at 0.05 strain/s. Therefore, Figure 15 does not provide a direct comparison since the loading rates for these previous studies were between the rates used in the current study. With that in mind, Figure 15 shows that the values and trends for ultimate stress and strain vary between studies due to either differences in bone type or subject pool. Despite these differences in material property values and trends with age, the material values obtained in the current study were comparable to the previous studies even though the thicknesses of the rib cortical bone coupons (0.2286 to 0.4318 mm) were considerably smaller than the 2 mm sample thicknesses used by both Burstein et al. (1976) and McCalden et al. (1993). In addition, there were no significant correlations between sample thickness and age in the current study (Figure A12). Finally, a two-factor ANVOA showed that no material properties varied significantly with either thickness or the interaction between age and thickness (Table A4). The comparisons to previous studies along with the statistical analyses pertaining to sample thickness indicate that the sample thicknesses used in the current study should be large enough to meet the continuum assumption, and that the variation in the material properties was not related to the specimen size. Overall, while the trends in material properties with respect to age for the tibia and femur agree with the trends in the current study, the material property values from rib cortical bone testing should be used to model the material response of the thorax. Future work should be conducted to quantify rib histomorphometry and focus on relationships between osteon population density, osteon size, and other microstructural parameters with the rib material properties reported here.

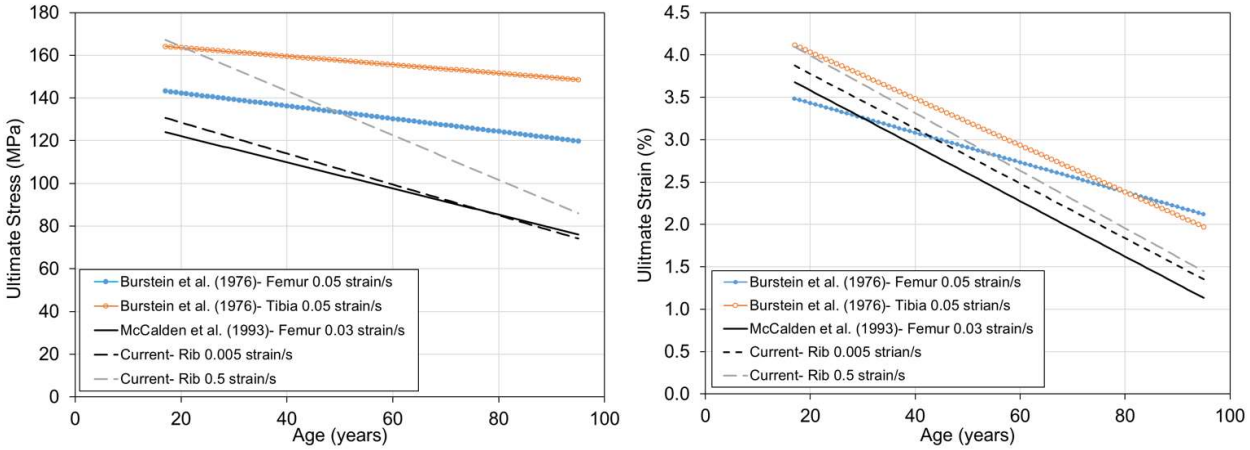

Figure 15: Comparison of trends in ultimate stress (left) and ultimate strain (right) versus age between different studies.

Finite element models have been increasingly valuable in the automotive industry due to their ability to virtually analyze the response and injury risk of a vehicle occupant during MVCs. The cost and time needed to simulate a MVC using a model is much lower than physical crash testing. As a result, more loading conditions can be analyzed faster and cheaper with the use of FEMs. Several researchers have leveraged this unique advantage of FEMs to perform parametric studies aimed at assessing the relative effects of age and/or sex related changes in the geometric or material properties on the structural response of the thorax [36-38]. These studies reported that the age dependence of both material and geometric properties affects the response and predicted injury risk of the model. However, the conclusions regarding the relative effects of these properties varies between studies. Kent et al. (2005) varied the angle of the ribs, cortical thickness, and material properties to simulate "young" and "old" occupants, and reported that the "structural and material changes played approximately equal roles in modulating the force deflection response of the thorax." Conversely, the changes in the material properties were reported to play the largest role in the injury tolerance of the chest, which was assessed using predicted rib fractures. Schoell et al. (2015) varied the material properties and the 3-dimensional shape of the thorax to simulate a 30 year old male and a 70 year old female subject, but did not vary the cortical thickness. This study reported that while differences across age and sex were observed due to changes in geometry, material properties, and a combination of both, changing only the material properties had very little effect on the peak force, compression, or number of rib fractures. However, the results of these FEM studies must be regarded with a certain degree of caution, since the global responses of the different models were not validated against matched tests performed on PMHS of the same

age, sex, height, and weight. In addition, FEMs of both the whole body and isolated ribs have both demonstrated a limited ability to accurately predict the number, location, and/or timing of rib fractures deterministically [36, 39-41]. Overall, the differences in biomechanical response, e.g., force versus deflection and/or fracture prediction, between rib FEM simulations and experimental data have been attributed to simplified geometry, simplified material properties, or both.

Although FEMs are invaluable tools that can be used to provide insight into injury mechanisms and the factors that affect them, the response and accuracy of these models is dependent on the data used to develop and validate them. The thin cortical shell of the ribs makes it extremely difficult and time consuming to obtain accurate cross-sectional geometry measurements of the ribs. If the resolution of the equipment/methodology used to quantify the thickness of the cortical shell is not high enough, then extremely thin and/or porous regions of the rib, which can act as stress concentrations/risers, will be overestimated. This can result in errors in the estimation of the biomechanical response and/or fracture prediction. In addition, due to the fact that accounting for the anisotropic, asymmetric, age-dependent, viscoelastic behavior of cortical bone is relatively challenging, many FEMs use simplified material models (non-rate dependent, isotropic, elastic-plastic) when modeling rib cortical bone [36, 43]. To date, FEM studies that have implemented tensile material properties from human rib cortical bone have been limited the use of data from Kemper et al. (2005, 2007), which only provides material data for small number of primarily male subjects at a single loading rate [36, 39, 43]. The results of the current study help fill this gap in the literature by providing the necessary data to more accurately model and assess differences in the material response of the rib cage for nearly all vehicle occupants of driving age, as well as more accurately evaluate the relative effects of geometric and material variables. However, quantifying the changes in the material response with respect to age, sex, and loading rate is likely only part of the potential solution to improving the response and fracture prediction of rib FEMs. Given that gross and cross-sectional geometry have also been shown to be important factors in the structural response of the rib, substantial improvements in fracture predictions may not occur until both material properties and geometry can be accurately represented. Consequently, additional FEM and experimental studies should be performed to determine which geometric or material variables account for the majority of the variance in the structural properties of the ribs.

The current study has several limitations. While multiple samples were tested per subject in previous rib coupon studies [14, 25], only two samples were tested (one at each loading rate) per subject in the current study due to the limited material available. Obtaining more samples from each subject for each loading rate could have decreased the potential effects of intra-subject variation. An additional limitation is that the location of the sample on the rib was often different between the two loading rates. For several subjects, the coupon tested at 0.005 strain/s was taken from a different rib level, side, and/or location than the coupon tested at 0.5 strain/s. While the differences in the material properties with respect to rib side, rib level, and coupon location were assumed to be insignificant, some intra-subject variance could be captured by our data, potentially reducing or increasing the p-values for the statistical tests pertaining to the effects of loading rate and age. However, it should be noted that when two samples were tested from the same subject at the same loading rate (0.005 strain/s: Srb383, Srb244, Srb227, and Srb235; 0.005 strain/s: Xrb/Frb103), the material responses were similar, regardless of side, rib level, or location (designated as "(1)" and "(2)" in Figure A3, Figure A7- Figure A10). A quantitative comparison between matched samples showed that the average percent difference for yield stress, yield strain, failure stress, and failure strain was 11.2%, 18.2%, 16.3% and 14.8%, respectively. Another limitation was not accounting for the potential effect of porous areas in the geometric measurements of sample gage length. Samples were sanded to a constant thickness, but a minimum thickness was required for testing in order to clamp the coupon in place and prevent it from slipping. Consequently, porous areas were unavoidable for some of the coupons. Given that the outer dimensions of the gage length were measured with calipers to quantify area, the measured cortical area in a porous coupon would be higher than the true bone area. This would result in lower stress or modulus calculations. Additionally, all coupons were aligned with the main axis of the rib, since it has been shown that the principal strain on the rib corresponded to approximately the main axis of the rib during frontal shoulder belt loading [73]. Testing tension coupons in a different orientation relative to the long axis of the rib would likely result in lower material properties due to the anisotropic nature of cortical bone [31]. In future research, multiple samples should be taken at different orientations along the rib to evaluate this phenomenon. Lastly, the effects of BMD or other histological/morphometric variables with respect to age were not evaluated in the current study. As stated previously, these variables should be evaluated in future studies to better understand the underlying variables associated with increased fracture risk.

It should be noted that although eight subjects included in the analysis were 17-24 years of age, a linear fit was applied to all material property data with respect to age. Agnew et al. (2018) performed rib bending tests from 182 subjects ranging in age from 4 - 108 years (mean 53 ± 23 years) and noted a bilinear fit for stiffness, yield force, peak force, and energy with respect to age between pediatric subjects aged 4-21 years (n = 18) and adult subjects aged 22-108 years (n = 166) [54]. Stiffness, yield force, peak force, and energy showed significant positive relationships with respect to age for the pediatric group, but significant negative relationships with respect to age for the adult group. However, only peak force for the pediatric group and energy for both groups had trends with R^2 values large enough to be considered practically significant. In the current study, there were no obvious trends or apparent inflection points between pediatric and adult subjects for any of the material properties. The exclusion of subjects ≤21 years of age from the statistical analysis did not notably affect the correlations between tensile material properties and advanced age (Table A5, Figure A13 - Figure A20). The correlation for modulus versus increased age changed from statistically insignificant to statistically significant at 0.005 strain/s , but the R^2 value remained low ($R^2 = 0.169$). The significance in trends of material properties with respect to age at 0.5 strain/s did not change due to the exclusion of subjects aged ≤21 years. Additionally, the material property values for subjects ≤21 years were within the scatter surrounding the fit line for subjects >21 years for each material property, which was relatively consistent across all decades for a given property. However, there were only seven subjects (n=7) ≤ 21 years, and none less than 17 years. Skeletal maturity, which is measured by fusion of the epiphyseal plates, begins in childhood and is generally complete by 25 years of age [74, 75]. However, the complete fusion or union of the epiphyseal plates is highly variable depending on the individual's sex and genetics, environmental factors, and skeletal element [74-77]. While fusion is observed as early as 12-14 years of age for some skeletal elements, complete fusion of secondary ossification centers in the rib, specifically, can occur anytime between 17-25 years of age [78]. Given that no subjects in this sample were less than 17 years, it would be inappropriate to separate the sample into immature vs mature specimens since it is unknown if the bone is actually immature in these samples. Differences in the microstructure between immature and mature bone could result in differences in rib material and/or structural properties. However, cortical drift in the rib ceases around the age of 13 years [79], resulting in less variation in the age of the compacta after this point in development and a more consistent mean tissue age throughout the cortex that is generally

differentiated through remodeling, not modeling processes [80]. Although the ribs should be skeletally mature within 21 years of age for the majority of the population, it is possible that skeletal maturity could be reached sooner. Given these factors and the degree of scatter observed within a given decade, a considerably larger group of younger subjects (0-21yrs) and histological analysis would be needed to evaluate the effects of skeletal development on the material properties of rib cortical bone, both of which are outside the scope of the current study.

Conclusions

The tensile material response of human rib cortical bone was quantified at two different loading rates over a wide range of subject demographics in this study. There were no significant differences in material properties between sexes and no significant differences in the interaction between age and sex. Several material properties were found to be significantly higher at 0.5 strain/s than at 0.005 strain/s, including yield stress, yield strain, failure stress, ultimate stress, and plastic, elastic, and total SED. This supports the hypothesis that the material response of rib cortical bone is rate dependent. However, additional strain rates need to be evaluated to fully characterize the viscoelastic properties of rib cortical bone. Trends in material properties with respect to increasing age were congruent with the results of previous studies. Yield stress, failure stress, ultimate stress, failure strain, elastic SED, plastic SED, and total SED all decreased significantly with increased age at both 0.005 strain/s and 0.5 strain/s. The R^2 values were highest for total and plastic SED with respect to age at both loading rates. The corresponding trends in plastic stress and strain and the lack of trends in yield stress and strain with age indicate that post-yield behavior drove the correlation between SED and age. These results also provide data for a larger age range than previous studies, which supports the goal of FE modelers to develop models across the full age spectrum. However, the R^2 values for material properties with respect to age only ranged from 0.15 - 0.62, indicating that there may be other underlying variables that better explain the variance within a given population. Overall, this is the first study to evaluate the material properties of human ribs at multiple loading rates over a large range of subject demographics. Additionally, this study provides the necessary data to more accurately model and assess differences in the material response of the rib cage for nearly all vehicle occupants of driving age.

CHAPTER 3: EFFECTS OF SEX, LOADING RATE, AND AGE ON THE COMPRESSIVE MATERIAL PROPERTIES OF HUMAN RIB CORTICAL BONE

Introduction

While rib fractures commonly occur on the cutaneous surface of the antero-lateral portion of the rib due to tensile loading in a frontal loading condition experienced in an MVC, fractures that occur on the pleural surface of the lateral-posterior portion of the rib during frontal loading can be due to compressive loading. Additionally, in a side impact loading condition, the cutaneous surface of the antero-lateral portion of the rib is placed in compression, while the pleural surface of the lateral-posterior portion of the rib is placed in compression as the rib as bent against the radius of curvature. Currently, the only data available to model the material response of rib cortical bone have been obtained from dog-bone coupons tested in tension [14, 25, 26, 45]. Studies have shown that cortical bone behaves differently depending on the mode of loading, i.e., tension versus compression. Several studies that have tested bovine and human femoral and tibial cortical bone samples reported that the yield stress, yield strain, and failure stress were all higher in compression than in tension [81, 82]. Given that bone is known to remodel in response to the forces/stresses it is subjected to and that the ribs withstand different types of loading in everyday life than the femur and tibia, the microstructure and material properties of the ribs are likely inherently different than the long bones in the lower extremity. Therefore, the goals of the current study were to develop novel methods to fabricate and test cylindrical samples of human rib cortical bone in order to quantify the compressive material properties over a wide age range, evaluate differences in the material response with respect to sex, age, and loading rate, and compare the compressive material response to the tensile material response of rib cortical bone across all decades of life.

Methods

Thirty (n = 30) subjects (M = 19, F = 11) ranging from 18 to 95 years of age (Avg. = 49.0 ± 23.9 yrs.) were used in the compression testing portion of this study. It should be noted that tension coupons were also obtained and tested for these subjects (See Chapter 2). Thirty (n = 30) compression samples were tested at 0.005 strain/s, and thirty (n = 30) compression samples were tested at 0.5 strain/s in the current study. Subject demographics including sex, age, height, and weight are included in Table A1.

All ribs used in this study were ethically obtained through the Body Donor Program at The Ohio State University and Lifeline of Ohio with no known bone disease reported. Whole ribs were excised from the body, wrapped in normal saline soaked gauze, stored in air-tight plastic bags, and frozen at -20 °C until testing [46-50]. Rib levels 5-7 were used to analyze the compressive material properties. The rib level and rib side (left/right) were selected at random; however, the rib level and rib side taken from each subject were occasionally limited by the tissue available. Based on the studies by Kemper *et al.* (2005, 2007), differences in material property data with respect to rib level were assumed to be insignificant [14, 25]. In addition, it was assumed there were no differences in material properties between the left and right ribs due to symmetry [10]. Due to the fact that the thickness of the cortical shell generally increases from the anterior to posterior region, all samples were taken from the lateral-posterior portion of the rib, but anterior of the angle of the rib to avoid changes in material properties associated with changes in microstructure. All compression samples were taken from the pleural side of the rib, which is the side of the rib most commonly placed in compression during a frontal loading condition.

A series of steps were taken to obtain two cylindrical compression samples from each subject. All specimens were kept hydrated with normal saline throughout each fabrication process. First, ribs were thawed and the soft tissue was removed. Then, a 1 cm longitudinal segment of the rib was cut using a low speed diamond saw (Model 650, South Bay Technology, San Clemente, CA). The segment was placed in a cylindrical bone chuck and secured with nylon tipped set screws such that the long axis of the rib was parallel with the end mill (Figure 16). The bone chuck was filled with saline and the top surface of the rib section was then milled flat using a Computer Numerical Control (CNC) mill (MAXNC 10, MAXNC Inc., Chandler, AZ). A cylindrical sample 1 mm in diameter and 4 to 5 mm in height was then milled from the pleural surface of the cortical shell along the main axis of the rib. Next, the sample was cut from the base of the cylinder using a low speed diamond saw. The last step was to mill the bottom surface in order to generate two parallel loading surfaces at a target specimen height of 2 mm. This was done by placing the sample in a custom clamp with v-slots of different depths (1.5 mm, 2 mm, and 2.5 mm), and then milling the top surface flat (Figure 17). The final dimensions of the cylindrical samples ranged from 0.914 mm to 1.067 mm (Avg. = 1.016 ± 0.041 mm) in cross-sectional diameter and 1.854 mm to 2.083 mm (Avg. = 2.003 ± 0.065 mm) in height, which were measured with dial calipers prior to testing (Figure 18). The height to diameter ratio (H:D = 2:1) was consistent with previous studies and

testing standards [83-85]. Prior to testing, the mass of each hydrated compression sample was measured on a precision scale (AR0640, OHAUS, Pinebrook, NJ).

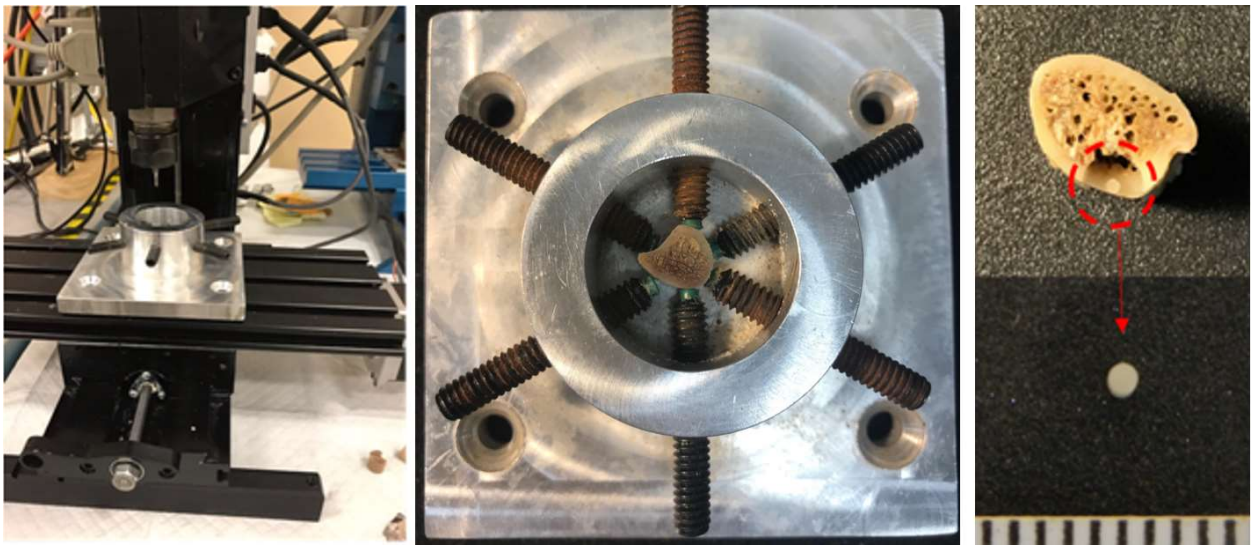

Figure 16: Cylindrical bone chuck mounted on CNC (left), rib section mounted in bone chuck (center), and cylindrical bone sample milled from pleural side of rib section (right).

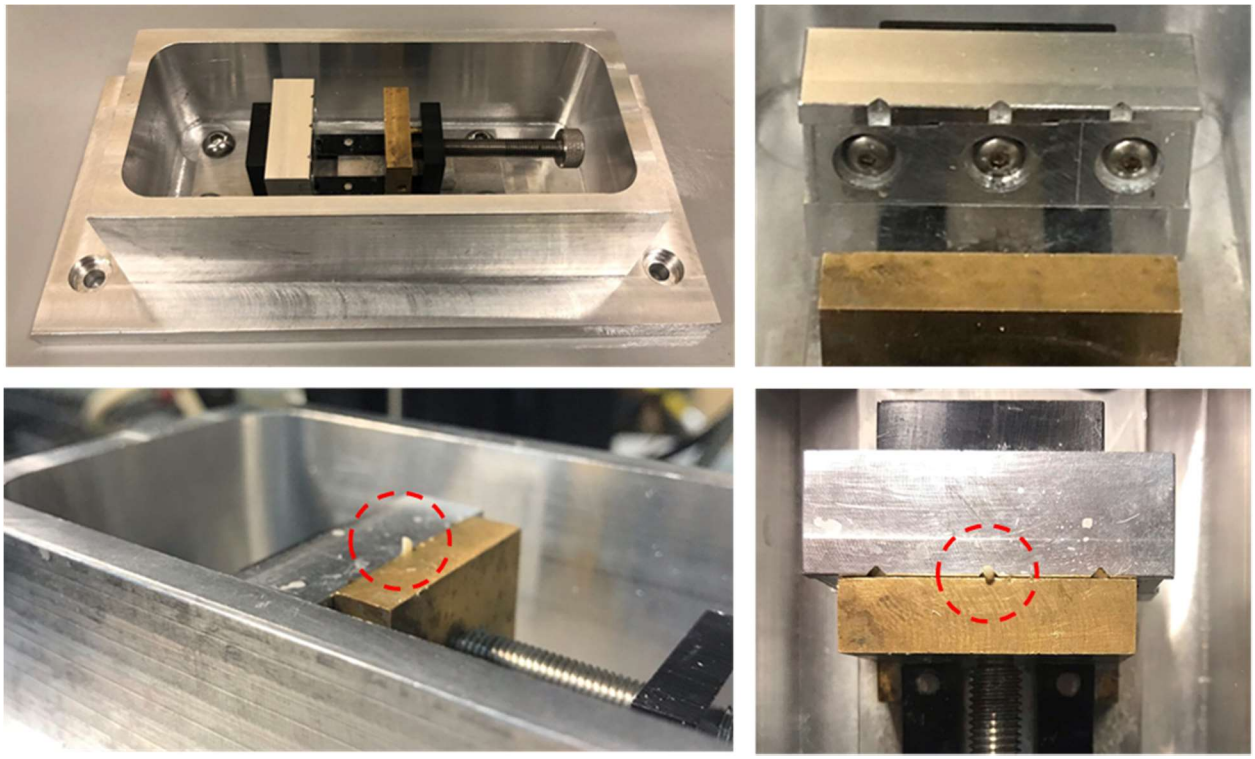

Figure 17: Custom clamp and saline bath for cylindrical bone samples (top-left), v-slots of different depths (top-right), sample in clamp (bottom-left, bottom-right).

Figure 18: Final 2 mm height (left), 1 mm diameter (right) sample with a U.S. penny for size reference.

Uniaxial compression tests were performed to failure on an electric-dynamic material testing machine (800LE4, Test Resources Inc., Shakopee, MN). The experimental test setup consisted of a custom-designed small-sample compression press with rigid loading platens, a high-accuracy, high-precision deflectometer (Model 3540-001M-ST, Epsilon Technology Corp, Jackson, WY) to measure the deflection of the press piston/sample, a uniaxial load cell (1210ACK-300-B, Interface, Scottsdale, AZ) to measure the piston load, and a three-axial load cell (5768, Humanetics, Farmington Hills, MI) to measure the reaction load (Figure 19 -

Figure **20**). The samples were tested at the same target strain rates (0.5 strain/s and 0.005 strain/s) that were tested in the previous tension study (See Chapter 2). For the 0.005 strain/s tests, data were collected at 100 Hz and filtered with a 1-49 Hz notch filter (Figure A21). For the 0.5 strain/s tests, data were collected at 20000 Hz and filtered with a CFC 30 filter (Figure A21).

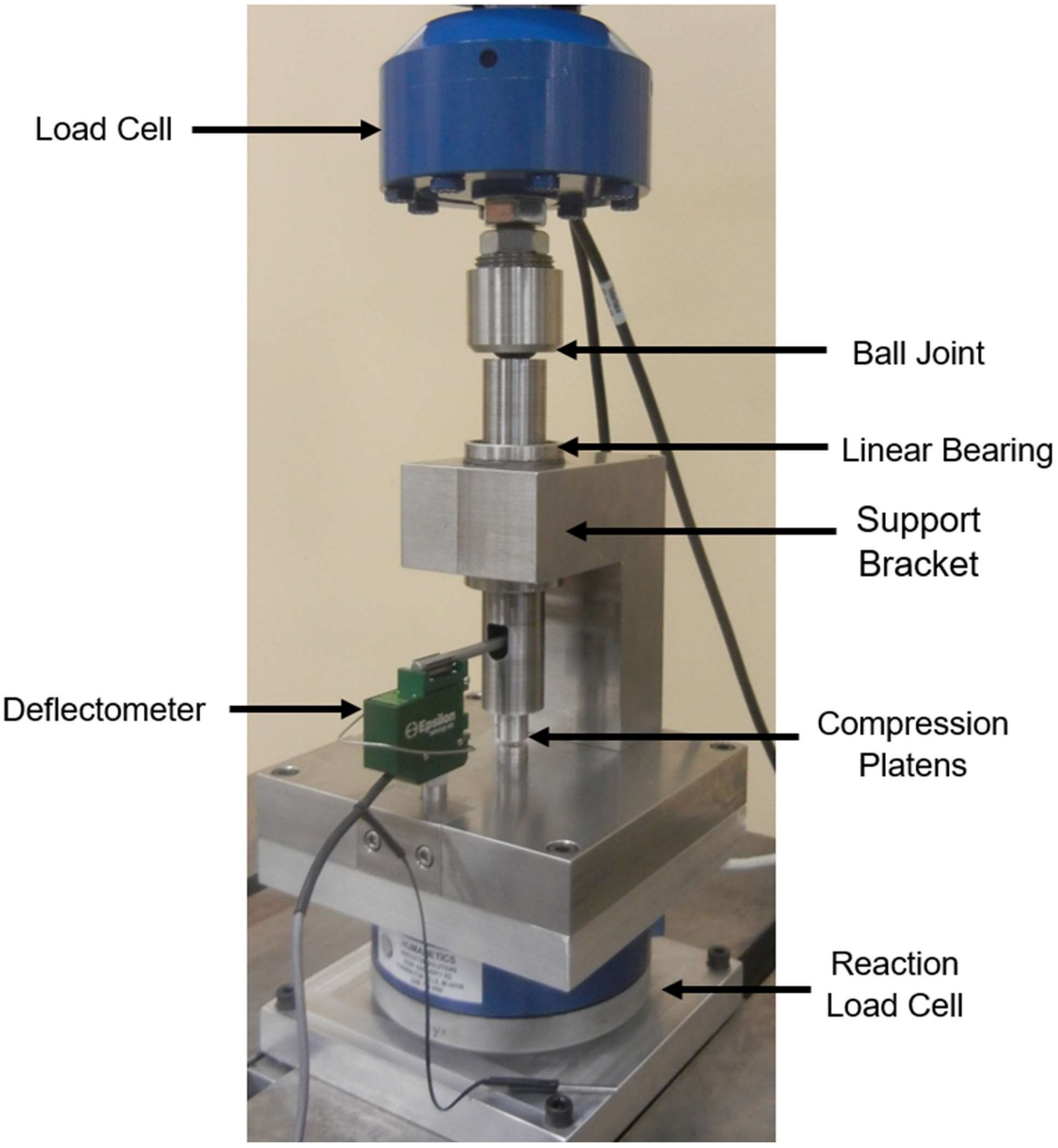

Figure 19: Front view of compression experimental test setup.

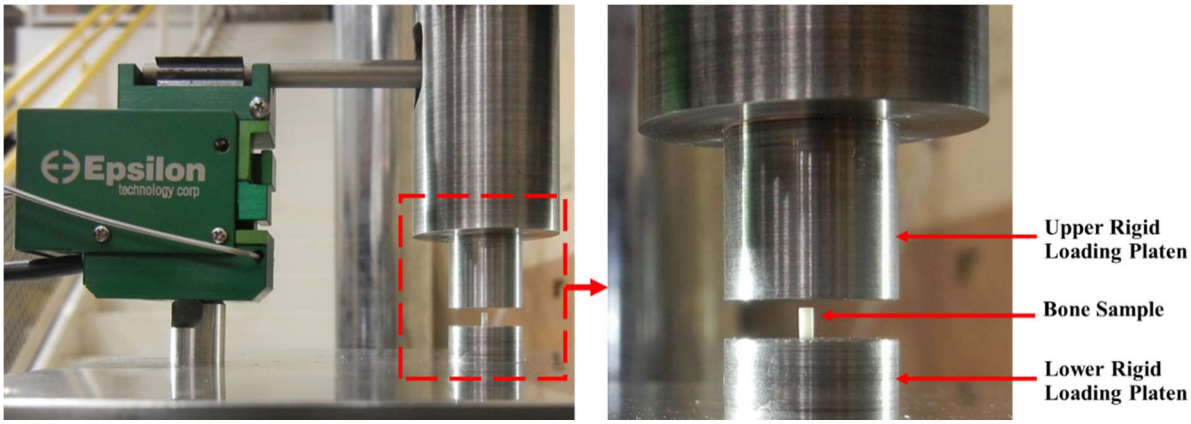

Figure 20: Side view of compression experimental test setup and sample.

The filtered data were used to calculate the elastic modulus, yield stress, yield strain, ultimate stress, ultimate strain, elastic strain energy density (SED), plastic SED, and total SED (Figure A22-Figure A23). Stress was calculated by dividing the force by the initial cross-sectional area of the specimen. Strain was calculated by dividing the change in height by the initial height. Compressive stress and strain values were made positive for plotting and comparisons. To determine yield and ultimate stress and strain, the toe region of the stress-strain curve was compensated according to ASTM D695-15 [86]. A continuation of the linear region of the curve was constructed through the x-axis, and the strain values were shifted until the point of zero strain corresponded to the point of zero stress, i.e., the continuation of the linear region of the curve passed through the origin (Figure A23). All strain values were hence measured from the shifted zero-strain point. The yield point was calculated as the point of intersection between the stress-strain curve and a straight line that was offset by 0.1% strain and parallel to the elastic portion of the curve [55, 56]. The elastic modulus was quantified by the slope of the elastic portion of the stress-strain curve between approximately 10% and 50% of the yield point. The ultimate stress for all tests was defined as the first point where an increase in strain did not result in an increase in stress. The ultimate strain was the strain value at the point of the ultimate stress (Figure A22). Total SED was calculated as the area under the stress-strain curve up to the point of ultimate stress, with elastic SED and plastic SED defined as the area under the stress-strain curve before and after the yield point, respectively. Density was calculated by dividing the total mass by the volume of the cylindrical sample. Characteristic average curves were quantified for each decade at both loading rates using the procedure published by Lessley *et al.* (2004) [57]. All statistical analyses conducted in this Chapter were the same as those conducted in the previous tension study (see Chapter 2). An additional

Spearman's correlation analysis was conducted to assess the relationship between density and material properties with alpha (α) set to 0.05 to determine significance. R^2 values were also reported.

Results

Material property data were successfully obtained at both 0.005 strain/s and 0.5 strain/s from all thirty (n = 30) subjects (Figure A24 - Figure A32, Table A1). The average strain rate for the 0.005 strain/s target rate compression tests was 0.0041 strain/s and the average strain rate for the 0.5 strain/s target rate compression tests was 0.404 strain/s.

Two statistical analyses were performed to evaluate the effect of sex on the material properties, where age was treated as either a continuous or discrete variable. No significant differences were detected in material properties with respect to sex as a continuous variable. A significant difference in ultimate stress and elastic SED was found with respect to the interaction between age and sex when age was treated as a continuous variable (Table 5). The ultimate stress and elastic SED were significantly lower in younger males than in younger females and higher in older males than in older females. However, only two female subjects in the study were greater than 60 years old. No significant results were obtained when analyzing the effect of sex on material properties within age groups (i.e., young, middle aged, and elderly) (Table 6).

When comparing material properties between loading rates, all material properties were significantly higher at 0.5 strain/s than at 0.005 strain/s (Figure 21, Table 7). It should be noted that several material properties were not normally distributed (Table A6). For those variables, the Wilcoxon signed-rank test was used.

Table 5: ANOVA results for the effect of sex on compressive material properties at both loading rates.

Material Property Variable	0.005 strain/s		0.5 strain/s	
	Sex	Sex*Age	Sex	Sex*Age
	p-value	p-value	p-value	p-value
Modulus	0.0835	0.2007	0.7883	0.1460
Yield Stress	0.1470	0.2296	0.9112	**0.0456**
Yield Strain	0.1274	0.2748	0.7743	0.0646
Ultimate Stress	0.0888	0.1914	0.8985	0.0666
Ultimate Strain	0.5194	0.5926	0.2657	0.8547
Elastic SED	0.5514	0.4867	0.9098	**0.0404**
Plastic SED	0.4713	0.7894	0.2438	0.9576
Total SED	0.3712	0.6100	0.3334	0.3791

Table 6: Tukey HSD results for the effect of sex on compressive material properties within each age group and loading rates.

Material Property Variable	0.005 strain/s			0.5 strain/s		
	Young	Middle	Elderly	Young	Middle	Elderly
	p-value	p-value	p-value	p-value	p-value	p-value
Modulus	0.8112	1.0000	0.3698	0.9900	0.9943	0.9867
Yield Stress	0.8969	0.9997	0.4946	0.8010	1.0000	0.9566
Yield Strain	0.9916	0.9569	0.7265	0.5674	0.8146	0.9585
Ultimate Stress	0.9481	0.9993	0.6021	0.9524	1.0000	0.9351
Ultimate Strain	0.9872	0.9885	0.8321	0.9817	0.9874	0.9965
Elastic SED	0.9890	0.9823	0.9189	0.5907	0.9947	0.9608
Plastic SED	1.0000	0.9523	1.0000	0.9119	0.9990	0.9933
Total SED	0.9985	0.9933	0.9971	1.0000	0.9938	0.9595

Table 7: Statistical analysis for the effect of loading rate on compressive material properties.

Material Property Variable	Paired t-test		Wilcoxon Signed Rank Test	
	t	p-value	S	p-value
Modulus	-3.558	**0.0013**	-153.5	**0.0003**
Yield Stress*	-5.872	<.0001	-208.0	**<.0001**
Yield Strain*	-2.245	0.0163	-117.0	**0.0134**
Ultimate Stress	-7.499	**<.0001**	-214.5	**<.0001**
Ultimate Strain	-6.023	**<.0001**	-216.5	**<.0001**
Elastic SED	-5.670	**<.0001**	-204.5	**<.0001**
Plastic SED	-6.157	**<.0001**	-209.5	**<.0001**
Total SED	-7.886	**<.0001**	-217.5	**<.0001**

Notes: An asterisk (*) indicates a parameter that was not normally distributed and that the Wilcoxon Signed Rank Test should be used. Bold text indicates a significant p-value for the appropriate statistical test.

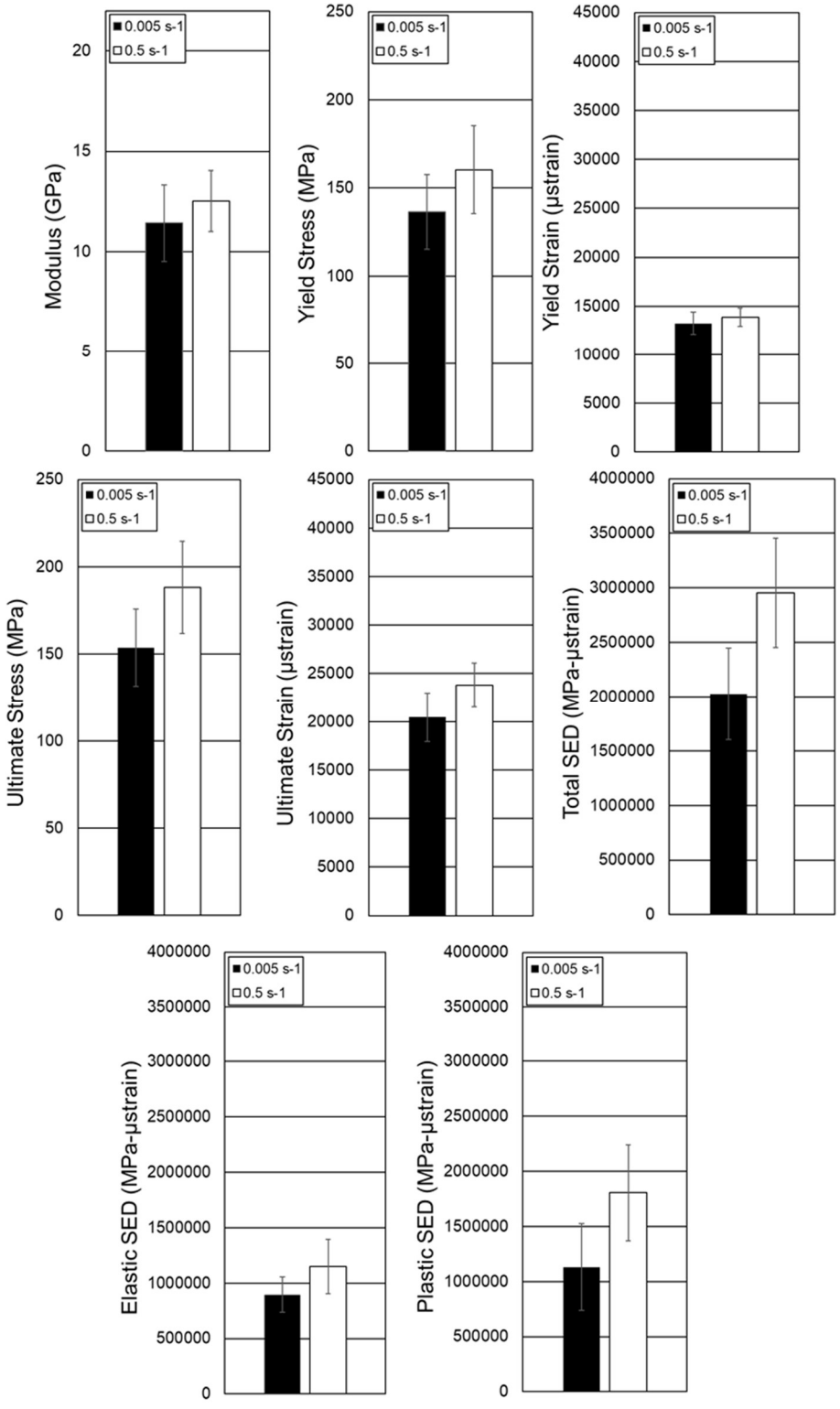

Figure 21: Average compressive material property values for each loading rate with ± 1 S.D. indicated by error bars.

There were no significant correlations with respect to increased age for any material properties at either loading rate (Figure 22 - Figure 29). Additionally, the R^2 values were below 0.2 for all material properties at both loading rates, indicating that less than 20% of the variance in material properties can be attributed to age. The characteristic stress-strain curves for all tests by loading rate and all tests by loading rate and decade are plotted in Figure 30 and Figure 31, respectively. Individual stress-strain curves with overlapped characteristic average curves are plotted for each decade in the Appendix (Figure A24 - Figure A32).

Table 8: Spearman's rank correlation analysis for the effect of age on compressive material properties.

Material Property Variable	0.005 strain/s tests				0.5 strain/s tests		
	ρ	R^2	p-value		ρ	R^2	p-value
Modulus	-0.1316	0.053	0.4883		-0.3328	0.143	0.0723
Yield Stress	-0.2400	0.059	0.2015		-0.3488	0.148	0.0588
Yield Strain	0.0000	0.021	1.0000		-0.1336	0.039	0.4816
Ultimate Stress	-0.1674	0.042	0.3766		-0.3001	0.134	0.1071
Ultimate Strain	0.1576	0.024	0.4055		0.2418	0.067	0.1981
Elastic SED	-0.3130	0.030	0.0922		-0.2910	0.123	0.1188
Plastic SED	0.0539	0.000	0.7774		0.1431	0.010	0.4505
Total SED	-0.0129	0.005	0.9460		-0.0069	0.008	0.9711

Notes: Bold text indicates a significant p-value or an R^2 value ≥ 0.49.

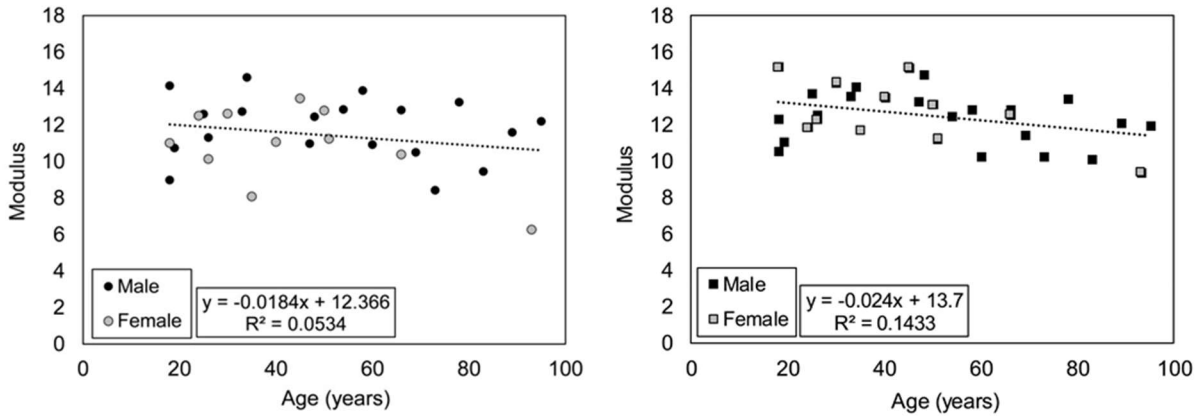

Figure 22: Modulus versus age at 0.005 strain/s (left) and 0.5 strain/s (right) in compression.

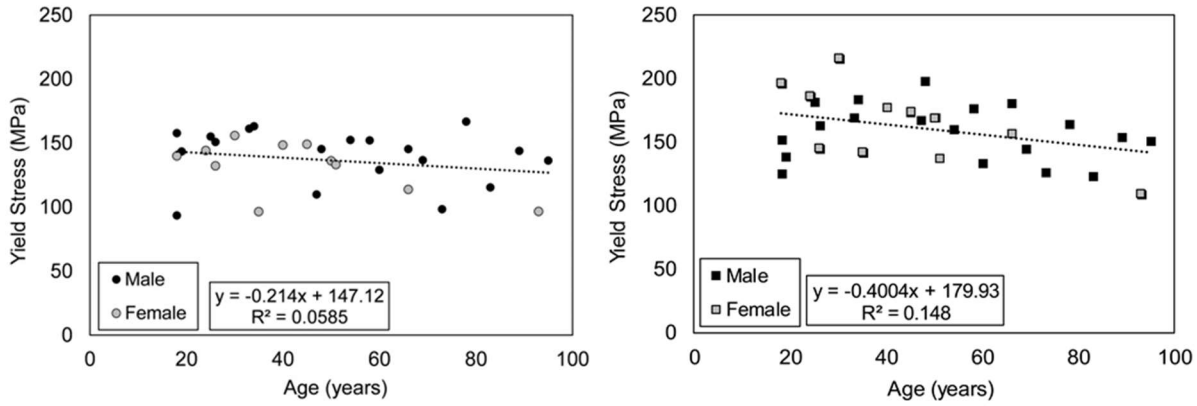

Figure 23: Yield stress versus age at 0.005 strain/s (left) and 0.5 strain/s (right) in compression.

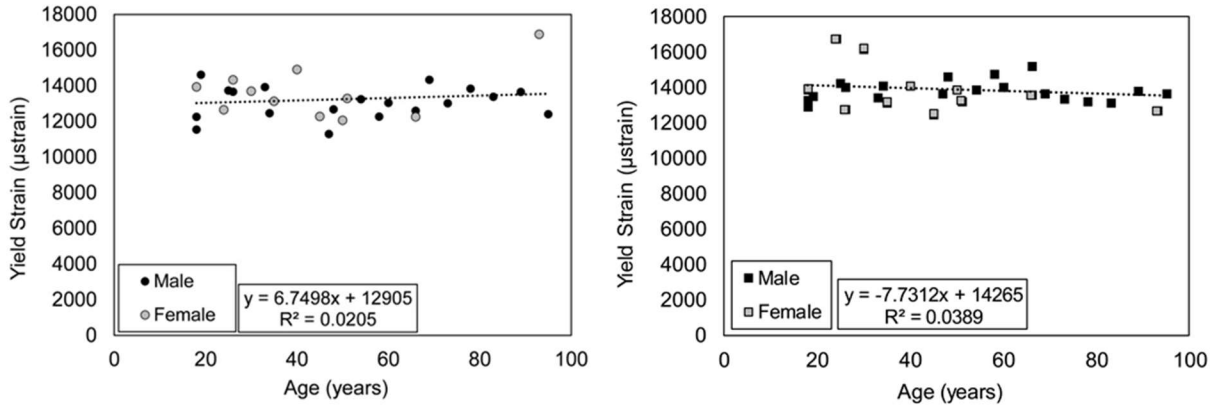

Figure 24: Yield strain versus age at 0.005 strain/s (left) and 0.5 strain/s (right) in compression.

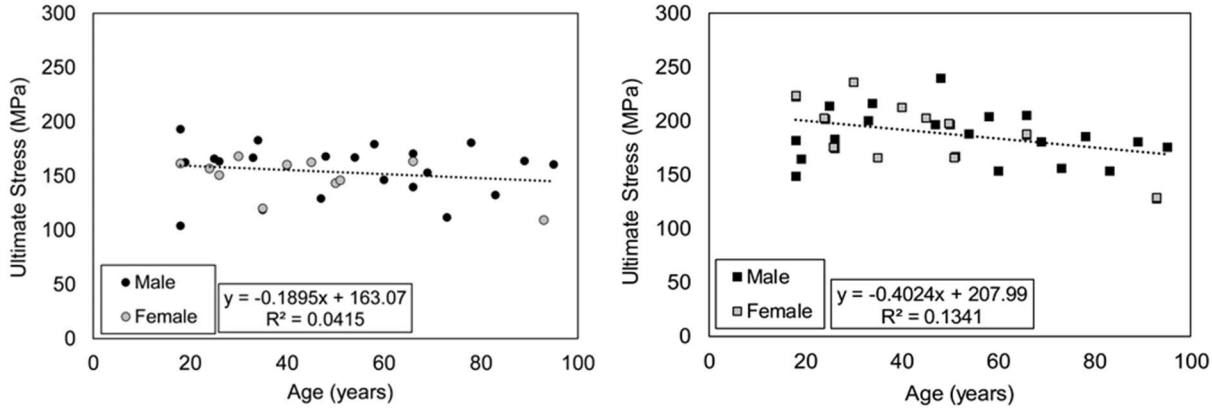

Figure 25: Ultimate stress versus age at 0.005 strain/s (left) and 0.5 strain/s (right) in compression.

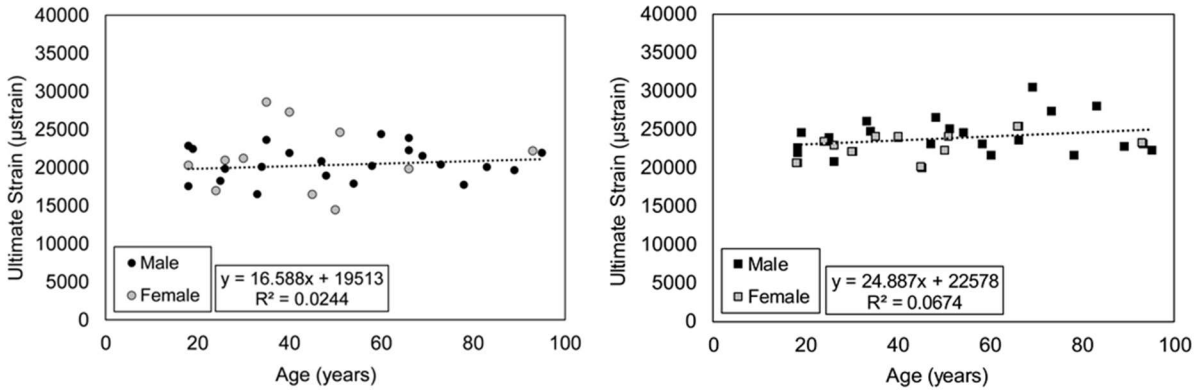

Figure 26: Ultimate strain versus age at 0.005 strain/s (left) and 0.5 strain/s (right) in compression.

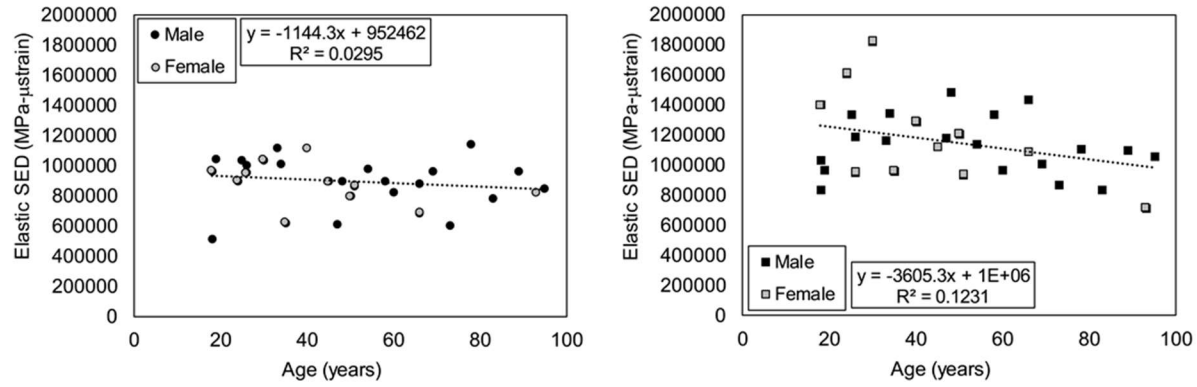

Figure 27: Elastic SED versus age at 0.005 strain/s (left) and 0.5 strain/s (right) in compression.

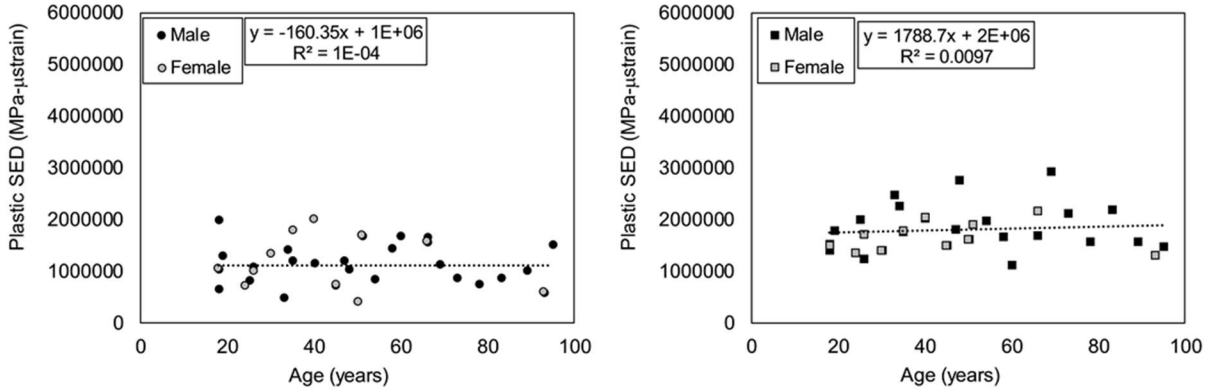

Figure 28: Plastic SED versus age at 0.005 strain/s (left) and 0.5 strain/s (right) in compression.

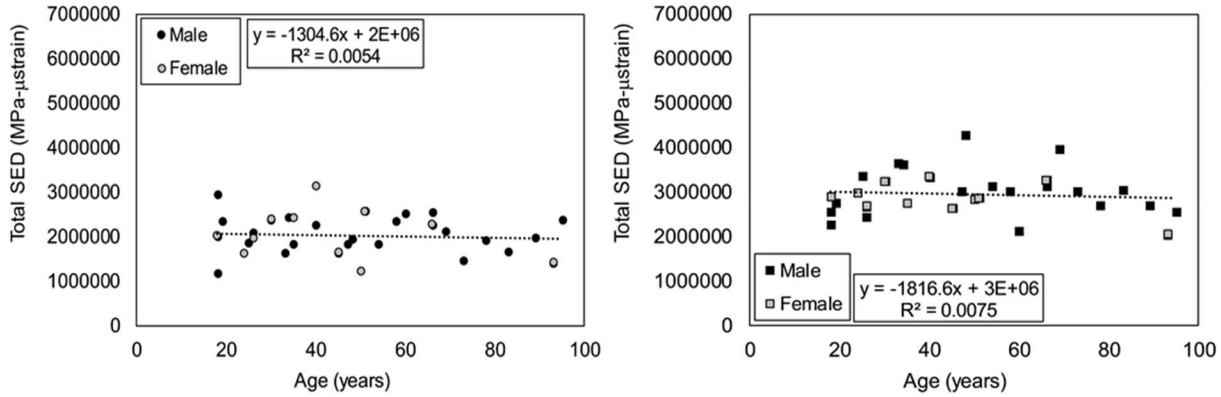

Figure 29: Total SED versus age at 0.005 strain/s (left) and 0.5 strain/s (right) in compression.

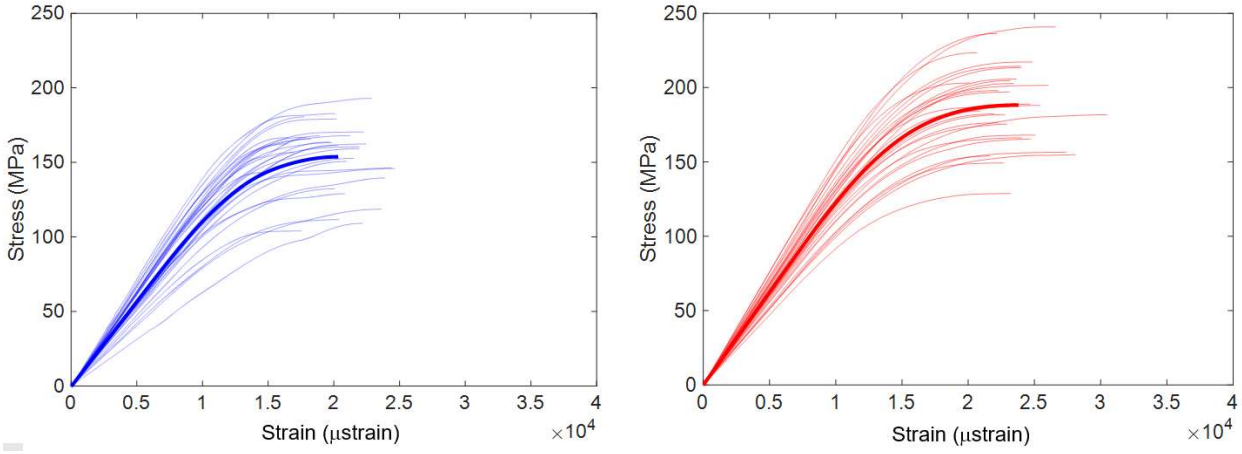

Figure 30: Characteristic average stress-strain curves for all compression tests at 0.005 strain/s (left) and 0.5 strain/s (right).

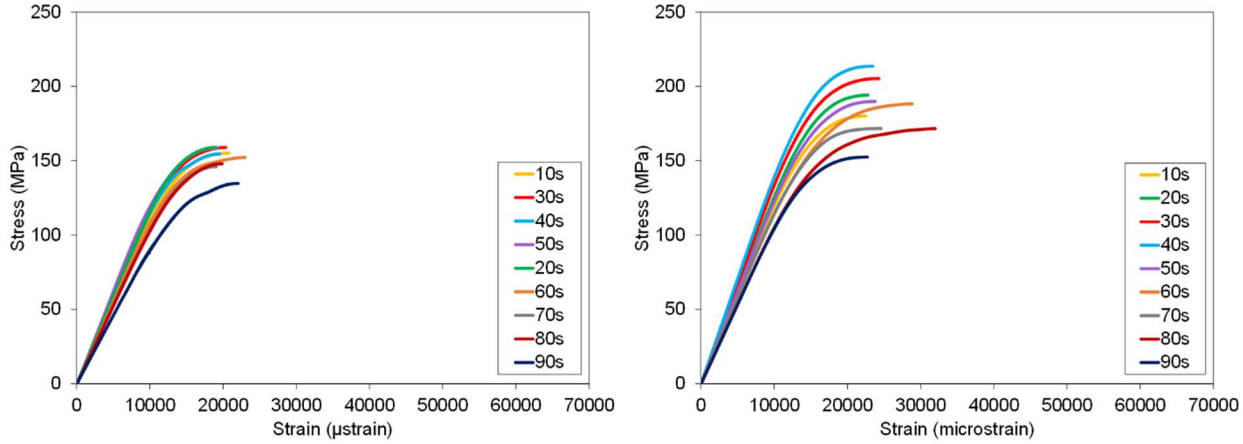

Figure 31: Characteristic average stress-strain curves for each decade at 0.005 strain/s (left) and 0.5 strain/s (right).

At both loading rates, the modulus, yield stress, ultimate stress, and elastic SED significantly increased with increased density (Table 9, Figure 32 - Figure 39). R^2 values for significantly correlated material properties ranged from 0.163 to 0.295 at 0.005 strain/s and 0.286 to 0.358 at 0.5 strain/s.

Table 9: Spearman's rank correlation analysis for the effect of density on compressive material properties.

Material Property Variable	0.005 strain/s tests				0.5 strain/s tests		
	ρ	R^2	p-value		ρ	R^2	p-value
Modulus	0.3994	0.279	**0.0288**		0.5498	0.358	**0.0016**
Yield Stress	0.4795	0.295	**0.0073**		0.5282	0.342	**0.0027**
Yield Strain	0.0839	0.033	0.6594		0.1448	0.069	0.4451
Ultimate Stress	0.4107	0.219	**0.0242**		0.5291	0.295	**0.0026**
Ultimate Strain	-0.2410	0.116	0.1996		-0.1457	0.055	0.4422
Elastic SED	0.4390	0.163	**0.0152**		0.4543	0.286	**0.0117**
Plastic SED	-0.0699	0.001	0.7137		-0.0558	0.001	0.7694
Total SED	0.1184	0.014	0.5333		0.2040	0.059	0.2795

Notes: Bold text indicates a significant p-value or an R^2 value ≥ 0.49.

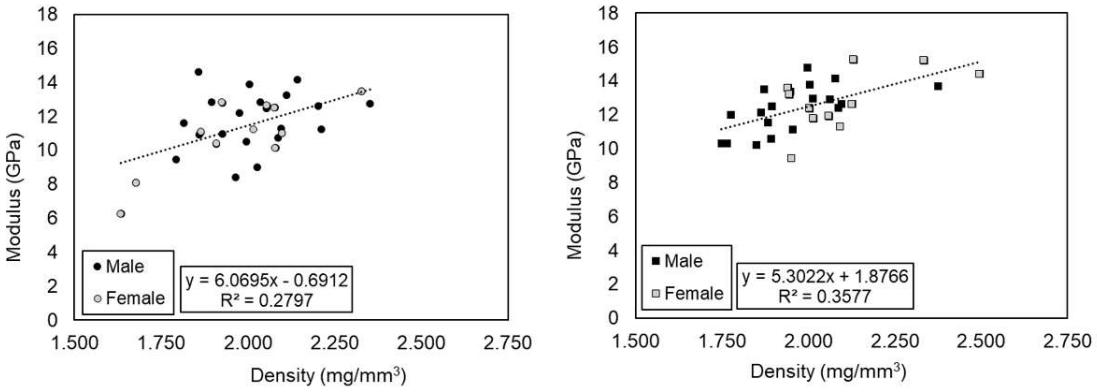

Figure 32: Modulus versus density at 0.005 strain/s (left) and 0.5 strain/s (right) in compression.

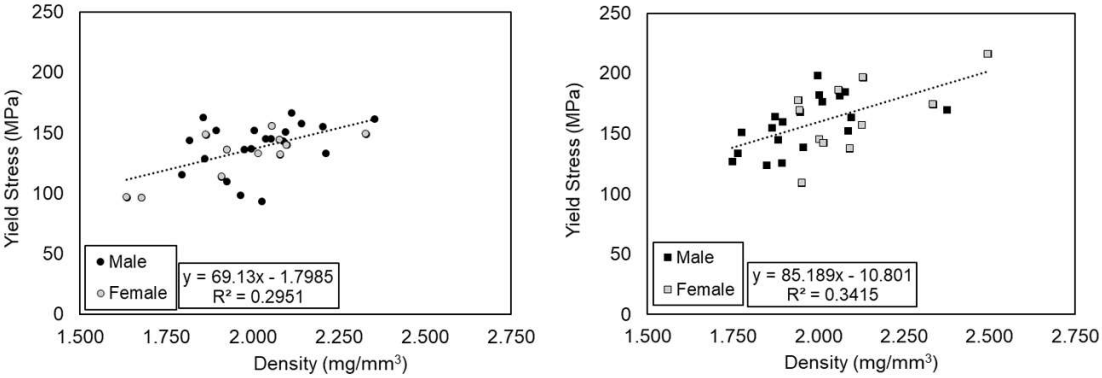

Figure 33: Yield stress versus density at 0.005 strain/s (left) and 0.5 strain/s (right) in compression.

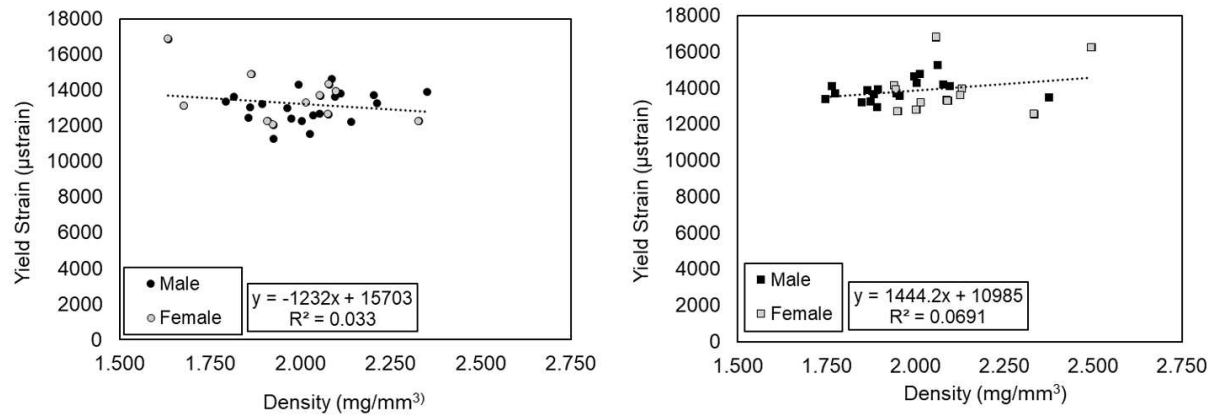

Figure 34: Yield strain versus density at 0.005 strain/s (left) and 0.5 strain/s (right) in compression.

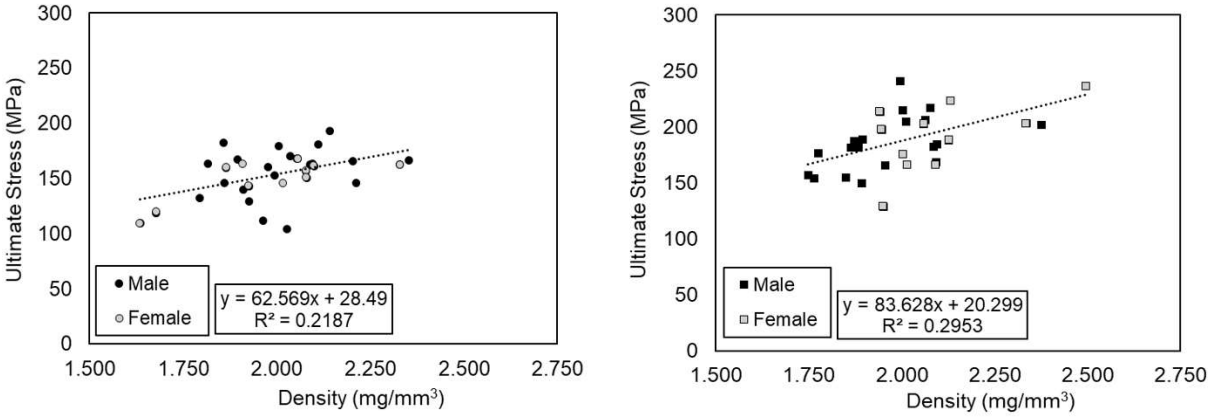

Figure 35: Ultimate stress versus density at 0.005 strain/s (left) and 0.5 strain/s (right) in compression.

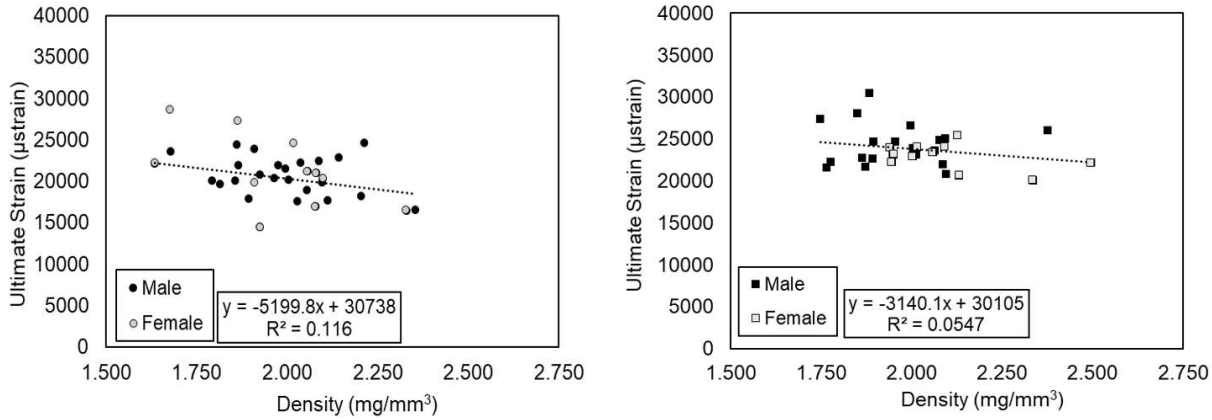

Figure 36: Ultimate strain versus density at 0.005 strain/s (left) and 0.5 strain/s (right) in compression.

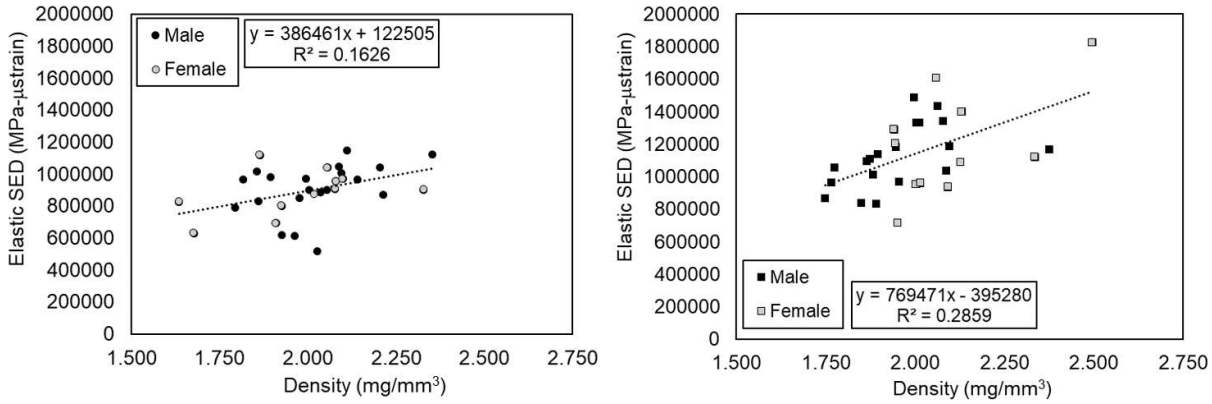

Figure 37: Elastic SED versus density at 0.005 strain/s (left) and 0.5 strain/s (right) in compression.

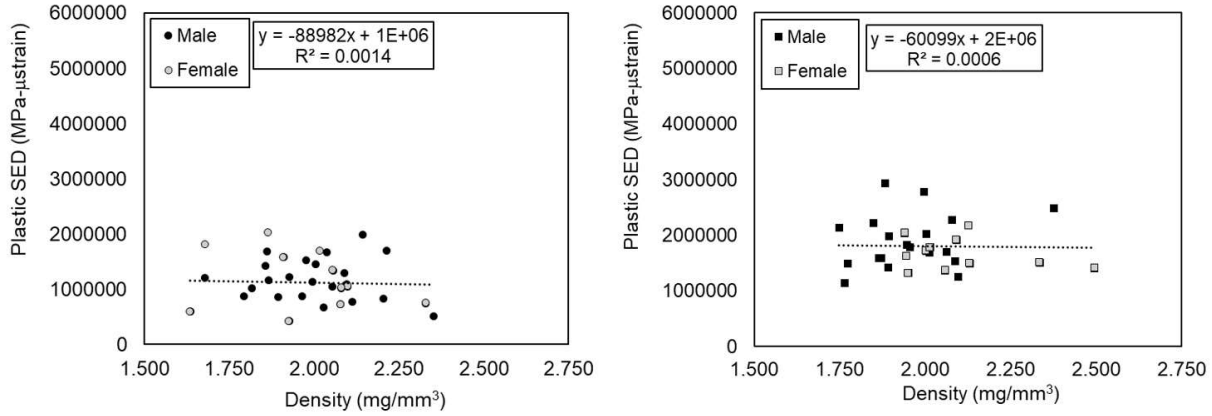

Figure 38: Plastic SED versus density at 0.005 strain/s (left) and 0.5 strain/s (right) in compression.

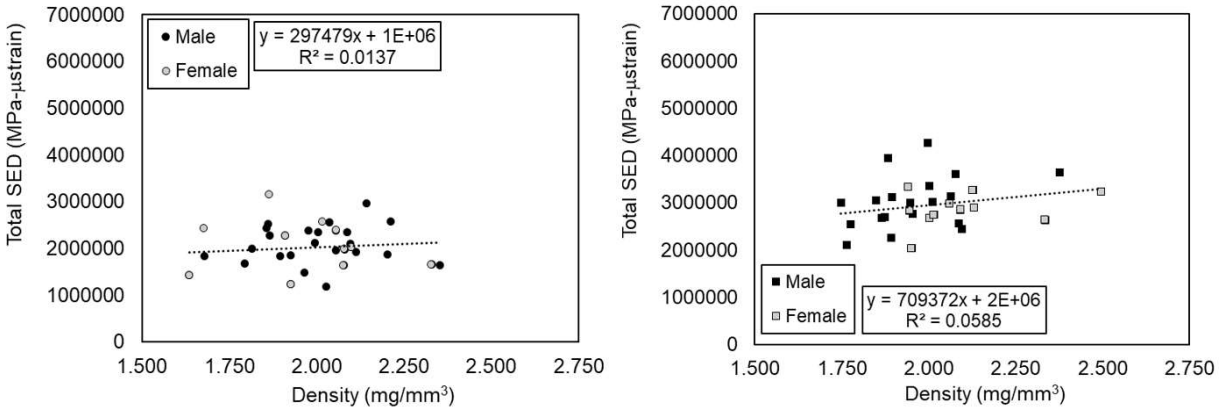

Figure 39: Total SED versus density at 0.005 strain/s (left) and 0.5 strain/s (right) in compression.

Discussion

As mentioned in Chapter 2, previous studies have quantified the material properties of human cortical bone in compression for the tibia and femur. The average modulus, ultimate stress, and ultimate strain values obtained at similar strain rates by McElhaney (1966), Reilly *et al.* (1974), Burstein *et al.* (1976), and Hansen *et al.* (2008) are displayed in Table 10 [23, 28, 81, 87]. The ultimate stress values obtained from rib cortical bone in the current study were similar to those from tibial or femoral cortical bone tested at approximately the same strain rates. However, the current study produced slightly lower average elastic modulus values and higher average ultimate strain values than previous studies in compression. This could be due to the potential microstructural differences between the femur and the ribs. It is well established in the literature that bone remodels based on the normal loading conditions that a particular bone is subjected to in everyday life. The femur, tibia, and fibula are load bearing long bones that are primarily subjected to compressive loading in mid-shaft. Conversely, the ribs are non-load bearing flat bones that elevate and expand in diameter (transverse plane) during inspiration, and depress and contract during expiration. Consequently, the microstructure and material properties of the ribs may be inherently different than the long bones in the lower extremity. Specifically, the lower modulus and higher ultimate strain observed in the ribs compared to long bones may be due to remolding in order to facilitate the motion of the ribs during breathing, as opposed to axial load bearing.

Table 10: Cortical bone compressive material property values from other studies at similar strain rates.

Study	Strain Rate [s^{-1}]	Bone Tested	Age Range [years]	Avg. Elastic Modulus (GPa)	Avg. Ultimate Stress [MPa]	Avg. Ultimate Strain [strain]
Current Study	0.5	Human Rib	18-95	12.49	189.20	0.0247
McElhaney (1966)	0.1	Human Femur	24 (one subject)	17.93	199.95	0.0175
Reilly et al. (1974)	0.05	Human Femur	20-86	17.28	190.42	0.0211
Burstein et al. (1976)	0.05	Human Femur	21-86	17.56	194.14	N/A
Burstein et al. (1976)	0.05	Human Tibia	21-86	28.02	195.33	N/A
Hansen et al. (2008)	0.14	Human Femur	51 (one subject)	17.04	173.63	0.0184
Current Study	0.005	Human Rib	18-95	11.43	153.68	0.0204
McElhaney (1966)	0.001	Human Femur	24 (one subject)	15.17	150.31	0.0165

In regard to the effects of loading rate on the compressive material response of human rib cortical bone, the results of the current study were consistent with previous research performed at similar loading rates in compression. As mentioned in Chapter 2, multiple studies have reported differences in compressive material properties of femoral cortical bone from both human and bovine subjects with respect to strain rate [28, 81]. McElhaney (1966), whose findings were thoroughly discussed in Chapter 2, reported considerable increases in the ultimate compressive stress and modulus in human cortical bone with increased loading rate. McElhaney (1966) also reported that ultimate strain considerably decreased when the loading rate increased from 1 strain/s to 1500 strain/s, but observed a slight increase in ultimate strain from 0.001 strain/s to 0.1 strain/s at the lower end of the loading rate spectrum. This slight increase in ultimate strain was also observed in the current study from 0.005 strain/s to 0.5 strain/s. Hansen *et al.* (2008) tested human femoral cortical bone in compression at strain rates ranging between 0.14 – 29.1 strain/s, and reported that post-yield stress, ultimate stress, post-yield strain, and failure strain increased with increased strain rate while yield stress and strain decreased from 0.14 strain/s to 10 strain/s. After approximately 10 strain/s, several material properties seem to reach a maximum and then begin to decrease as the loading rate increases. When analyzing the Hansen *et al*. (2008) data at the lower end of the strain rate spectrum, the results were found to be similar to those obtained for human rib cortical bone in the current study with the exception of yield values. In regard to the energy absorption to failure, it is important to note that the data from McElhaney (1966) showed that energy absorption increases slightly from 0.001 strain/s to ~0.1 strain/s before transitioning to a distinct steady decrease in energy absorption with increased loading rate. The characteristic average stress-strain curves from the current study display the increases in modulus, yield and failure values, and energy absorption between the two loading rates and show similar differences in the average stress-strain curves with respect to loading rate as those reported by McElhaney (1966) at 0.001 and 0.1 strain/s (Figure 40). Overall, these data illustrate that FEMs should model these loading rate effects, given the fact that the ribs experience various dynamic strain rates during MVCs. However, additional strain rates need to be evaluated to fully characterize the viscoelastic properties of rib cortical bone.

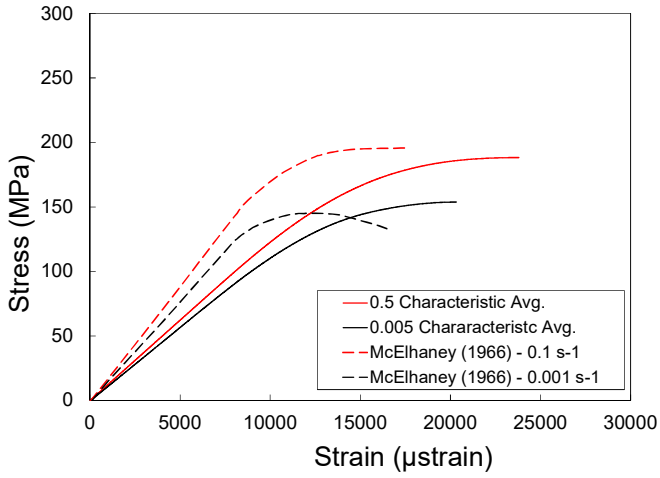

Figure 40: Characteristic average stress-strain curves for each strain rate tested in the current study (0.005 strain/s and 0.5 strain/s) plotted against the curves reported in McElhaney (1966) at 0.001 s^{-1} and 0.1 s^{-1}.

The correlations in material properties with respect to age were much less apparent in compression than they were in tension (see Chapter 2). No significant correlations were observed in material properties with respect to age at either loading rate. However, some weak to moderate trends have been noted in previous studies. Evans and Vincentelli (1974) tested an average of 11 human tibial specimens per subject from six male subjects (26 to 75 years of age) at approximately 0.005 strain/s [88]. This study reported that the samples from the 26-year-old subject experienced the lowest ultimate compressive stress (UCS), while the next oldest subject (aged 31 years) experienced the highest UCS. After the subject that was 31 years of age, the UCS steadily declined with advancing age. This is similar to the trends observed in the current study. For the 0.005 strain/s tests, the UCS from subjects aged 18 to 26 years (n = 6, Avg. UCS = 156.2 MPa) was lower on average than the UCS from subjects aged 30 to 50 (n = 10, Avg. UCS = 157.5 MPa). After age 50, the yield and UCS values in the current study gradually decreased with increased age (n = 14, Avg. UCS = 150.1 MPa). A similar, stronger trend was observed in the current study at 0.5 strain/s, with average ultimate stresses of 187.6 MPa, 206.7 MPa, and 178.9 MPa for subjects aged 18-26 years, 30-50 years, and 51+ respectively. Other material properties reported by Evans and Vincentelli (1974), including elastic modulus and ultimate strain, showed no significant correlations with increased age, which is consistent with the findings of the current study. Burstein *et al.* (1976) tested multiple samples from both tibial and femoral samples (21 to 86 years of age) in compression at approximately 0.05 strain/s [23]. The authors reported higher average ultimate stress values for the

subjects aged between 20 and 29 relative to the rest of the population, and these values were higher than those reported by Evans and Vincentelli (1974) and the current study. Additionally, Burstein *et al.* (1976) observed a significant decrease in ultimate stress as age increased across the entire sample size. Burstein *et al.* (1976) did not observe significant changes in modulus with increased age and did not report yield values or ultimate strain values in compression. Conversely, the data from the current study showed slight decreases in modulus and yield stress with advanced age at 0.5 strain/s. Although it was non-significant, a decrease in ultimate stress at 0.5 strain/s was also observed. Given that these correlations were weak and/or non-significant, the gradual decreases in modulus and ultimate stress with advanced age indicate that there may be underlying variables, e.g., bone density or micro-architecture, that are driving the changes in compressive material properties of rib cortical bone with age.

The lower stress and energy absorption values reported in the current study for younger subjects compared to older subjects could be due to differences in the histological and micro-architectural composition of the samples. While collagen provides strength and ductility to cortical bone in tension, hydroxyapatite and other minerals/inorganic materials in cortical bone provide strength in compression. It has been shown that the bone mineral crystal size and perfection increases during the first 25-30 years of life, and then decreases thereafter, slightly increasing in the oldest individuals [89]. As mentioned in Chapter 2, differences in the microstructure between immature and mature bone could result in differences in rib material and/or structural properties. It is possible that the inorganic material that provides compressive strength to cortical bone is not fully developed in the subjects under 25 years of age in the current study, i.e., maturation and ossification have not been completed, resulting in lower ultimate and yield stresses in compression. However, not enough subjects or samples per subject were tested in the current portion of the study in order to apply a non-linear fit to the data. In addition, Evans and Vincentelli (1974) attributed the decreases in ultimate stress and strain with respect to age to osteon count and point of osteon maturation in the sample [88]. The decrease in mineral crystal size or other changes due to mineral loss in cortical bone, e.g., increased porosity or decreased BMD, after peak skeletal maturation could also potentially contribute to the decreases in compressive stress with age [62, 63, 90]. Several material properties had significant positive correlations with density in the current study. As density increased, the modulus, yield stress, ultimate stress, and elastic SED increased at each loading rate. This supports the hypothesis that density may be a better indicator of the material

response of cortical bone than chronological age, considering none of the material properties in the current study were significantly correlated with age across the entire subject pool. In previous studies, wet and dry density were also reported to have significant positive correlations with modulus and ultimate strength in cortical bone [22, 71, 91, 92]. However, the R^2 values in the current study only range from 0.163 to 0.358, and bone mineral density (BMD), mineralization content, and osteon size/count were not measured. Therefore, additional tests from subjects less than 18 years and greater than 70 years of age, along with a more comprehensive histological analysis, should be performed to provide a more in-depth analysis of the effect of microstructure on the compressive material properties of rib cortical bone.

While the inclusion or omission of immature subjects in the statistical analysis of tensile properties with age in Chapter 2 did not affect the overall significance of the correlations with age, the trends considerably shift from statistically insignificant to statistically significant when the immature subjects are excluded in the compressive analysis, especially at 0.5 strain/s. A supplementary Spearman correlation statistical analysis was performed to determine the trends in compressive material properties with age for skeletally mature subjects (>21 years) at both loading rates (Table A7, Figure A33 - Figure A40). At 0.005 strain/s, elastic SED shifted from insignificant to significant, but the R^2 value remained low (R^2 = 0.072). At 0.5 strain/s, several correlations in material properties with respect to age were significant with the exclusion of subjects ≤21 years, including modulus, yield stress, ultimate stress, and elastic SED. Additionally, the R^2 values increase from 0.143 to 0.275, 0.148 to 0.321, 0.134 to 0.299, and 0.123 to 0.280 for modulus, yield stress, ultimate stress, and elastic SED, respectively. These trends align more with the previous literature that analyzed the effect of aging on the human cortical bone in compression. However, the R^2 values for material properties that varied significantly with respect to advancing age only ranged from 0.072 - 0.321, indicating that there may be other underlying variables, e.g., BMD or micro-architecture, that better explain the variance within a given population. Finally, more subjects are necessary to determine if skeletal development, i.e., changes from 0-21 years, has a significant effect on material properties of rib cortical bone.

Limitations in the manufacturing and testing of compression samples of rib cortical bone should be addressed. Firstly, the data set consists of more male subjects (M = 19) than female subjects (F = 11) due to most elderly female subjects in the current study having a small, thin cortical shell.

The cortical shell was too thin to obtain compression samples from the ribs of several elderly subjects, male and female, that were used to obtain tension coupons. The samples taken from the ribs of elderly subjects in the current study had thicker cortical shells from which it was physically possible to obtain a 1 mm diameter sample. It is possible that selecting only the subjects with adequately thick cortical shells biased the results with respect to age. Decreasing the diameter and/or height of the sample in order to obtain samples from more subjects could provide the opportunity to include more elderly subjects in future research studies and therefore more thoroughly analyze the effect of age on material properties. While the approximate location of the sample was kept constant, the remaining rib material of certain subjects was limited, so the compression sample was not taken from the same exact location along the rib for each subject. Finally, the effects of BMD or other histological/morphometric variables were not evaluated. The data from the current study should be analyzed with complementary histological variables in future studies to more thoroughly analyze the material properties of rib cortical bone.

Tensile versus Compressive Material Properties of Rib Cortical Bone

Material response data were obtained in both tension and compression from 28 subjects (Avg. age = 50.5 ± 24.1 yrs.) at 0.005 strain/s and from 29 subjects (Avg. age = 49.9 ± 24.1 yrs.) at 0.5 strain/s. Two-sided paired t-tests (t) or Wilcoxon signed-rank (S) tests were conducted on the matched tension and compression data at 0.5 strain/s and 0.005 strain/s (Table 11). A positive test statistic (t or S) indicates that the tensile material property was higher than the corresponding compressive material property, while a negative test statistic indicates that the compressive material property was higher than the corresponding tensile material property. Average values for each material property were reported in Figure 41. At 0.005 strain/s, the modulus and plastic SED were significantly higher in tension than in compression, and the yield stress, yield strain, ultimate stress, and elastic SED were significantly higher compression than in tension (Figure 41). The same trends were observed at 0.5 strain/s, as well as significantly higher failure strain in tension than in compression. Characteristic average stress-strain curves were also plotted for compression and tension matched data per decade in the Appendix (Figure A41 - Figure A45). Per each decade, the plastic strain was higher in tension than in compression, while the yield stress, yield strain, and elastic SED were higher in tension than in compression at both loading rates (Figure A41 - Figure A45). In regard to existing literature, Reilly *et al.* (1974) and Burstein *et al.* (1976) tested human

tibial and femoral samples in both tension and compression [23, 87]. Each study reported no significant differences in modulus with respect to loading mode and a significantly higher ultimate stress in compression than in tension. A more recent study tested bovine cortical bone in compression and tension and also reported no difference in modulus, a higher ultimate stress in compression, and a lower ultimate strain in tension [82]. The collagen in cortical bone provides ductility and strength in tension, which explains higher ultimate strain and plastic SED values observed in tension in the current study and Burstein *et al.* (1976). Conversely, hydroxyapatite and other inorganic materials provide strength in compression, which explains the higher ultimate stress observed in compression. While the current study tested samples from relatively younger human subjects on average than Reilly *et al.* (1974) and Burstein *et al.* (1976), the differences in average ultimate stress values between compressive and tensile loading were similar to those that were reported in Reilly *et al.* (1974) and Burstein *et al.* (1976) (Table 12). However, the modulus values for each decade in the current study were lower on average than those reported in previous studies. In addition, the current study produced higher modulus values in tension than in compression, which disagrees with the previous literature. The differences in the modulus values between the current study and previous studies could be due to micro-architectural differences between the ribs, which are flat bones, and the femur or tibia, which are load bearing long bones, resulting from remodeling that occurs in response to everyday loading. Histological studies could help elucidate the potential reasons for the material differences observed between these bones, as well as underlying variables driving the changes in material response with respect to development and advanced aging. Overall, the results of the current study illustrate that the material response of human rib cortical bone differs between tensile and compressive loading. Given that the ribs experience dynamic tensile and compressive loading during MVC, the data from the current study could allow FEMs to more accurately model the rate-dependent, asymmetric material response of the ribs in an MVC.

Table 11: Statistical analysis for the effect of loading mode (tension versus compression) on material properties.

Material Property Variable	0.005 strain/s				0.5 strain/s			
	Paired t-test		Wilcoxon Signed Rank Test		Paired t-test		Wilcoxon Signed Rank Test	
	t	p-value	S	p-value	t	p-value	S	p-value
Modulus	5.058	**<.0001**	169	**<.0001**	5.261	**<.0001**	180.0	**<.0001**
Yield Stress*	-13.498	<.0001	-203	**<.0001**	-17.140	**<.0001**	-217.5	**<.0001**
Yield Strain†	-24.051	**<.0001**	-203	**<.0001**	-30.594	<.0001	-217.5	**<.0001**
Ultimate Stress†	-40.437	**<.0001**	-203	**<.0001**	-9.508	<.0001	-217.5	**<.0001**
Ultimate Strain*†	2.116	0.0437	-199	0.0674	2.397	0.0234	95.5	**0.0365**
Elastic SED	-18.713	**<.0001**	-203	**<.0001**	-18.485	**<.0001**	-217.5	**<.0001**
Plastic SED*†	2.792	0.0095	105	**0.0139**	2.962	**0.0062**	117.5	**0.0085**
Total SED*†	0.377	0.7093	-6	0.8942	0.499	0.6218	-8.5	0.8579

Notes: An asterisk (*) indicates a parameter that was not normally distributed at 0.005 strain/s for either loading mode; a dagger (†) indicates a parameter that was not normally distributed at 0.5 strain/s for either loading mode. The Wilcoxon Signed-Rank Test should be used for those parameters. Bold text indicates a significant p-value for the appropriate statistical test.

Table 12: Average material properties in compression versus tension from previous literature compared to the current study's average results.

Study	Strain Rate [s^{-1}]	Bone Tested	Age Range [years]	Avg. Elastic Modulus [GPa]		Avg. Ultimate Stress [MPa]		Avg. Ultimate Strain [strain]	
				T	C	T	C	T	C
Current Study	0.5	Human Rib	18-95	15.45	12.49	135.1	189.2	0.0292	0.0247
Reilly et al. (1974)	0.05	Human Femur	20-86	16.40	17.28	128.3	190.4	0.0274	0.0211
Burstein et al. (1976)	0.05	Human Femur	21-86	16.84	17.56	132.0	194.1	0.0283	N/A
Burstein et al. (1976)	0.05	Human Tibia	21-86	23.83	28.02	156.4	195.3	0.031	N/A
Current Study	0.005	Human Rib	18-95	14.63	11.43	104.1	153.7	0.0247	0.0204
Li et al. (2013)	0.001	Bovine Femur	N/A	20.22	19.09	97.4	214.4	0.0185	0.0237

Notes: "T" and "C" represent Tension and Compression, respectively.

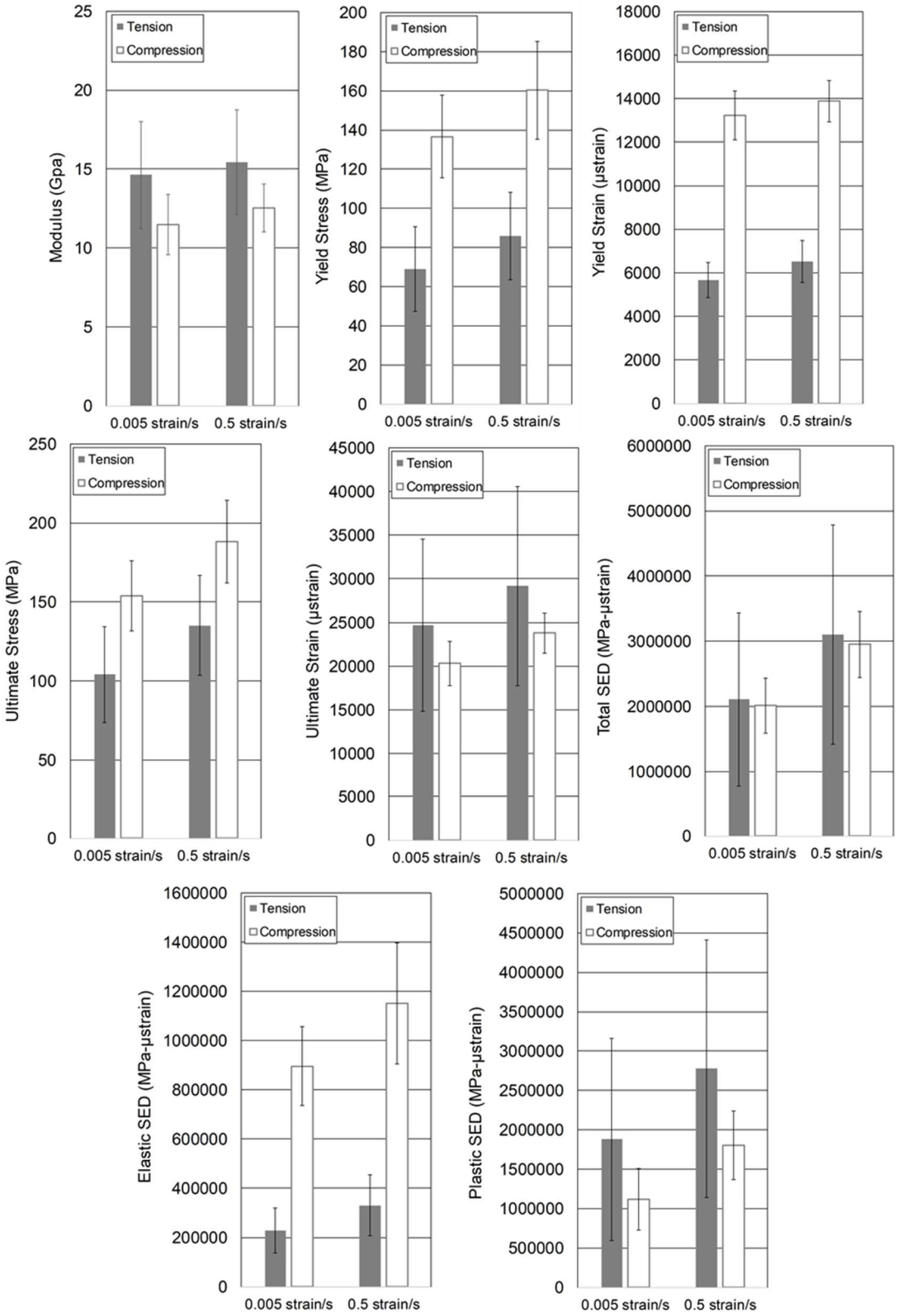

Figure 41: Average compressive and tensile material property values from matched subjects for each loading rate with ±1 S.D. indicated by error bars

Conclusion

To the author's knowledge, this is the first study to quantify the compressive material properties of human rib cortical bone. The compressive modulus, ultimate stress, and ultimate strain values obtained in the current study were in the range of values reported by previous studies for other bones. However, the modulus was considerably lower and the ultimate strain was considerably higher than the average values from previous studies that tested femur and/or tibia cortical bone samples at loadings rates that were on the same order of magnitude. This could be due to the micro-architectural composition of the ribs, as compared to the tibia and femur. Therefore, the values reported in the current study should be incorporated into FEMs to more accurately model the compressive material response of the ribs. The trends with respect to loading rate were also consistent with the trends from previous studies, signifying the rate-dependent nature of rib cortical bone at relatively low strain rates. The compressive material properties at both loading rates did not show strong correlations with advancing age, but several material properties, including modulus, yield stress, and ultimate stress, showed moderate downward trends as age increased. When the potentially skeletally immature subjects (≤ 21) were removed from that analysis, the trends were considerably stronger. However, the R^2 values were still low for most material properties with respect to increased chronological age, indicating that there may be other underlying variables that better explain the variance within a given population. A statistical analysis of the compressive material properties with respect to density yielded several significant positive correlations with better R^2 values than the correlations with respect to age. However, the R^2 values did not exceed 0.358, and no other histological variables were measured. Consequently, more histological research should be conducted in parallel with material response testing in order to better assess the factors that affect the correlation between rib material properties and chronological age. When comparing the compressive material properties to the tensile material properties of matched subjects, it was apparent that the ultimate and yield stress of rib cortical bone was much larger in compression than in tension, while failure strain and plastic energy absorption were greater in tension. However, additional testing at multiple loading rates with a larger subject size is necessary in order to more fully assess the differences in material properties with respect to age, loading rate, and mode of loading. Overall, finite element models will be able to implement the data provided in the current study to more accurately model the material response of the thorax in the various dynamic loading conditions experience in MVCs.

REFERENCES

1. Kent R, Woods W, Bostrom O. Fatality Risk and the Presence of Rib Fractures. Annals of Advances in Automotive Medicine/Annual Scientific Conference; 2008.
2. Page Y, Cuny S, Hermitte T, Labrousse M. A comprehensive overview of the frequency and the severity of injuries sustained by car occupants and subsequent implications in terms of injury prevention. Annals of Advances in Automotive Medicine/Annual Scientific Conference: Association for the Advancement of Automotive Medicine; 2012. p. 165.
3. Elhagediab AM, Rouhana SW. Patterns of abdominal injury in frontal automotive crashes. 16th International Technical Conference on the Enhanced Safety of Vehicles. Washington, D.C.: NHTSA; 1998. p. 327-37.
4. Weaver AA, Talton JW, Barnard RT, Schoell SL, Swett KR, Stitzel JD. Estimated injury risk for specific injuries and body regions in frontal motor vehicle crashes. Traffic Injury Prevention. 2015;**16**(sup1):S108-S16.
5. Bulger EM, Arneson MA, Mock CN, Jurkovich GJ. Rib Fractures in the Elderly. Journal of Trauma and Acute Care Surgery. 2000 2000;**48(6)**:1040-7.
6. Augenstein J, Digges K, Bahouth G, Dalmotas D. Investigation of the Performance of Safety Systems for Protection of the Elderly. Annual Proceedings: Association for the Advancement of Automotive Medicine. 2005 2005;**49**:361.
7. Crandall JR, Bass CR, Pikey W, Miller H, Sikorski J, Wilkins M. Thoracic Response and Injury with Belt, Driver Side Airbag, and Force Limited Belt Restraint Systems. International Journal of Crashworthiness. 1996;**2(1)**:119-32.
8. Kent R, Patrie J. Chest Deflection Tolerance to Blunt Anterior Loading Is Sensitive to Age but Not Load Distribution. Forensic Science International. 2005;**149(2)**:121-8.
9. Kroell C, Schneider D, Nahum A. Impact Tolerance and Response of the Human Thorax. 15th Stapp Car Crash Conference: SAE International; 1971.
10. Yoganandan N, Pintar FA. Biomechanics of human thoracic ribs. Journal of Biomechanical Engineering. 1998;**120**(1):100-4.
11. Cormier JM, Stitzel JD, Duma SM, Matsuoka F. Regional variation in the structural response and geometrical properties of human ribs. Annual Proceedings/Association for the Advancement of Automotive Medicine: Association for the Advancement of Automotive Medicine; 2005. p. 153.
12. Stein ID, Granik G. Rib structure and bending strength: an autopsy study. Calcified Tissue International. 1976;**20**(1):61-73.
13. Granik G, Stein I. Human ribs: static testing as a promising medical application. Journal of Biomechanics. 1973;**6**(3):237-40.
14. Kemper AR, McNally C, Pullins CA, Freeman LJ, Duma SM, Rouhana SW. The biomechanics of human ribs: material and structural properties from dynamic tension and bending tests. Stapp Car Crash Journal. 2007;**51**.

15. Feuer G, Saha S. Effect of Strain Rate on the Bending Properties of Human Ribs. ASME 2011 Summer Bioengineering Conference: American Society of Mechanical Engineers; 2011. p. 907-8.
16. Schafman MA, Kang Y-S, Moorhouse K, White SE, Bolte IV JH, Agnew AM. Age and sex alone are insufficient to predict human rib structural response to dynamic AP loading. Journal of Biomechanics. 2016;**49**(14):3516-22.
17. Agnew AM, Moorhouse K, Murach M, White SE, Kang Y-S. Tensile stress in human ribs throughout the lifespan. Proceedings of IRCOBI Conference, IRC-14-44; 2014. p. 397-407.
18. Murach MM, Kang Y-S, Goldman SD, et al. Rib geometry explains variation in dynamic structural response: Potential implications for frontal impact fracture risk. Annals of Biomedical Engineering. 2017;**45**(9):2159-73.
19. Charpail E, Trosseille X, Petit P, Laporte S, Lavaste F, Vallancien G. Characterization of PMHS ribs: a new test methodology. Stapp Car Crash Journal. 2005;**49**:183-98.
20. Kindig M, Lau AG, Kent RW. Biomechanical response of ribs under quasistatic frontal loading. Traffic Injury Prevention. 2011;**12**(4):377-87.
21. Agnew AM, Schafman M, Moorhouse K, White SE, Kang Y-S. The effect of age on the structural properties of human ribs. Journal of the Mechanical Behavior of Biomedical Materials. 2015;**41**:302-14.
22. McCalden RW, McGeogh JA, Barker MB. Age-related changes in the tensile properties of cortical bone. Journal of Bone and Joint Surgery. 1993;**75**(8):1193-205.
23. Burstein AH, Reilly DT, Martens M. Aging of bone tissue: mechanical properties. The Journal of Bone and Joint Surgery. 1976;**58**(1):82-6.
24. Lindahl O, Lindgren AGH. Cortical bone in man ii. Variation in tensile strength with age and sex. Acta Orthopaedica Scandinavica. 1967;**38**(1-4):141-7.
25. Kemper AR, McNally C, Kennedy EA, et al. Material properties of human rib cortical bone from dynamic tension coupon testing. Stapp Car Crash Journal. 2005;**49**:199-230.
26. Subit D, de Dios EdP, Valazquez-Ameijide J, Arregui-Dalmases C, Crandall JR. Tensile material properties of human rib cortical bone under quasi-static and dynamic failure loading and influence of the bone microstucture on failure characteristics. https://arxivorg/abs/11080390. 2011.
27. Albert DL. Biomechanical Responses of Human Surrogates under Various Frontal Loading Conditions with an Emphasis on Thoracic Response and Injury Tolerance [Dissertation]. Blacksburg, VA: Virginia Polytechnic Institute and State University; 2018.
28. McElhaney J. Dynamic response of bone and muscle tissue. Journal of Applied Physiology. 1966;**21**(4):1231-6.
29. Silva LdMS, Ebacher V, Liu D, McKay H, Oxland TR, Wang R. Elasticity and Viscoelasticity of Human Tibial Cortical Bone Measured by Nanoindentation. Material Research Society Online Proceedings Library (MRS OPL). 2005;**874**.

30. Wood JL. Dynamic response of human cranial bone. Journal of Biomechanics. 1971;**4**(1):1-12.
31. Crowninshield RD, Pope MH. The response of compact bone in tension at various strain rates. Annals of Biomedical Engineering. 1974;**2**(2):217-25.
32. Nyman JS, Leng H, Dong XN, Wang X. Differences in the mechanical behavior of cortical bone between compression and tension when subjected to progressive loading. Journal of the Mechanical Behavior of Biomedical Materials. 2009;**2**(6):613-9.
33. Li S, Demirci E, Silberschmidt VV. Variability and anisotropy of mechanical behavior of cortical bone in tension and compression. Journal of the Mechanical Behavior of Biomedical Materials. 2013;**21**:109-20.
34. Carter DR, Hayes WC. Bone compressive strength: the influence of density and strain rate. Science. 1976;**194**(4270):1174-6.
35. Abrams E, Mohr M, Engel C, Bottlang M. Cross-sectional geometry of human ribs. Cortex. 2003;**80**:2.
36. Schoell SL, Weaver AA, Vavalle NA, Stitzel JD. Age-and sex-specific thorax finite element model development and simulation. Traffic Injury Prevention. 2015;**16**(sup1):S57-S65.
37. Antona-Makoshi J, Yamamoto Y, Kato R, et al. Age-dependent factors affecting thoracic response: a finite element study focused on Japanese elderly occupants. Traffic Injury Prevention. 2015;**16**(sup1):S66-S74.
38. Kent R, Lee S-H, Darvish K, et al. Structural and material changes in the aging thorax and their role in crash protection for older occupants: SAE Technical Paper; 2005.
39. Golman AJ, Danelson KA, Miller LE, Stitzel JD. Injury prediction in a side impact crash using human body model simulation. Accident Analysis & Prevention. 2014;**64**:1-8.
40. Li Z, Kindig MW, Kerrigan JR, et al. Rib fractures under anterior–posterior dynamic loads: experimental and finite-element study. Journal of Biomechanics. 2010;**43**(2):228-34.
41. Li Z, Kindig MW, Subit D, Kent RW. Influence of mesh density, cortical thickness and material properties on human rib fracture prediction. Medical Engineering & Physics. 2010;**32**(9):998-1008.
42. Cai Z, Lan F, Chen J, Zhao F. Development and validation of a finite element model of the human thoracic for rib fractures prediction in automobile collisions. Proceedings of the FISITA 2012 World Automotive Congress: Springer; 2013. p. 375-88.
43. Forman JL, Kent RW, Mroz K, Pipkorn B, Bostrom O, Segui-Gomez M. Predicting rib fracture risk with whole-body finite element models: development and preliminary evaluation of a probabilistic analytical framework. Annals of Advances in Automotive Medicine/Annual Scientific Conference: Association for the Advancement of Automotive Medicine; 2012. p. 109.
44. IIHS. Fatality Facts, Teenagers. 2017 [cited 2019 2/15/19]
45. Albert DL, Kang Y-S, Agnew AM, Kemper AR. A Comparison of Rib Structural and Material Properties from Matched Whole Rib Bending and Tension Coupon Tests. IRCOBI Conference Proceedings; 2017.

46. Borchers RE, Gibson LJ, Burchardt H, Hayes WC. Effects of selected thermal variables on the mechanical properties of trabecular bone. Biomaterials. 1995;**16**(7):545-51.
47. Hamer AJ, Strachan JR, Black MM, Ibbotson CJ, Stockley I, Elson RA. Biomechanical properties of cortical allograft bone using a new method of bone strength measurement: a comparison of fresh, fresh-frozen and irradiated bone. The Journal of Bone and Joint Surgery. 1996;**78**(3):363-8.
48. Linde F, Sørensen HCF. The effect of different storage methods on the mechanical properties of trabecular bone. Journal of Biomechanics. 1993;**26**(10):1249-52.
49. Panjabi MM, Krag M, Summers D, Videman T. Biomechanical time-tolerance of fresh cadaveric human spine specimens. Journal of Orthopaedic Research. 1985;**3**(3):292-300.
50. Pelker RR, Friedlaender GE, Markham TC, Panjabi MM, Moen CJ. Effects of freezing and freeze-drying on the biomechanical properties of rat bone. Journal of Orthopaedic Research. 1983;**1**(4):405-11.
51. Duma S, Stitzel J, Kemper A, McNally C, Kennedy E, Matsuoka F. Non-censored rib fracture data from dynamic belt loading tests on the human cadaver thorax. Proc 19th International Technical Conference on the Enhanced Safety of Vehicles. Washington, DC: NHTSA; 2005.
52. Thomas P, Frampton R. Large and small cars in real-world crashes-patterns of use, collision types and injury outcomes. Annual Proceedings/Association for the Advancement of Automotive Medicine; 1999: Association for the Advancement of Automotive Medicine; 1999. p. 101.
53. Carter DR, Hayes WC. The Compressive Behavior of Bone as a Two-Phase Porous Structure. The Journal of Bone and Joint Surgery. 1977;**59**(7):954-62.
54. SAE. Instrumentation for Impact Test. Society of Automotive Engineers. Warrendale, PA; 1995.
55. Stefan U, Michael B, Werner S. Effects of three different preservation methods on the mechanical properties of human and bovine cortical bone. Bone. 2010;**47**(6):1048-53.
56. Albert D, Kang YS, Agnew A, Kemper A. The effect of injurious whole rib loading on rib cortical bone material properties. International Council on Biomechanics of Injury. 2018:680-7.
57. Lessley D, Crandall J, Shaw G, Kent R, Funk J. A normalization technique for developing corridors from individual subject responses. 2004 SAE World Congress. Detroit, MI; 2004.
58. Zhou Q, Rouhana SW, Melvin JW. Age effects on thoracic injury tolerance. 40th Stapp Car Crash Conference; 1996.
59. Kirchner H. Ductility and brittleness of bone. International Journal of Fracture. 2006;**139**(3-4):509-16.
60. Currey JD. The effects of strain rate, reconstruction and mineral content on some mechanical properties of bovine bone. Journal of Biomechanics. 1975;**8**(1):81-6.

61. Tomar V. Insights into the effects of tensile and compressive loadings on microstructure dependent fracture of trabecular bone. Engineering Fracture Mechanics. 2009;**76**(7):884-97.
62. Wachter NJ, Krischak GD, Mentzel M, et al. Correlation of bone mineral density with strength and microstructural parameters of cortical bone in vitro. Bone. 2002;**31**(1):90-5.
63. Smith CB, Smith DA. Relations between age, mineral density and mechanical properties of human femoral compacta. Acta Orthopaedica Scandinavica. 1976;**47**(5):496-502.
64. Dominguez VM, Agnew AM. Patterns in resorptive spaces in elderly rib cortices. American Journal of Physical Anthropology. 2014;**153**:107-.
65. Zebaze R, Seeman E. Cortical bone: a challenging geography. Journal of Bone Mineral Research. 2015;**30**(1):24-9.
66. Team RC. R Core Team. A language and environment for statistical computing. R Foundation for Statistical Computing, Vienna, Austria 2015. ISBN 3–900051–07–0, URL: https://www.R-project.org/; 2015.
67. Champely S, Ekstrom C, Dalgaard P, Gill J, Wunder J, De Rosario H. Basic functions for power analysis. R; 2015.
68. Wang X, Bank RA, TeKoppele JM, Agrawal CM. The role of collagen in determining bone mechanical properties. Journal of Orthopaedic Research. 2001;**19**(6):1021-6.
69. Ritchie RO, Buehler MJ, Hansma P. Plasticity and toughness in bone. Physics Today. 2009:41-7.
70. Wynnyckyj C, Willett TL, Omelon S, Wang J, Wang Z, Grynpas MD. Changes in bone fatigue resistance due to collagen degradation. Journal of Orthopaedic Research. 2011;**29**(2):197-203.
71. Martin RB, Ishida J. The relative effects of collagen fiber orientation, porosity, density, and mineralization on bone strength. Journal of Biomechanics. 1989;**22**(5):419-26.
72. Zebaze RMD, Ghasem-Zadeh A, Bohte A, et al. Intracortical remodelling and porosity in the distal radius and post-mortem femurs of women: a cross-sectional study. The Lancet. 2010;**375**(9727):1729-36.
73. Duma SM, Kemper AR, Stitzel JD, McNally C, Kennedy EA, Matsuoka F. Rib fracture timing in dynamic belt tests with human cadavers. Journal of Clinical Anatomy. 2011;**24**(3):327-38.
74. Cech D, Martin S. Functional movement development across the life span. LWW; 1995.
75. White TD, Black MT, Folkens PA. Human osteology: Academic press; 2011.
76. Crowder C, Austin D. Age ranges of epiphyseal fusion in the distal tibia and fibula of contemporary males and females. Journal of Forensic Science. 2005;**50**(5):JFS2004542-7.
77. O'Connor J, Bogue C, Spence L, Last J. A method to establish the relationship between chronological age and stage of union from radiographic assessment of epiphyseal fusion at the knee: an Irish population study. Journal of Anatomy. 2008;**212**(2):198-209.
78. Scheuer L, Black S. The juvenile skeleton: Elsevier; 2004.

79. Wu K, Schubeck KE, Frost HM, Villanueva A. Haversian bone formation rates determined by a new method in a mastodon, and in human diabetes mellitus and osteoporosis. Calcified Tissue Research. 1970;**6**(1):204-19.
80. Agnew AM, Moorhouse K, Kang Y-S, et al. The response of pediatric ribs to quasi-static loading: mechanical properties and microstructure. Annals of Biomedical Engineering. 2013;**41**(12):2501-14.
81. Hansen U, Zioupos P, Simpson R, Currey JD, Hynd D. The effect of strain rate on the mechanical properties of human cortical bone. Journal of Biomechanical Engineering. 2008;**130**(1):011011.
82. Li S, Demirci E, Silberschmidt VV. Variability and anisotropy of mechanical behavior of cortical bone in tension and compression. Journal of the Mechanical Behavior of Biomedical Materials. 2013;**21**:109-20.
83. ASTM C. Standard test method for compressive strength of cylindrical concrete specimens. ASTM C39/C39M-12; 2012.
84. Dong XN, Acuna RL, Luo Q, Wang X. Orientation dependence of progressive post-yield behavior of human cortical bone in compression. Journal of Biomechanics. 2012;**45**(16):2829-34.
85. McAlister G, Moyle D. Some mechanical properties of goose femoral cortical bone. Journal of Biomechanics. 1983;**16**(8):577-89.
86. ASTM. D695-15. Standard test method for compressive properties of rigid plastics. 2015.
87. Reilly DT, Burstein AH, Frankel VH. The elastic modulus for bone. Journal of Biomechanics. 1974;**7**(3):271-5.
88. Evans FG, Vincentelli R. Relations of the compressive properties of human cortical bone to histological structure and calcification. Journal of Biomechanics. 1974;**7**(1):1-10.
89. Handschin R, Stern W. X-ray diffraction studies on the lattice perfection of human bone apatite (Crista iliaca). Bone. 1995;**16**(4):S355-S63.
90. Hunter DJ, Sambrook PN, Therapy. Bone loss: epidemiology of bone loss. Arthritis Research. 2000;**2**(6):441.
91. Wright TM, Hayes WC. Tensile testing of bone over a wide range of strain rates: effects of strain rate, microstructure and density. Journal of Medical and Biological Engineering. 1976;**14**(6):671.
92. Keller TS. Predicting the compressive mechanical behavior of bone. Journal of Biomechanics. 1994;**27**(9):1159-68.

APPENDIX A

Table A1: Subject demographics and successful tensile and compression tests.

Subject Number	Age (years)	Sex	Weight (kg)	Height (cm)	Successful 0.5 s^{-1} Tensile Test	Successful 0.005 s^{-1} Tensile Test	Successful 0.5 s^{-1} Compression Test	Successful 0.005 s^{-1} Compression Test
0187	17	M	85	183	x	x		
300	18	M	62	170	x	x	x	x
379	18	F	50	165	x	x	x	x
383	18	M	66	168	x	xx		
385	18	M	66	178	x	x	x	x
293	19	M	113	183	x	x	x	x
152	21	M	53	168	x	x		
167	24	F	54	168	x	x	x	x
382	25	F	59	163	x	x		
262	25	M	73	178		x	x	x
155	26	F	64	170	x		x	x
98	26	M	55	173	x	x	x	x
0400	28	F	91	158		x		
350	30	F	69	165	x		x	x
386	32	M	61	178	x	x		
238	33	M	82	178	x	x	x	x
183	33	M	83	199	x	x		
222	34	F	73	173	x	x		
351	34	M	81	191	x	x	x	x
240	35	F	71	155	x	x		
175	35	F	82	173	x	x	x	x
228	40	F	127	165	x	x	x	x
260	45	F	66	166	x	x	x	x
377	47	M	38	173	x	x	x	x
267	48	M	67	175	x	x	x	x
229	50	F	77	168	x	x	x	x
219	51	F	77	157	x	x	x	x
249	54	M	79	183	x	x	x	x
259	54	F	47	163	x	x		
244	57	M	89	175	x	xx		
247	58	M	93	185	x	x	x	x
233	59	M	60	168	x	x		
242	59	M	75	191	x	x		
220	60	M	94	188	x	x	x	x
344	65	F	54	152		x		
227	66	F	63	167	x	xx	x	x

246	66	M	63	168	x	x	x	x
251	69	M	86	187	x	x	x	x
180	69	F	48	158	x	x		
239	70	F	n/a	n/a	x	x		
250	73	M	63	183	x	x	x	x
265	73	M	74	168	x	x		
221	74	F	44	155	x	x		
103	75	F	81	168	xx	x		
224	76	F	83	158	x	x		
225	78	M	102	183	x	x	x	x
223	82	F	59	160	x	x		
235	83	M	84	173	x	xx	x	x
236	84	F	46	165	x			
105	85	M	44	188	x	x		
367	87	F	32	163	x	x		
363	87	F	49	158	x	x		
234	89	M	83	183	x	x	x	x
352	90	F	54	158	x	x		
231	92	F	32	142	x	x		
261	93	F	61	158	x	x	x	x
226	94	M	100	175	x	x		
248	95	M	58	178	x	x	x	x
245	97	M	79	150	x	x		
384	98	M	86	191	x	x		
241	99	F	51	160	x	x		

Note: x = one (1) successful test, xx = two (2) successful tests averaged

Table A2: Shapiro-Wilk normality test statistics for all tensile test parameters at 0.5 strain/s and 0.005 strain/s.

Test Parameter	0.005 strain/s		0.5 strain/s	
	W	**p-value**	**W**	**p-value**
Age	0.9358	**0.0043**	0.9328	**0.0032**
Modulus	0.9789	0.4055	0.9894	0.8941
Yield Stress	0.9701	0.1621	0.9845	0.6666
Yield Strain	0.9740	0.2471	0.9815	0.5187
Failure Stress	0.9855	0.7175	0.9592	**0.0488**
Failure Strain	0.9407	**0.0069**	0.9221	**0.0012**
Ultimate Stress	0.9827	0.5778	0.9582	**0.0440**
Elastic SED	0.9625	0.0706	0.9883	0.8501
Plastic SED	0.9129	**0.0005**	0.9206	**0.0010**
Total SED	0.9155	**0.0006**	0.9290	**0.0022**

Note: Bold text indicates a significant p-value

Table A3: Distribution of subjects by decade of life for studies on the tensile material properties of human cortical bone versus age.

Decade of Life	Age Range	Burstein et al. (1976)	Burstein et al. (1976)	McCalden et al. (1993)	Current Study	Current Study	Current + Kemper et al. (2005, 2007)
		Femur 0.05 s^{-1}	**Tibia 0.05 s^{-1}**	**Femur 0.03 s^{-1}**	**Rib 0.005 s^{-1}**	**Rib 0.5 s^{-1}**	**Rib 0.5 s^{-1}**
		# of Subjects	# of Subjects	# of Subjects	# of Subjects	# of Subjects	# of Subjects
1st	0-9	-	-	-	-	-	-
2nd	10-19	-	-	-	6	6	7
3rd	20-29	5	3	6	6	5	5
4th	30-39	2	1	2	7	8	8
5th	40-49	3	4	3	4	4	8
6th	50-59	6	6	8	8	8	9
7th	60-69	8	9	8	6	5	9
8th	70-79	7	4	11	7	7	8
9th	80-89	2	1	6	6	7	8
10th	90-99	-	-	1	8	8	8
11th	100-109	-	-	1	-	-	-
Total # of Subjects		**33**	**28**	**46**	**58**	**58**	**70**
AVG # of Subjects/ Decade		**4.7**	**4.0**	**5.1**	**6.4**	**6.4**	**7.8**

Table A4: ANOVA for the effect of sample thickness on tensile material properties.

Material Property	0.005 strain/s				0.5 strain/s			
	Thickness		Thickness*Age		Thickness		Thickness*Age	
	p-value	R^2	p-value	R^2	p-value	R^2	p-value	R^2
Modulus	0.2802	0.0231	0.3014	0.0190	0.5742	0.0265	0.5259	0.0070
Yield Stress	0.8239	0.0000	0.3682	0.0140	0.2721	0.0515	0.3525	0.0150
Yield Strain	0.1744	0.0151	0.9388	0.0001	0.0674	0.0804	0.2079	0.0280
Failure Stress	0.7276	0.0001	0.9492	0.0001	0.2981	0.0599	0.1471	0.0370
Failure Strain	0.3224	0.0006	0.1761	0.0324	0.4069	0.0464	0.4852	0.0090
Ultimate Stress	0.6226	0.0000	0.9294	0.0001	0.2971	0.0600	0.1484	0.0370
Elastic SED	0.5140	0.0025	0.4689	0.0090	0.1087	0.0757	0.7128	0.0020
Plastic SED	0.5862	0.0002	0.3669	0.0140	0.3113	0.0542	0.6126	0.0050
Total SED	0.5614	0.0001	0.4045	0.0120	0.2476	0.0597	0.6054	0.0050

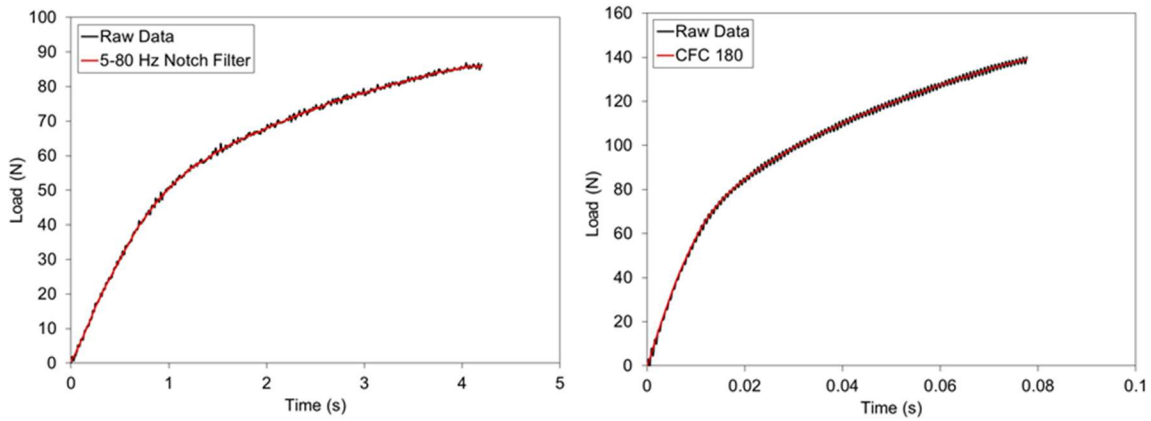

Figure A1: Filtered force versus time data plotted over the raw force versus time data for a tension coupon tested at 0.005 strain/s (left) and 0.5 strain/s (right).

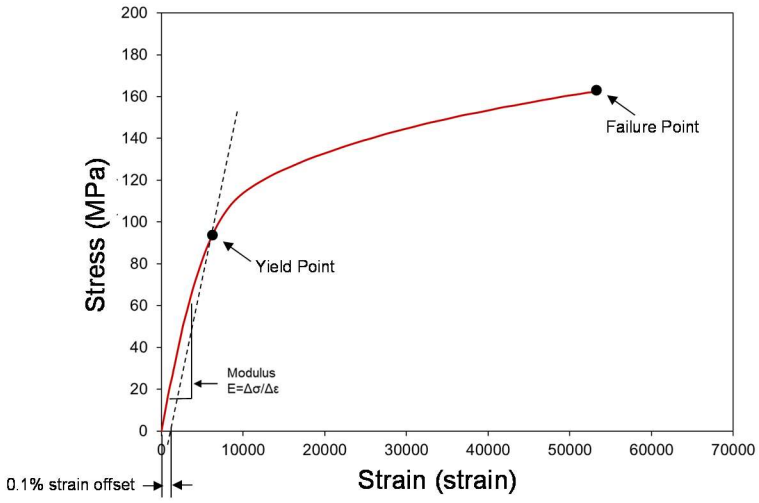

Figure A2: Material properties calculated for tension tests.

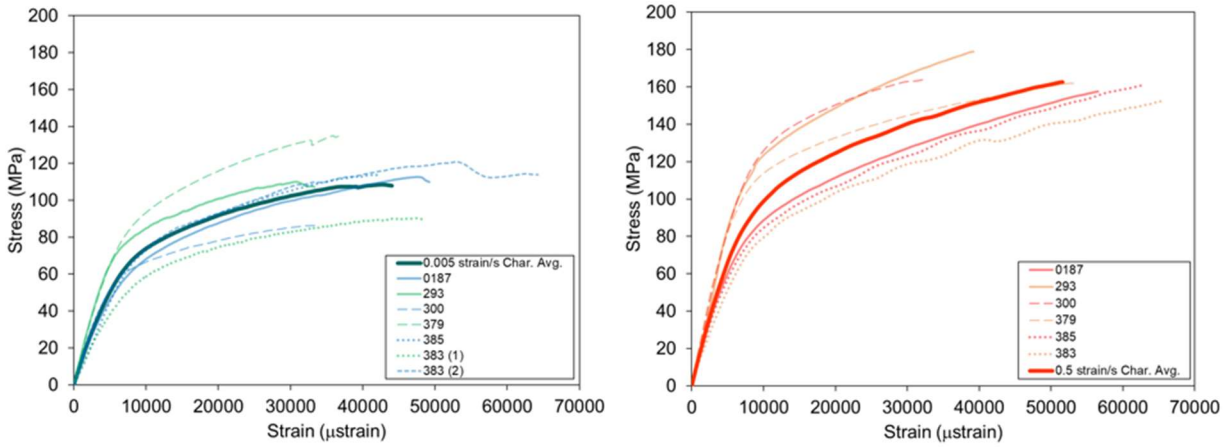

Figure A3: Stress-strain curves for tested tension coupons from subjects aged 10-19 years with characteristic average curve overlaid in bold for 0.005 strain/s loading rate (left) and 0.5 strain/s loading rate (right).

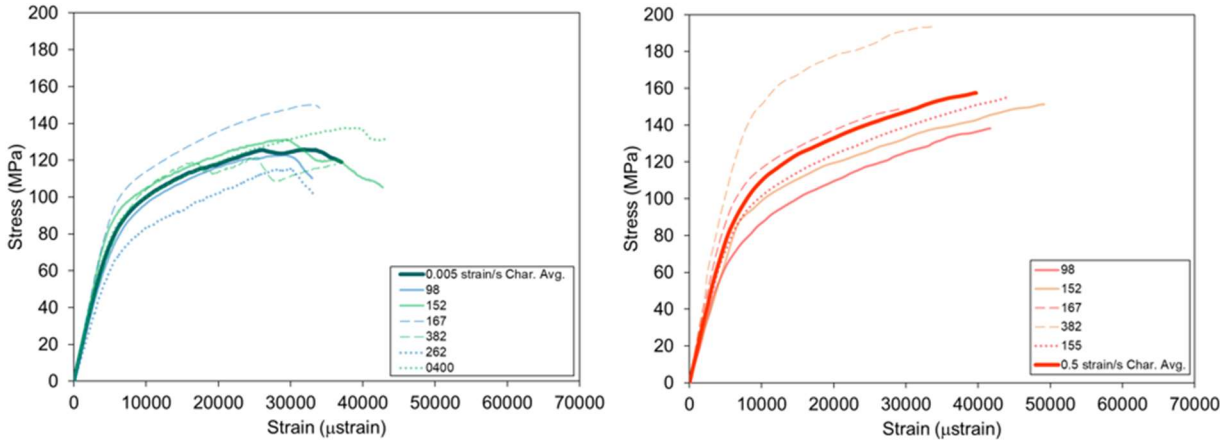

Figure A4: Stress-strain curves for tested tension coupons from subjects aged 20-29 years with characteristic average curve overlaid in bold for 0.005 strain/s loading rate (left) and 0.5 strain/s loading rate (right).

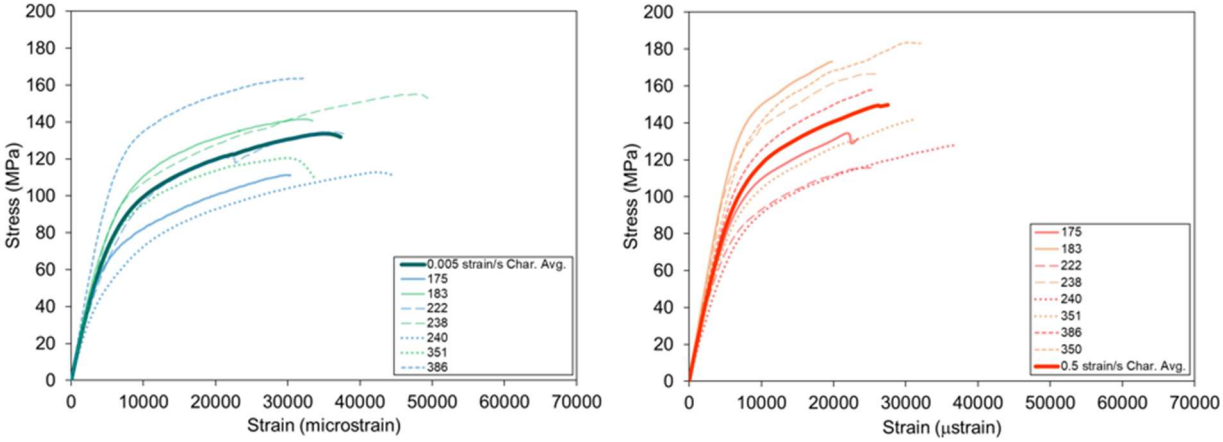

Figure A5: Stress-strain curves for tested tension coupons from subjects aged 30-39 years with characteristic average curve overlaid in bold for 0.005 strain/s loading rate (left) and 0.5 strain/s loading rate (right).

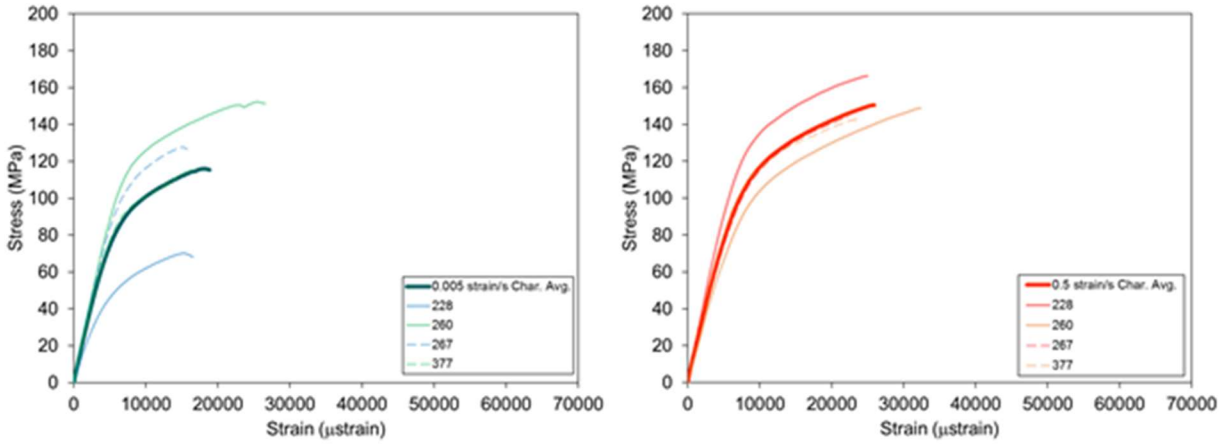

Figure A6: Stress-strain curves for tested tension coupons from subjects aged 40-49 years with characteristic average curve overlaid in bold for 0.005 strain/s loading rate (left) and 0.5 strain/s loading rate (right).

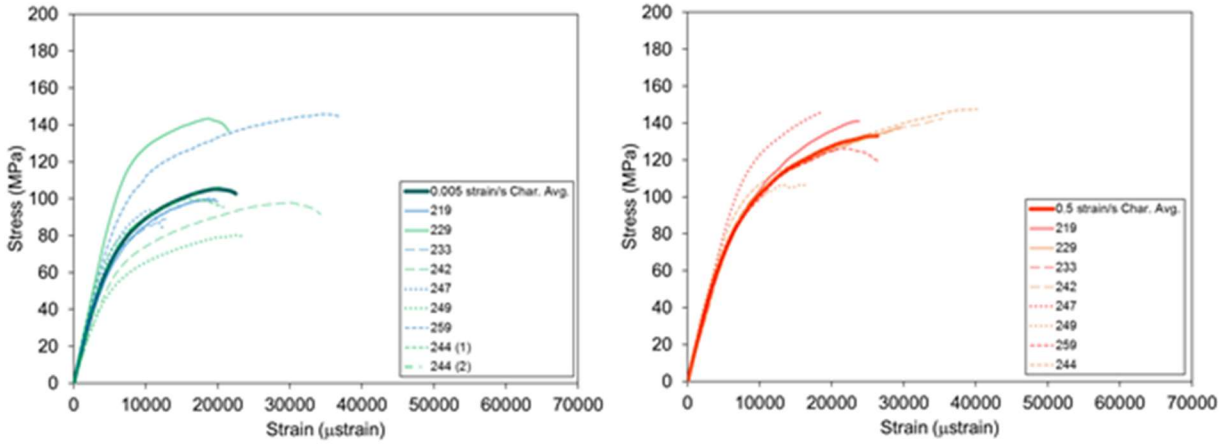

Figure A7: Stress-strain curves for tested tension coupons from subjects aged 50-59 years with characteristic average curve overlaid in bold for 0.005 strain/s loading rate (left) and 0.5 strain/s loading rate (right).

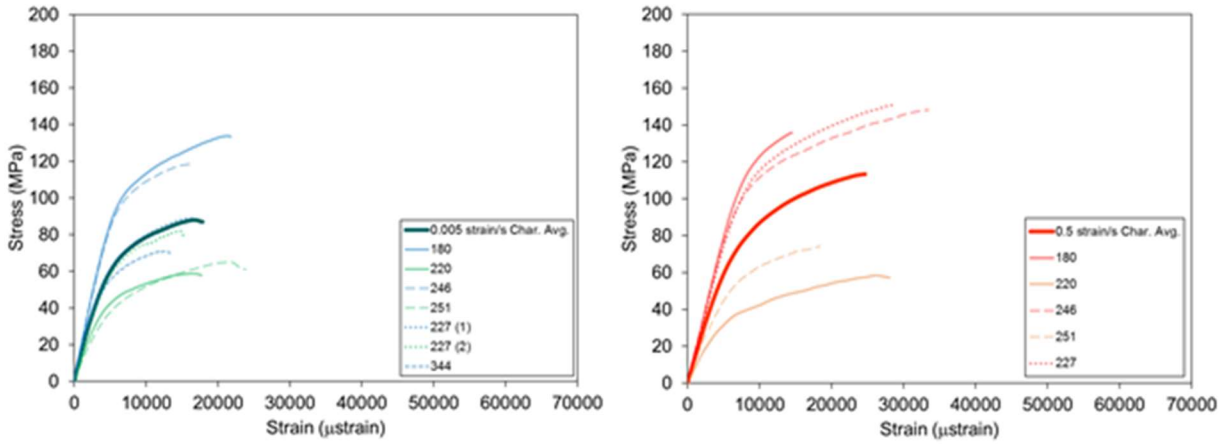

Figure A8: Stress-strain curves for tested tension coupons from subjects aged 60-69 years with characteristic average curve overlaid in bold for 0.005 strain/s loading rate (left) and 0.5 strain/s loading rate (right).

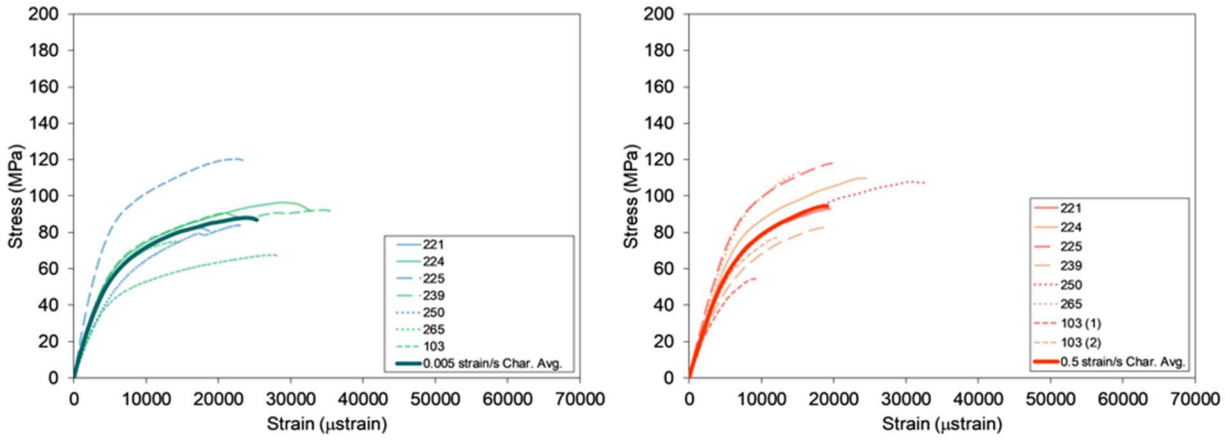

Figure A9: Stress-strain curves for tested tension coupons from subjects aged 70-79 years with characteristic average curve overlaid in bold for 0.005 strain/s loading rate (left) and 0.5 strain/s loading rate (right).

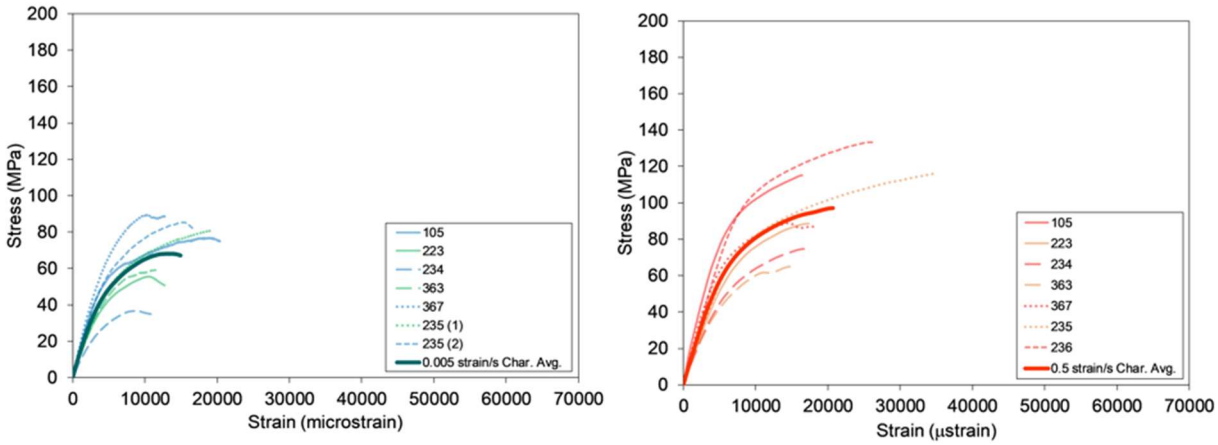

Figure A10: Stress-strain curves for tested tension coupons from subjects aged 80-89 years with characteristic average curve overlaid in bold for 0.005 strain/s loading rate (left) and 0.5 strain/s loading rate (right).

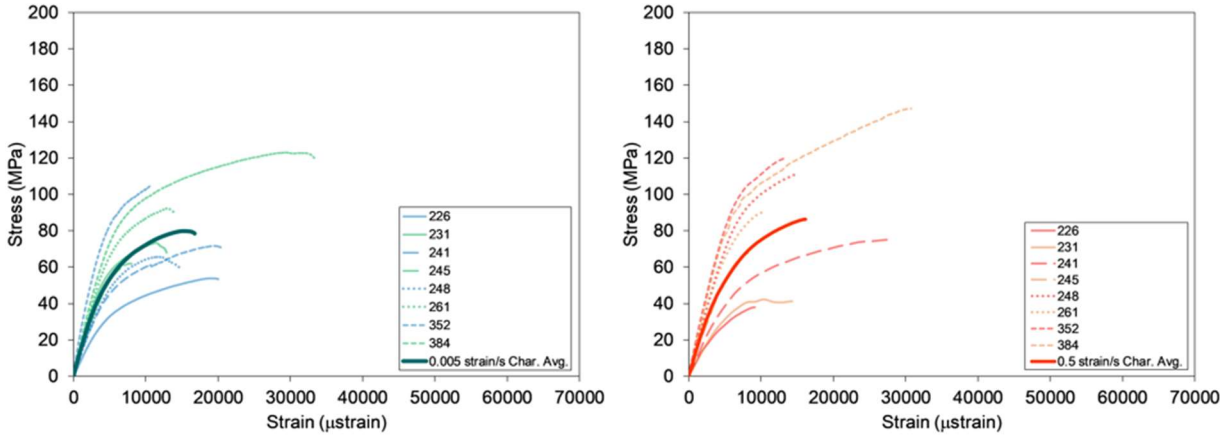

Figure A11: Stress-strain curves for tested tension coupons from subjects aged 90-99 years with characteristic average curve overlaid in bold for 0.005 strain/s loading rate (left) and 0.5 strain/s loading rate (right).

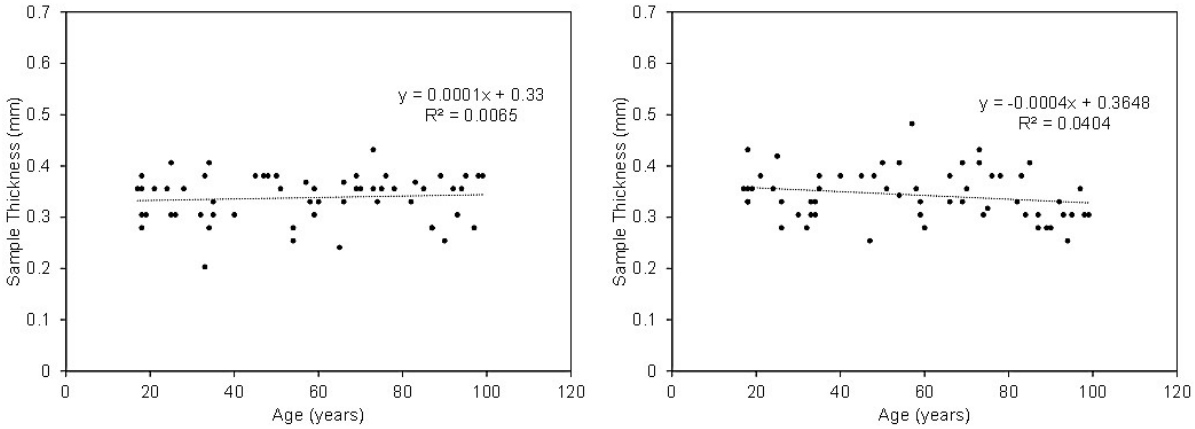

Figure A12: Correlation between sample thickness and age for 0.005 strain/s loading rate (left: p-value =0.5487) and 0.5 strain/s loading rate (right: p-value=0.1302) tensile tests.

Table A5: Spearman's rank correlation analysis for the effect of age on tensile material properties excluding subjects aged ≤21 years.

Material Property Variable	0.005 strain/s tests				0.5 strain/s tests		
	ρ	R^2	p-value		ρ	R^2	p-value
Modulus	-0.4262	0.169	**0.0018**		-0.5692	0.379	**<.0001**
Yield Stress	-0.5024	0.240	**0.0002**		-0.5126	0.283	**0.0001**
Yield Strain	-0.4485	0.156	**0.0010**		-0.1080	0.009	0.4507
Failure Stress	-0.6361	0.421	**<.0001**		-0.7184	**0.495**	**<.0001**
Failure Strain	-0.6027	0.409	**<.0001**		-0.5781	0.339	**<.0001**
Elastic SED	-0.4851	0.232	**0.0003**		-0.4287	0.179	**0.0017**
Plastic SED	-0.6918	0.482	**<.0001**		-0.6994	**0.490**	**<.0001**
Total SED	-0.6976	**0.491**	**<.0001**		-0.6998	**0.502**	**<.0001**

Notes: Bold text indicates a significant p-value or an R^2 value ≥ 0.49.

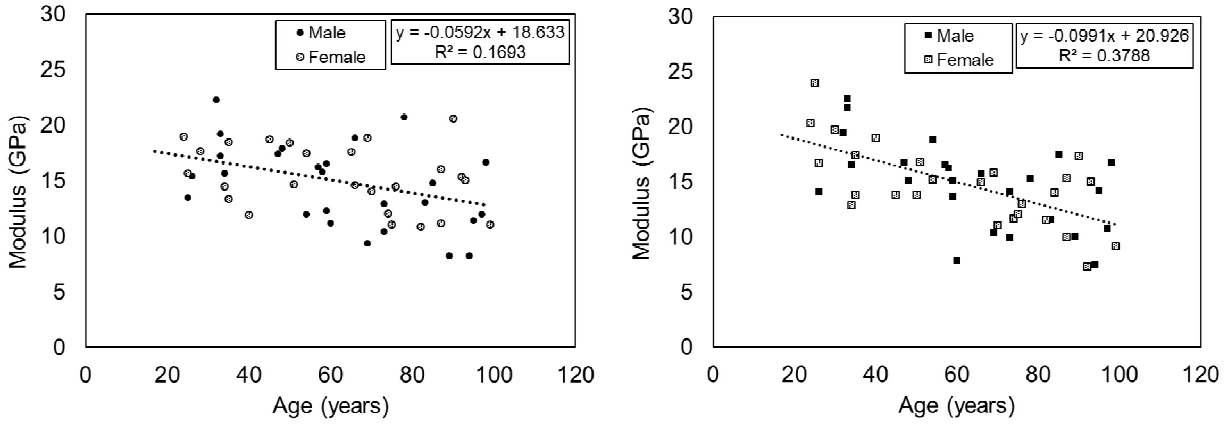

Figure A13: Modulus versus age for tensile tests at 0.005 strain/s (left) and 0.5 strain/s (right) for subjects >21 years old

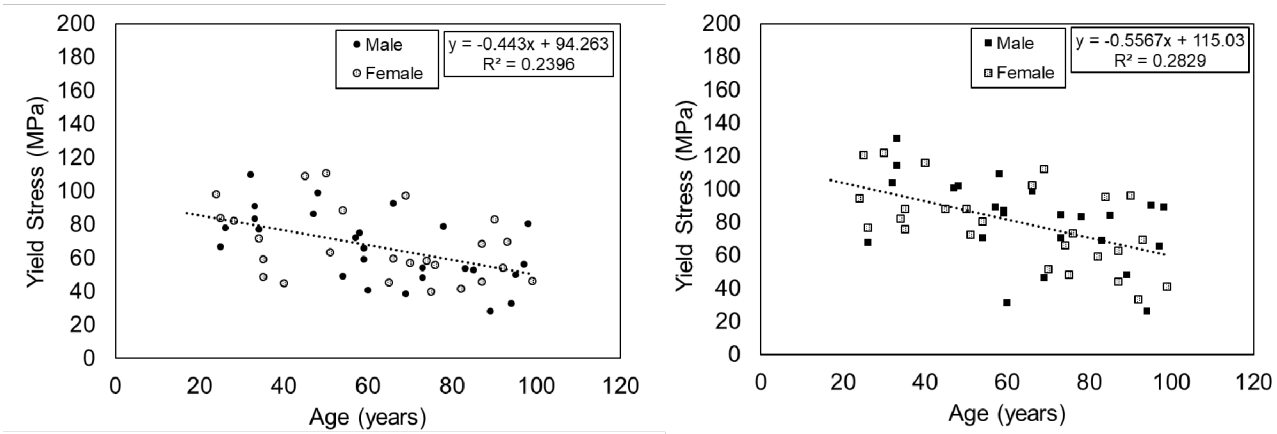

Figure A14: Yield stress versus age for tensile tests at 0.005 strain/s (left) and 0.5 strain/s (right) for subjects >21 years old

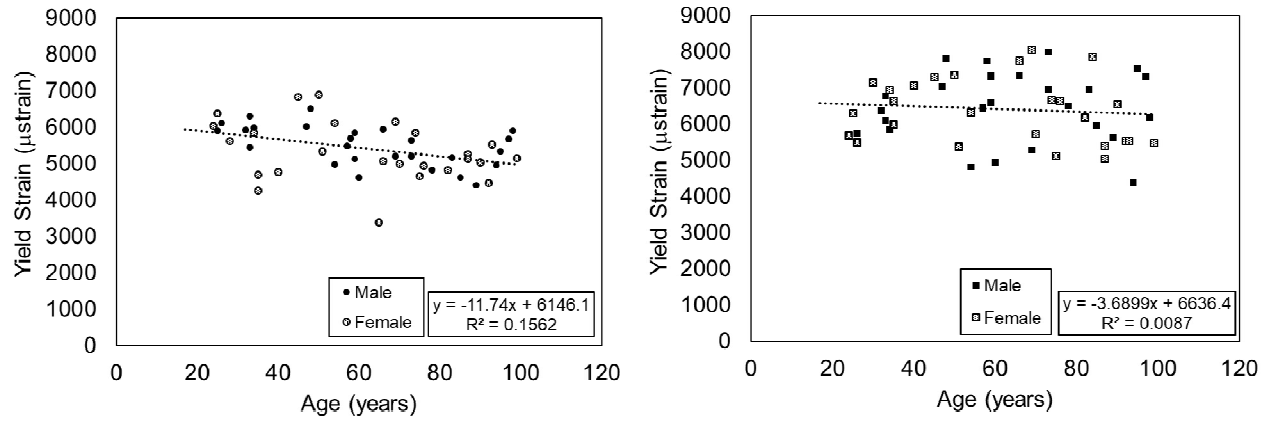

Figure A15: Yield strain versus age for tensile tests at 0.005 strain/s (left) and 0.5 strain/s (right) for subjects >21 years old

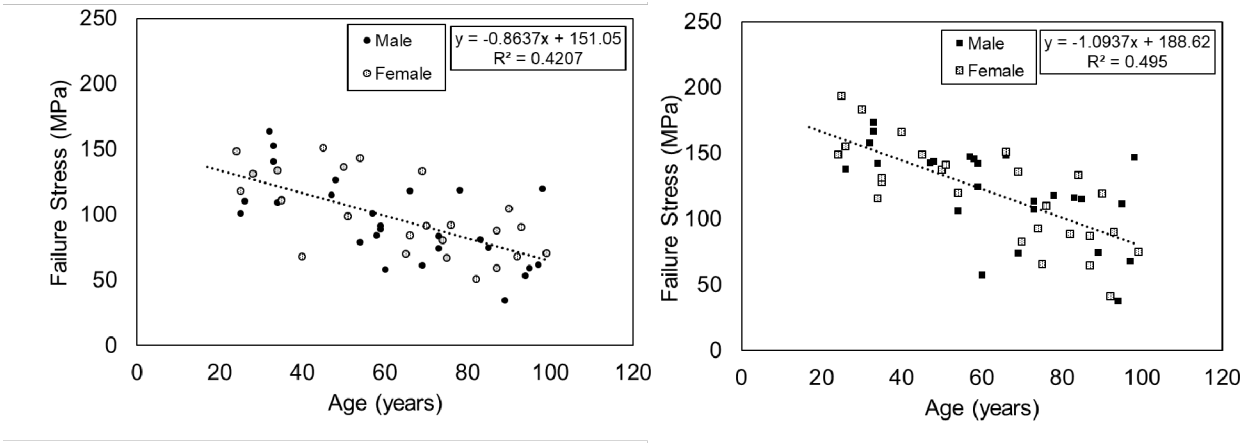

Figure A16: Failure stress versus age for tensile tests at 0.005 strain/s (left) and 0.5 strain/s (right) for subjects >21 years old

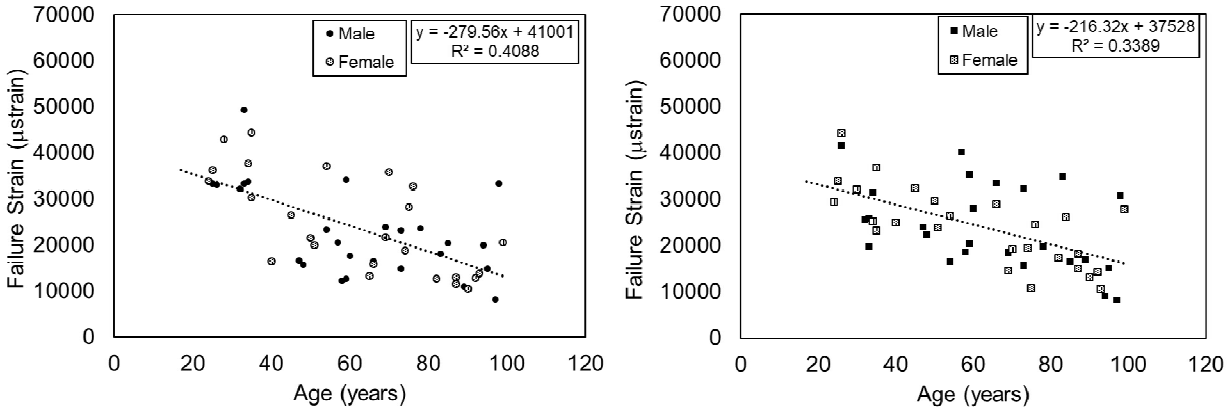

Figure A17: Failure strain versus age for tensile tests at 0.005 strain/s (left) and 0.5 strain/s (right) for subjects >21 years old

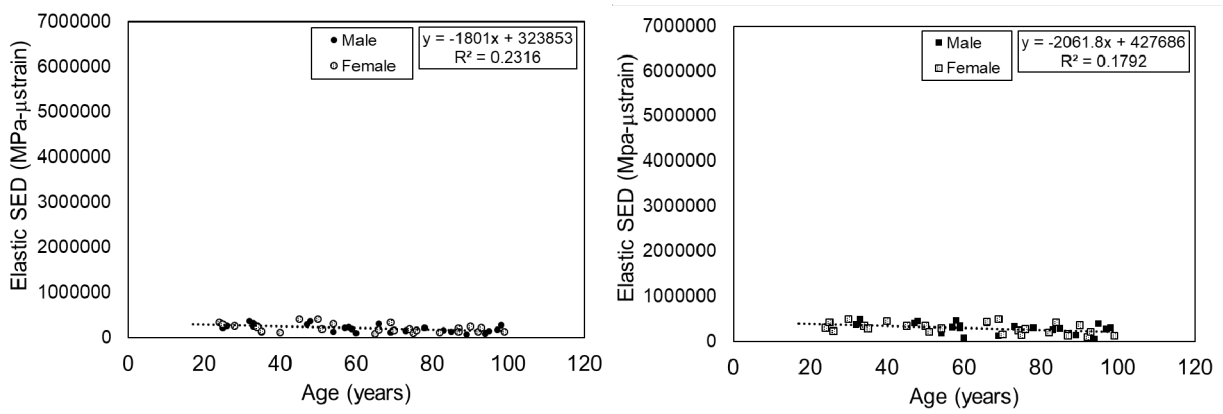

Figure A18: Elastic SED versus age for tensile tests at 0.005 strain/s (left) and 0.5 strain/s (right) for subjects >21 years old

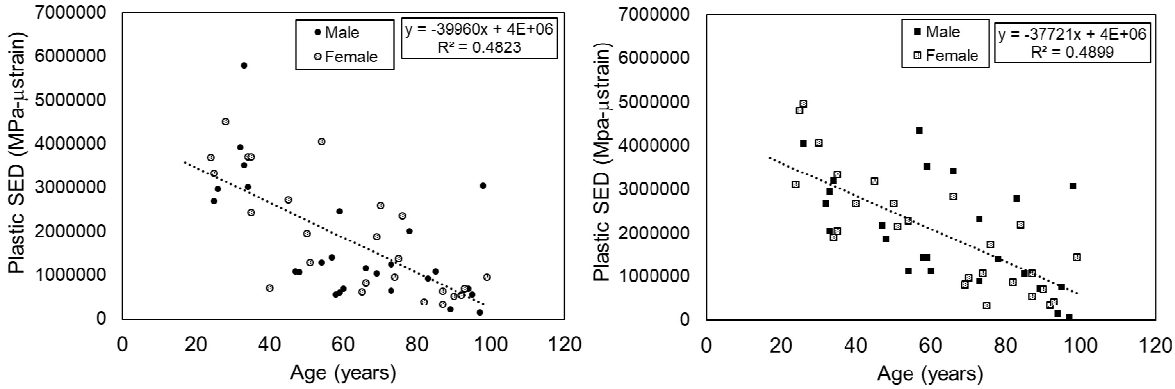

Figure A19: Plastic SED versus age for tensile tests at 0.005 strain/s (left) and 0.5 strain/s (right) for subjects >21 years old

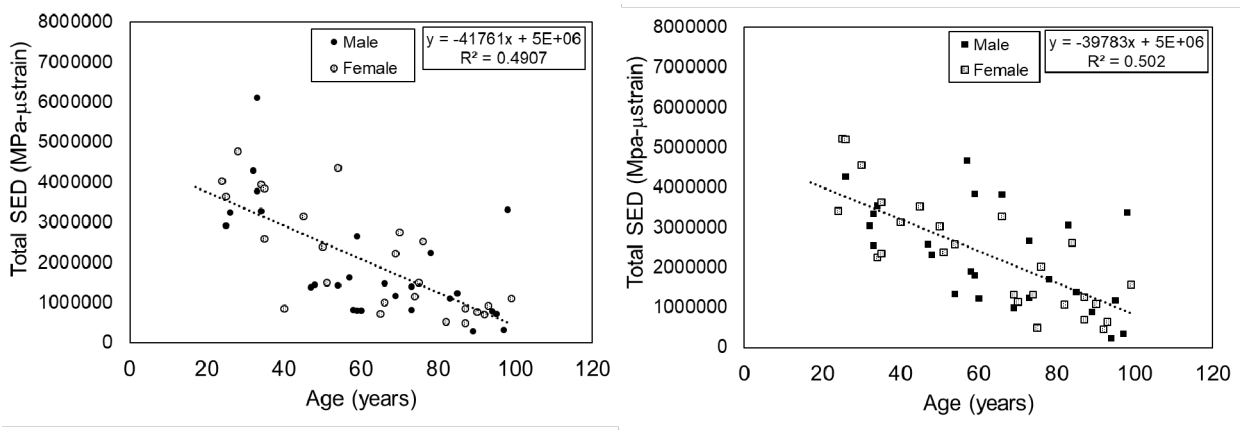

Figure A20: Total SED versus age for tensile tests at 0.005 strain/s (left) and 0.5 strain/s (right) for subjects >21 years old.

Table A6: Shapiro-Wilk normality test statistics for all compression test parameters at 0.5 strain/s and 0.005 strain/s.

Test Parameter	0.005 strain/s		0.5 strain/s	
	W	**p-value**	**W**	**p-value**
Age	0.9367	0.0742	0.9367	0.0742
Modulus	0.9563	0.2494	0.9826	0.8904
Yield Stress	0.9030	**0.0099**	0.9923	0.9983
Yield Strain	0.9391	0.0860	0.8768	**0.0024**
Ultimate Stress	0.9334	0.0607	0.9899	0.9905
Ultimate Strain	0.9772	0.7463	0.9462	0.1334
Elastic SED	0.9455	0.1282	0.9657	0.4300
Plastic SED	0.9804	0.8370	0.9399	0.0909
Total SED	0.9826	0.8894	0.9717	0.5873

Note: Bold text indicates a significant p-value

Table A7: Spearman's rank correlation analysis for the effect of age on compressive material properties excluding subjects aged ≤21 years.

Material Property Variable	0.005 strain/s tests				0.5 strain/s tests		
	ρ	**R^2**	**p-value**		**ρ**	**R^2**	**p-value**
Modulus	-0.2302	0.104	0.2580		-0.5055	0.275	**0.0084**
Yield Stress	-0.3653	0.123	0.0665		-0.5834	0.321	**0.0018**
Yield Strain	-0.0598	0.021	0.7715		-0.3369	0.122	0.0924
Ultimate Stress	-0.2093	0.070	0.3048		-0.5174	0.299	**0.0068**
Ultimate Strain	0.2890	0.056	0.1522		0.1180	0.031	0.5659
Elastic SED	-0.4001	0.072	**0.0428**		-0.5390	0.280	**0.0045**
Plastic SED	0.1447	0.007	0.4808		-0.0113	0.001	0.9564
Total SED	0.0458	0.001	0.8241		-0.2353	0.078	0.2472

Notes: Bold text indicates a significant p-value or an R^2 value ≥ 0.49.

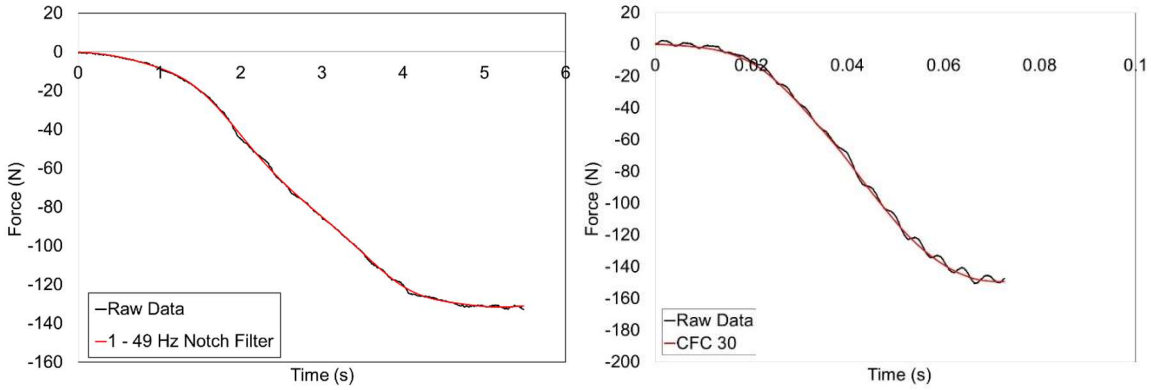

Figure A21: Filtered force versus time data plotted over the raw force versus time data for a compression sample tested at 0.005 strain/s (left) and 0.5 strain/s (right).

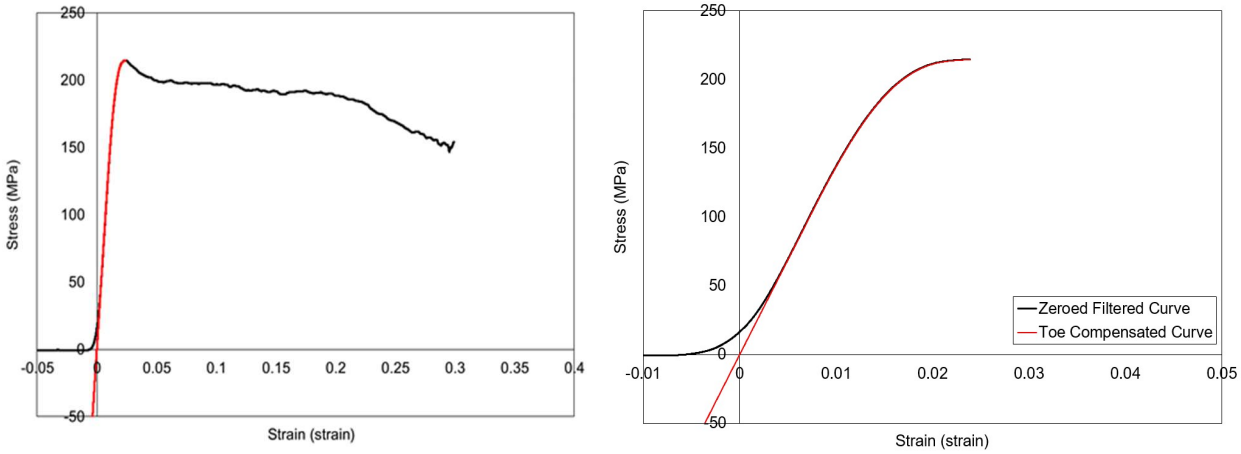

Figure A22: Full compression test filtered stress-strain curve with overlaid curve truncated at the ultimate stress (left) and zeroed, filtered stress-strain curve versus filtered toe-compensated curve (right).

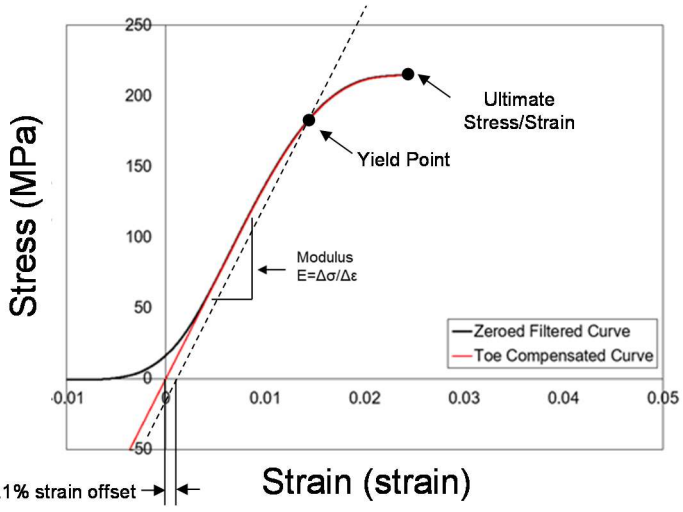

Figure A23: Material properties calculated for compression tests.

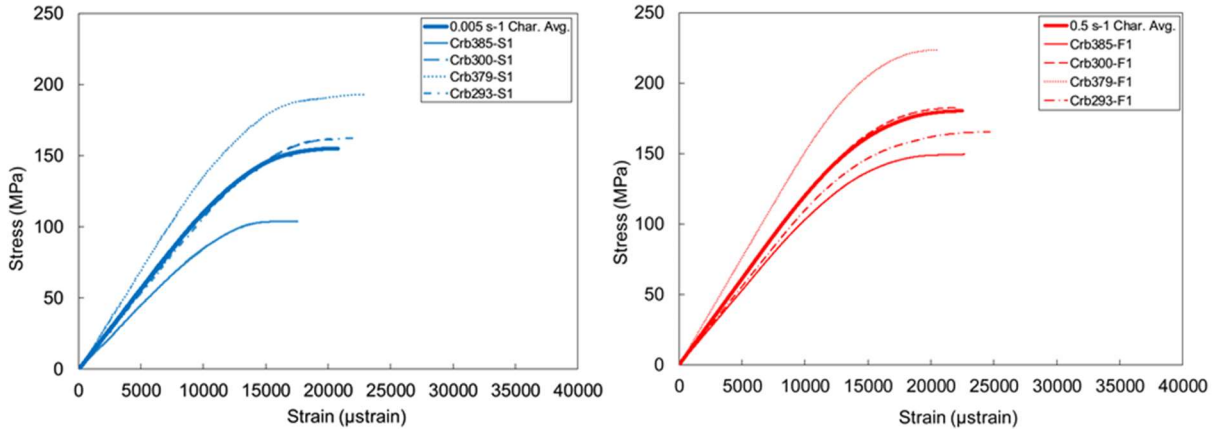

Figure A24: Stress-strain curves for tested compression samples from subjects aged 10-19 years for 0.005 strain/s loading rate (left) and 0.5 strain/s loading rate (right).

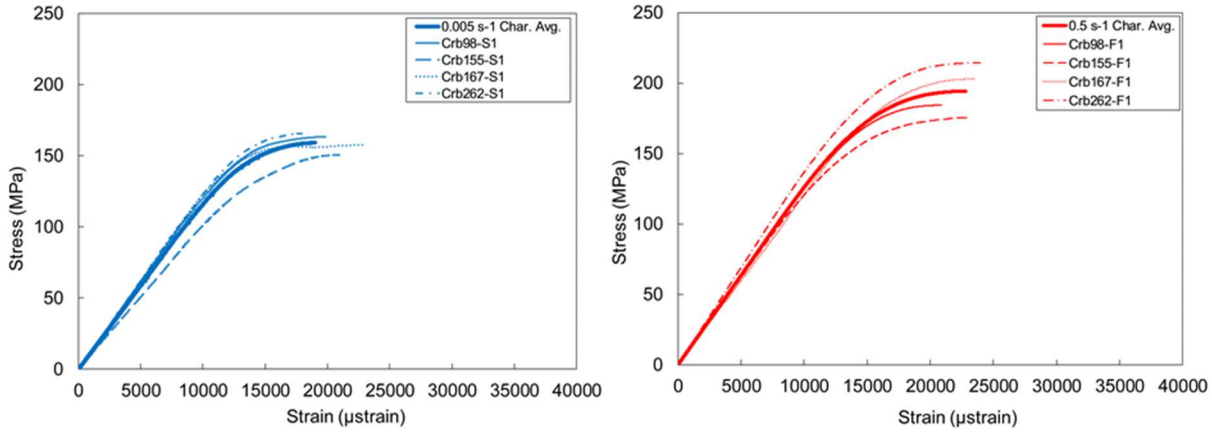

Figure A25: Stress-strain curves for tested compression samples from subjects aged 20-29 years for 0.005 strain/s loading rate (left) and 0.5 strain/s loading rate (right).

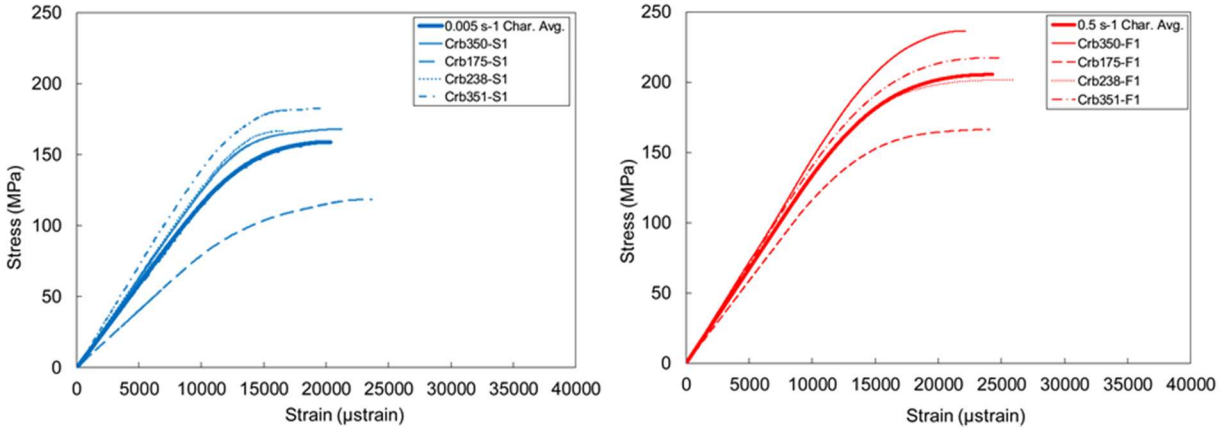

Figure A26: Stress-strain curves for tested compression samples from subjects aged 30-39 years for 0.005 strain/s loading rate (left) and 0.5 strain/s loading rate (right).

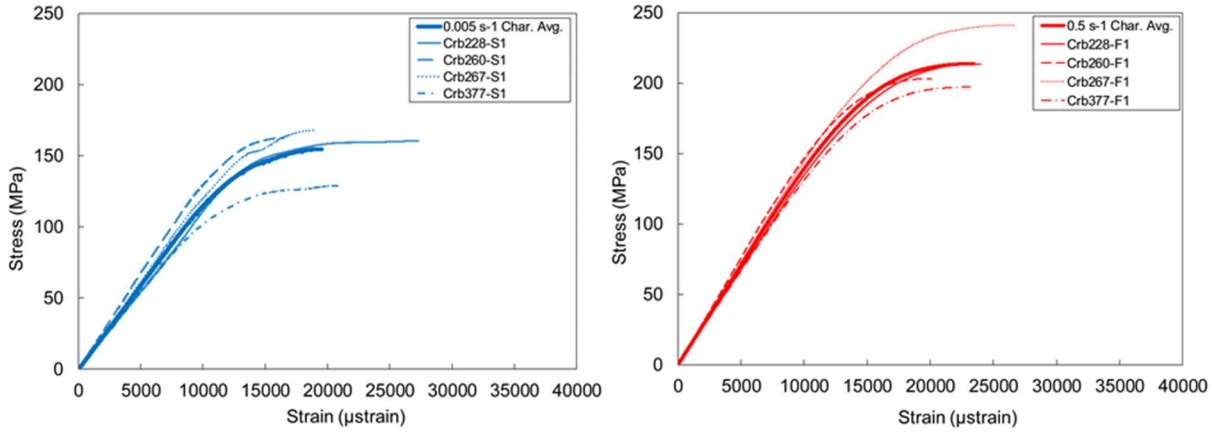

Figure A27: Stress-strain curves for tested compression samples from subjects aged 40-49 years for 0.005 strain/s loading rate (left) and 0.5 strain/s loading rate (right).

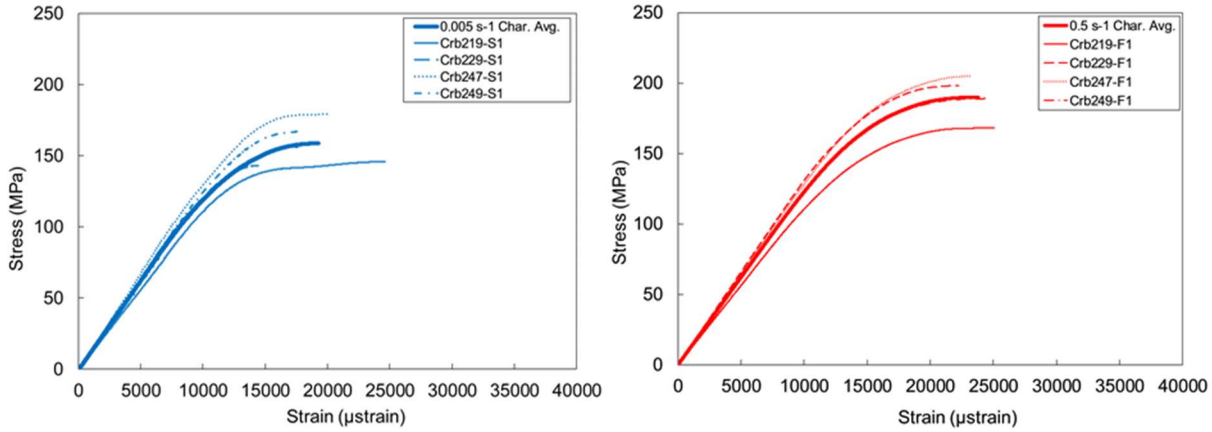

Figure A28: Stress-strain curves for tested compression samples from subjects aged 50-59 years for 0.005 strain/s loading rate (left) and 0.5 strain/s loading rate (right).

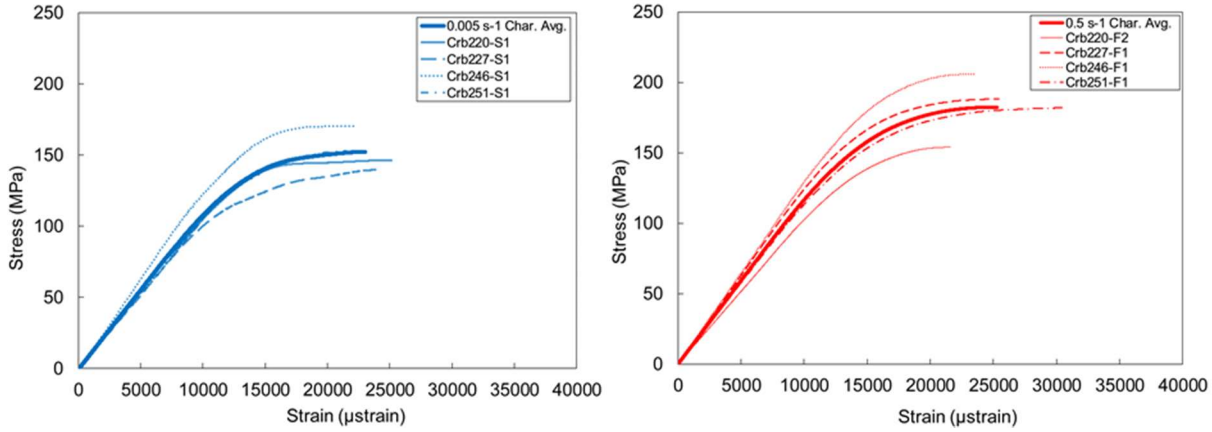

Figure A29: Stress-strain curves for tested compression samples from subjects aged 60-69 years for 0.005 strain/s loading rate (left) and 0.5 strain/s loading rate (right).

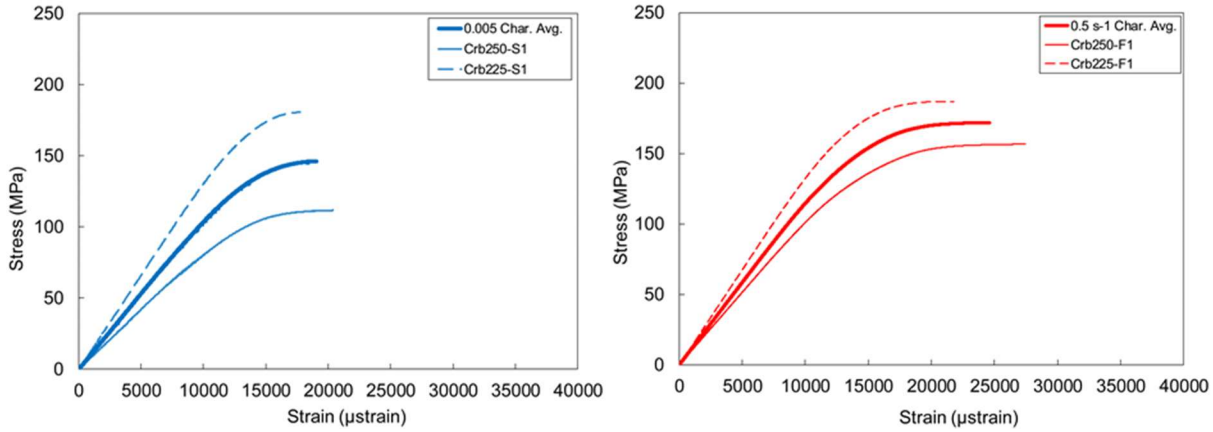

Figure A30: Stress-strain curves for tested compression samples from subjects aged 70-79 years for 0.005 strain/s loading rate (left) and 0.5 strain/s loading rate (right).

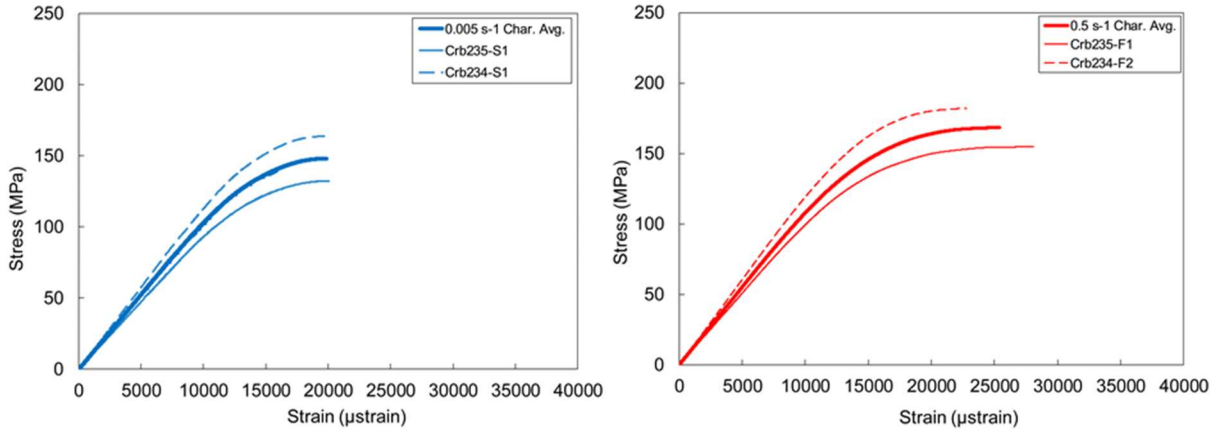

Figure A31: Stress-strain curves for tested compression samples from subjects aged 80-89 years for 0.005 strain/s loading rate (left) and 0.5 strain/s loading rate (right).

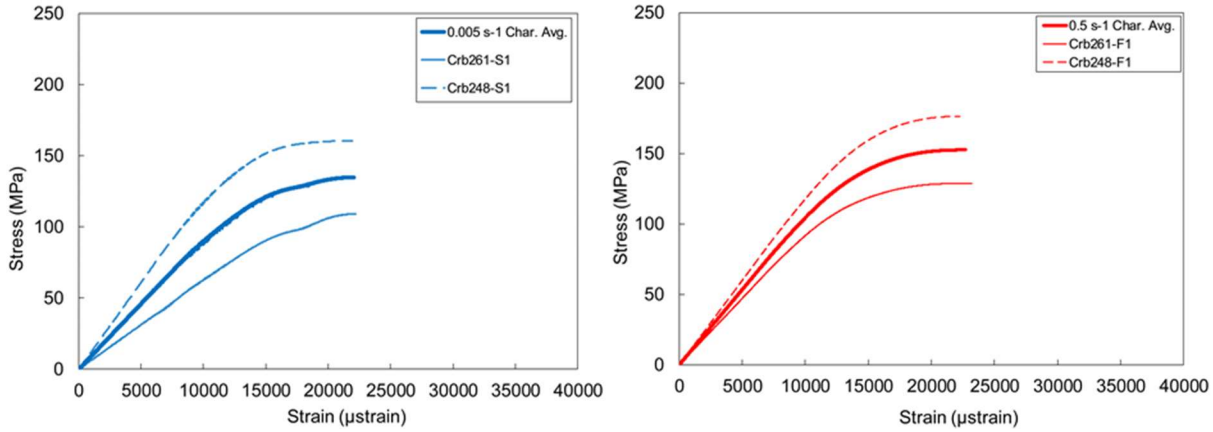

Figure A32: Stress-strain curves for tested compression samples from subjects aged 90-99 years for 0.005 strain/s loading rate (left) and 0.5 strain/s loading rate (right).

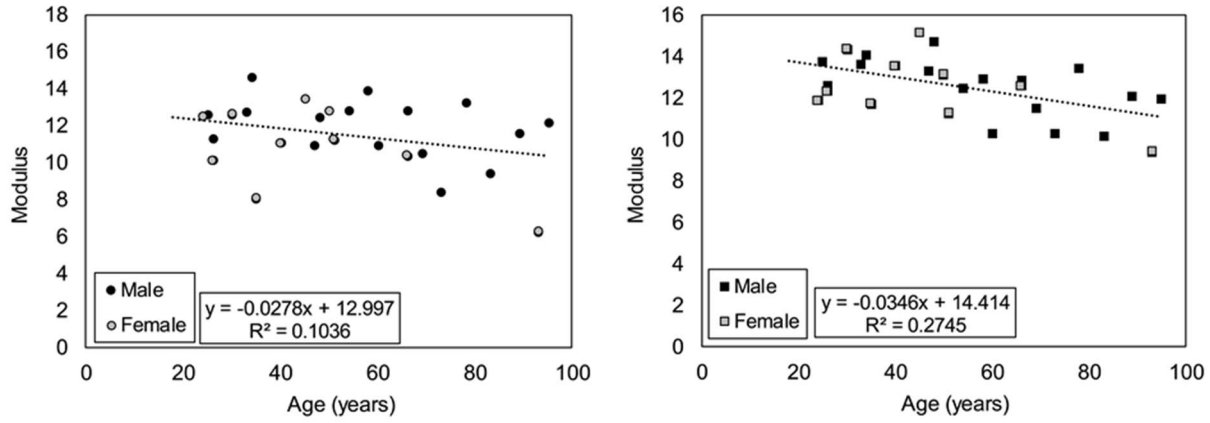

Figure A33: Modulus versus age for compression tests at 0.005 strain/s (left) and 0.5 strain/s (right) for subjects >21 years old.

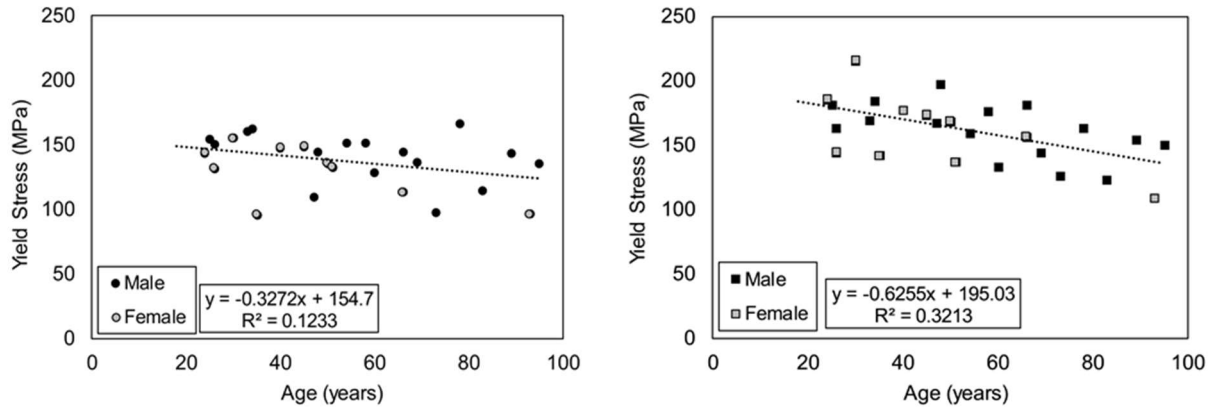

Figure A34: Yield stress versus age for compression tests at 0.005 strain/s (left) and 0.5 strain/s (right) for subjects >21 years old.

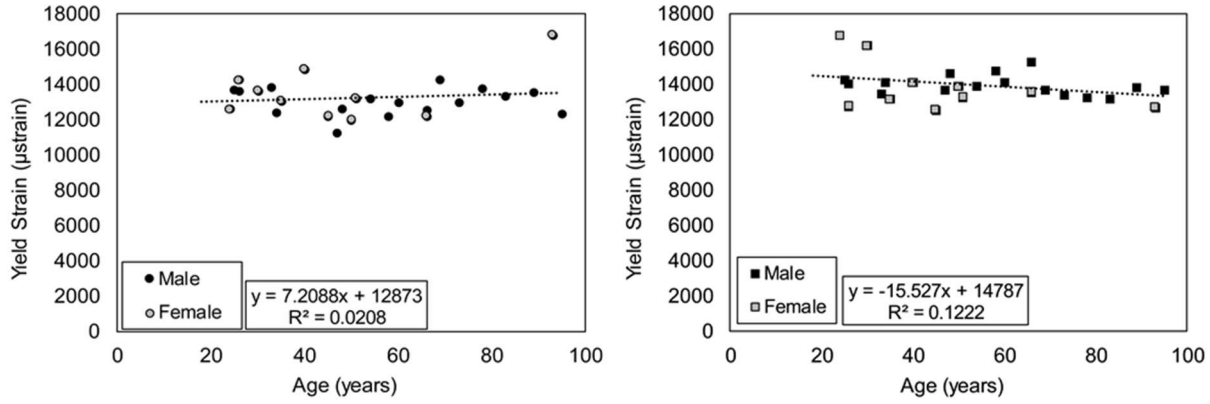

Figure A35: Yield strain versus age for compression tests at 0.005 strain/s (left) and 0.5 strain/s (right) for subjects >21 years old.

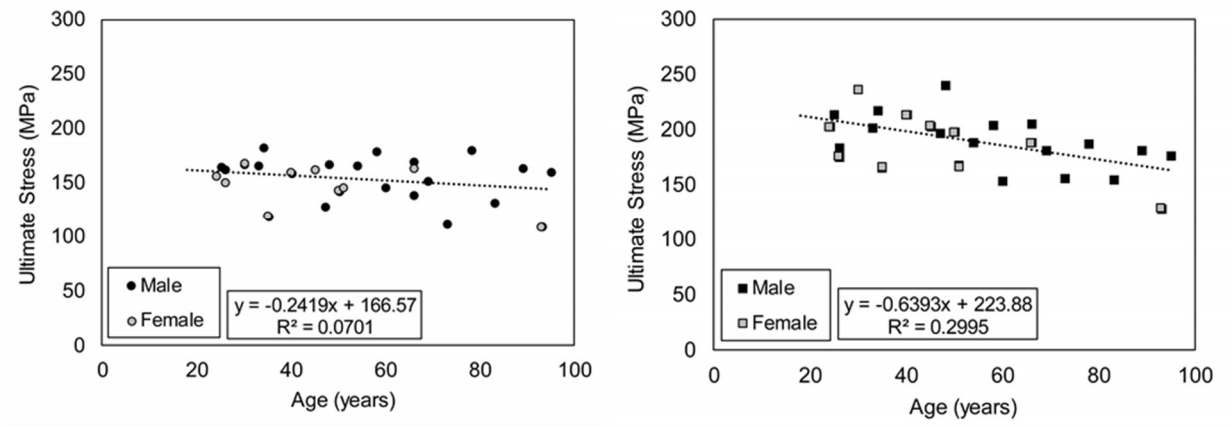

Figure A36: Ultimate stress versus age for compression tests at 0.005 strain/s (left) and 0.5 strain/s (right) for subjects >21 years old.

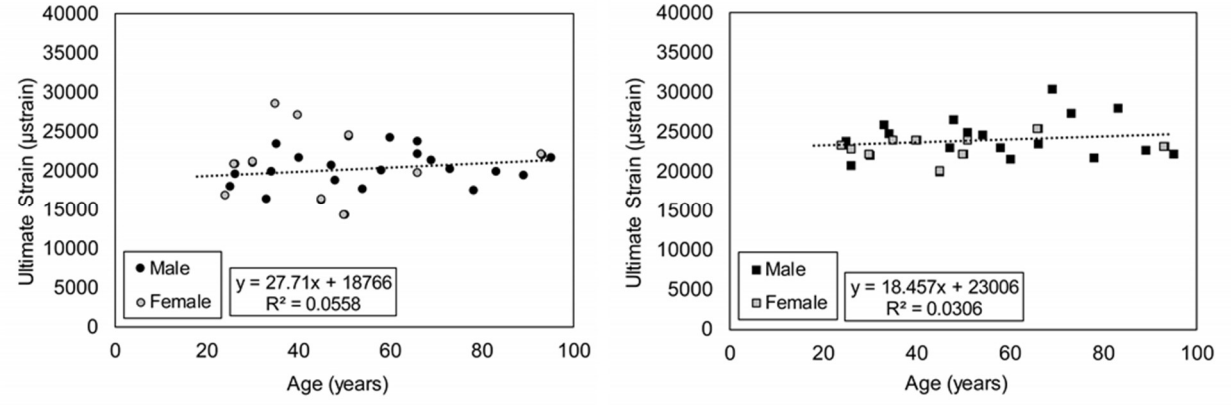

Figure A37: Ultimate strain versus age for compression tests at 0.005 strain/s (left) and 0.5 strain/s (right) for subjects >21 years old.

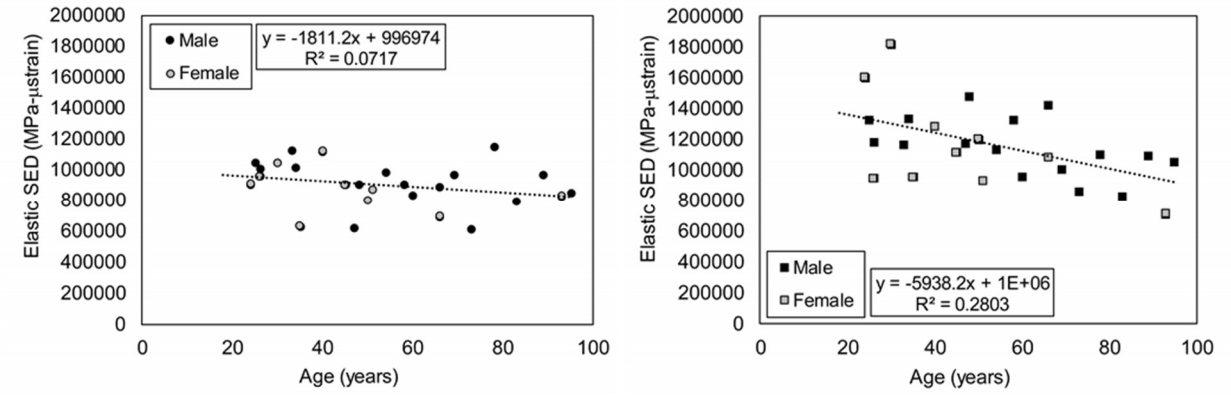

Figure A38: Elastic SED versus age for compression tests at 0.005 strain/s (left) and 0.5 strain/s (right) for subjects >21 years old.

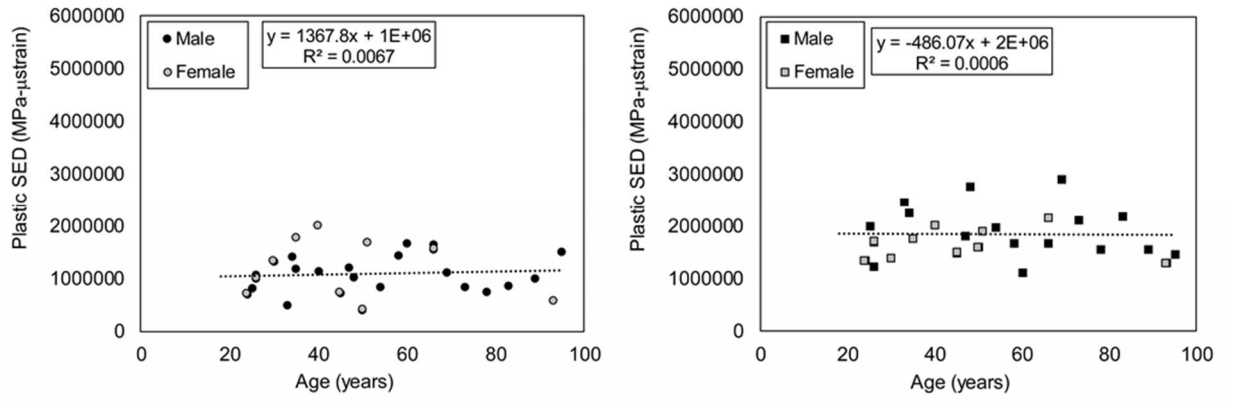

Figure A39: Plastic SED versus age for compression tests at 0.005 strain/s (left) and 0.5 strain/s (right) for subjects >21 years old.

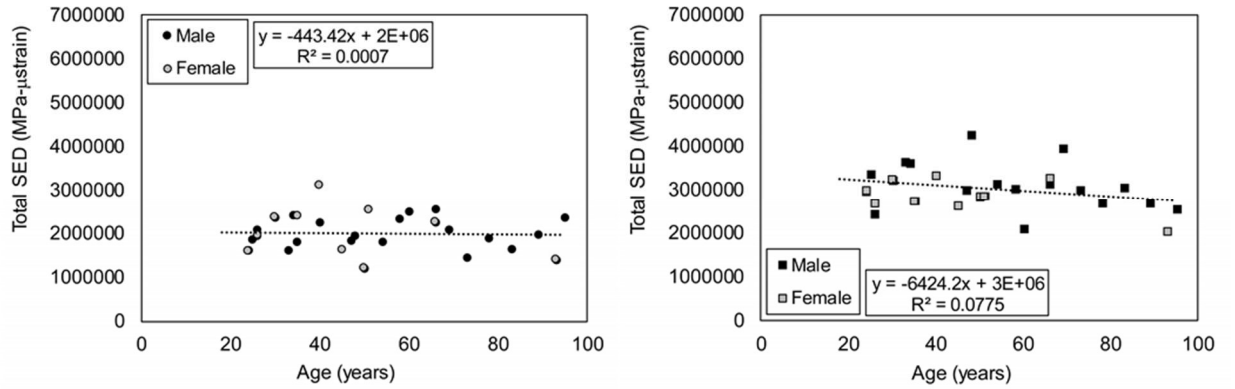

Figure A40: Total SED versus age for compression tests at 0.005 strain/s (left) and 0.5 strain/s (right) for subjects >21 years old.

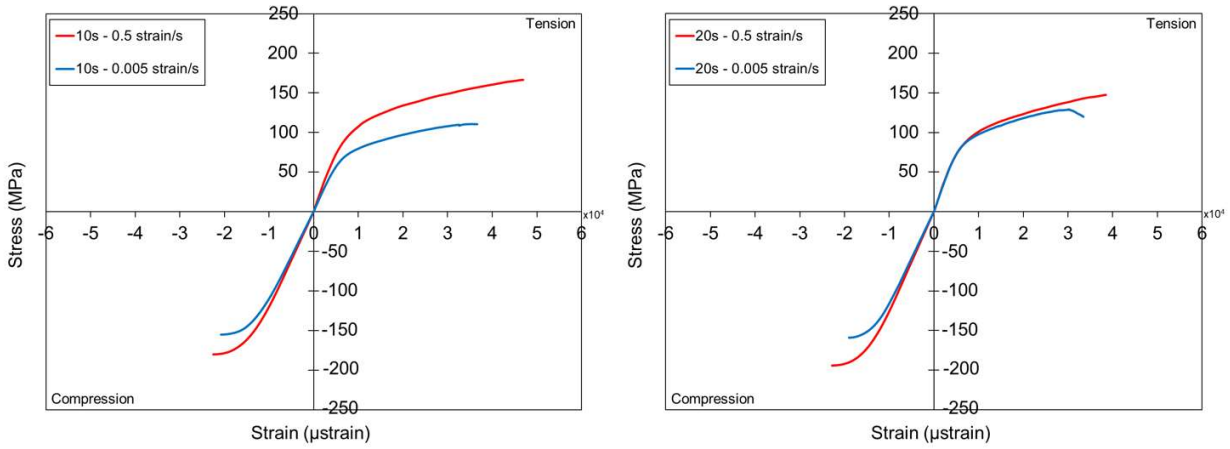

Figure A41: Tension (1st quadrant) and compression (3rd quadrant) characteristic average stress-strain curves at both strain rates for matched subjects aged 10-19 years (left) and 20-29 years (right).

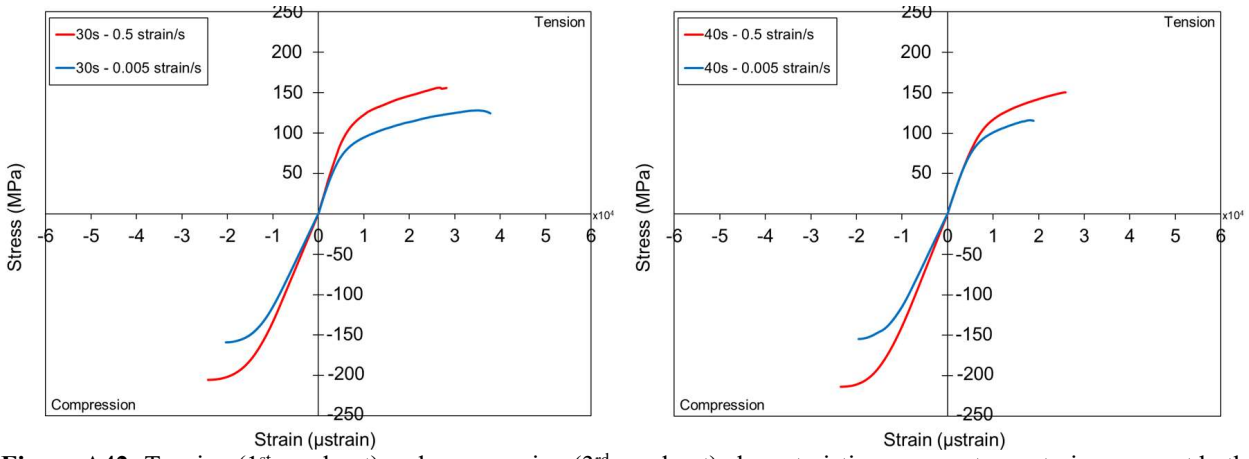

Figure A42: Tension (1st quadrant) and compression (3rd quadrant) characteristic average stress-strain curves at both strain rates for matched subjects aged 30-39 years (left) and 40-49 years (right).

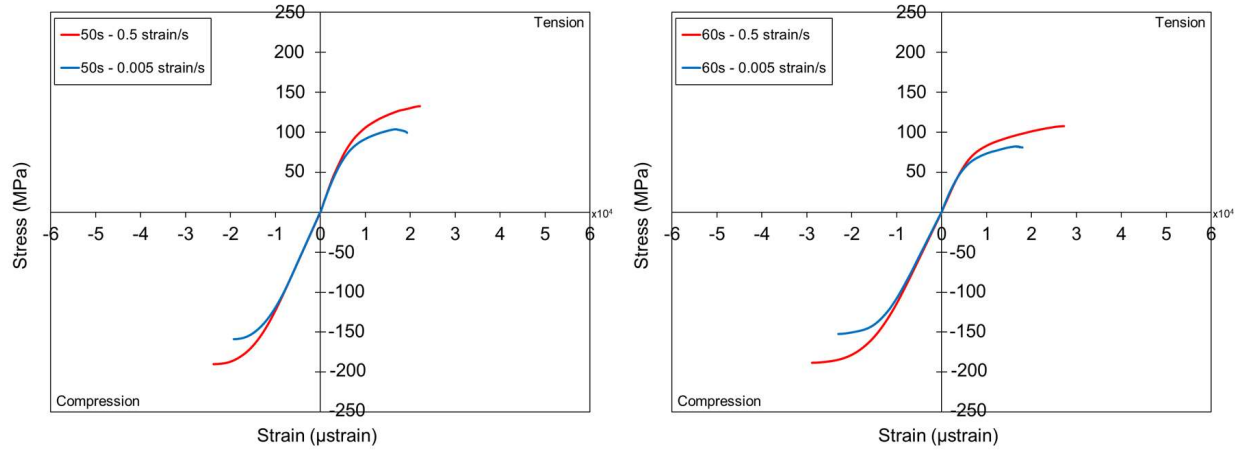

Figure A43: Tension (1st quadrant) and compression (3rd quadrant) characteristic average stress-strain curves at both strain rates for matched subjects aged 50-59 years (left) and 60-69 years (right).

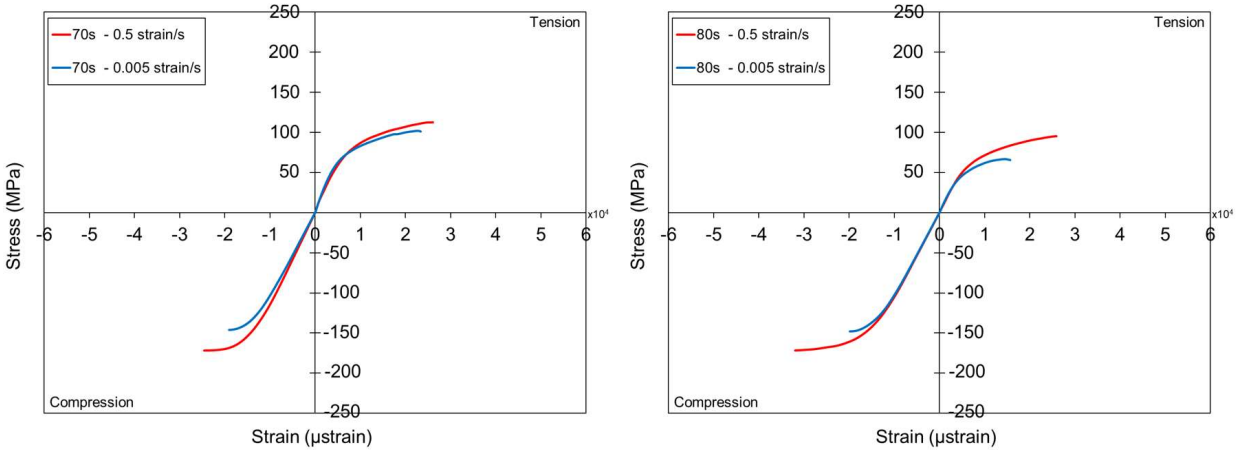

Figure A44: Tension (1st quadrant) and compression (3rd quadrant) characteristic average stress-strain curves t at both strain rates for matched subjects aged 70-79 years (left) and 80-89 years (right).

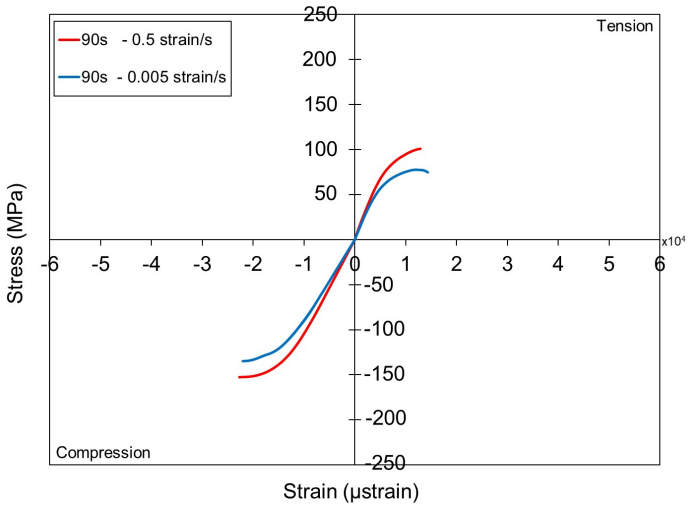

Figure A45: Tension (1st quadrant) and compression (3rd quadrant) characteristic average stress-strain curves at both strain rates for matched subjects aged 90-99 years.